AEDC-TR-76-26

Cy.4

THE DESIGN OF THE 4-MEGAWATT INDUCTION HEATING POWER SUPPLY AT AEDC

PROPULSION WIND TUNNEL FACILITY
ARNOLD ENGINEERING DEVELOPMENT CENTER
AIR FORCE SYSTEMS COMMAND
ARNOLD AIR FORCE STATION, TENNESSEE 37389

April 1976

Final Report for Period January 1971 — July 1974

Prepared for

DIRECTORATE OF TECHNOLOGY
ARNOLD ENGINEERING DEVELOPMENT CENTER
ARNOLD AIR FORCE STATION, TENNESSEE 37389

NOTICES

When U. S. Government drawings specifications, or other data are used for any purpose other than a definitely related Government procurement operation, the Government thereby incurs no responsibility nor any obligation whatsoever, and the fact that the Government may have formulated, furnished, or in any way supplied the said drawings, specifications, or other data, is not to be regarded by implication or otherwise, or in any manner licensing the holder or any other person or corporation, or conveying any rights or permission to manufacture, use, or sell any patented invention that may in any way be related thereto.

Qualified users may obtain copies of this report from the Defense Documentation Center.

References to named commercial products in this report are not to be considered in any sense as an endorsement of the product by the United States Air Force or the Government.

This report has been reviewed by the Information Office (OI) and is releasable to the National Technical Information Service (NTIS). At NTIS, it will be available to the general public, including foreign nations.

APPROVAL STATEMENT

This technical report has been reviewed and is approved for publication.

FOR THE COMMANDER

Marshall K Kingery

MARSHALL K. KINGERY
Research & Development
Division
Directorate of Technology

Robert O Dietz

ROBERT O. DIETZ
Director of Technology

REPORT DOCUMENTATION PAGE		READ INSTRUCTIONS BEFORE COMPLETING FORM
1 REPORT NUMBER AEDC-TR-76-26	2 GOVT ACCESSION NO.	3 RECIPIENT'S CATALOG NUMBER
4. TITLE *(and Subtitle)* THE DESIGN OF THE 4-MEGAWATT INDUCTION HEATING POWER SUPPLY AT AEDC		5 TYPE OF REPORT & PERIOD COVERED Final Report, January 1971 - July 1974 6. PERFORMING ORG. REPORT NUMBER
7. AUTHOR(s) J. W. Cunningham, ARO, Inc.		8. CONTRACT OR GRANT NUMBER(s)
9 PERFORMING ORGANIZATION NAME AND ADDRESS Arnold Engineering Development Center (DY) Air Force Systems Command Arnold Air Force Station, TN 37389		10. PROGRAM ELEMENT, PROJECT, TASK AREA & WORK UNIT NUMBERS Program Element 65807F
11 CONTROLLING OFFICE NAME AND ADDRESS Arnold Engineering Development Center (DYFS), Air Force Systems Command, Arnold Air Force Station, TN 37389		12. REPORT DATE April 1976 13. NUMBER OF PAGES 98
14 MONITORING AGENCY NAME & ADDRESS*(if different from Controlling Office)*		15. SECURITY CLASS. *(of this report)* UNCLASSIFIED 15a. DECLASSIFICATION/DOWNGRADING SCHEDULE N/A

16 DISTRIBUTION STATEMENT *(of this Report)*

Approved for public release; distribution unlimited.

17 DISTRIBUTION STATEMENT *(of the abstract entered in Block 20, if different from Report)*

18 SUPPLEMENTARY NOTES

Available in DDC.

19 KEY WORDS *(Continue on reverse side if necessary and identify by block number)*

induction heating

high power

oscillators

20. ABSTRACT *(Continue on reverse side if necessary and identify by block number)*

A large Class C oscillator, which is intended to be a power source for induction heating of gases, has been built at AEDC. The oscillator utilizes eight triode vacuum tubes in a push-pull parallel configuration and is capable of a continuous power output of 3.2 MW at frequencies between 10 and 50 kHz. This report describes in detail the design of the oscillator, its auxiliary equipment, and its protective devices. The report is not intended

DD FORM 1 JAN 73 1473 EDITION OF 1 NOV 65 IS OBSOLETE

20. ABSTRACT (CONTINUED)

as an operating manual; rather, it is intended to give the reader sufficient information to design experimental hardware which will properly load the oscillator, and to describe the capabilities and limitations of the oscillator. With this information, the user can write his own operating procedures. In the course of the design, a computer program was written to simulate the operation of the oscillator. The program produces a time history of the various voltages and currents within the oscillator and has proven to be an accurate analog of the actual hardware. It is a relatively simple matter to add to the program a description of a proposed experimental load and to study the behavior, both transient and steady state, of the oscillator with this particular load.

AFSC
Arnold AFS Tenn

PREFACE

The work reported herein was conducted by the Arnold Engineering Development Center (AEDC), Air Force Systems Command (AFSC), under Program Element 65807F. The results of the research were obtained by ARO, Inc. (a subsidiary of Sverdrup & Parcel and Associates, Inc.), contract operator of AEDC, AFSC, Arnold Air Force Station, Tennessee. The work was done under ARO Project Numbers PW3170, PW3270, PD205, RF416, and PF217. The author of this technical report was J. W. Cunningham, ARO, Inc. The manuscript (ARO Control No. ARO-PWT-TR-75-47) was submitted for publication on April 29, 1975.

Several people who participated in the design of the oscillator should be mentioned. Structural design of the oscillator and engineering on the cooling water supply were done by W. C. Rothe, ARO, Inc. The control system and the supply of electrical power to the oscillator were designed by J. B. Carson, ARO, Inc. Ashley Bock, who was retained as a consultant during the conceptual design of the oscillator, set the spacing between high voltage components, determined the lengths of high voltage insulators, and suggested sources for some of the components.

CONTENTS

ILLUSTRATIONS

TABLES

1.0 INTRODUCTION

This report describes the design of a large Class C oscillator which has been built at AEDC. The oscillator is intended as a power source for experiments in induction heating of gases. It utilizes eight vacuum tubes in a push-pull parallel configuration and is capable of a continuous power output of 3.2 MW at frequencies between 10 and 50 kHz. The tank capacitor of the oscillator consists of a bank of 42 individual capacitors which can be connected in various series-parallel combinations to allow operation at a number of frequencies over this range. The oscillator is coupled to the experiment by surrounding the plasma with a portion of the oscillator tank coil.

The oscillator was built in response to a requirement by the Lewis Laboratory of the National Aeronautics and Space Adminstration (NASA), where a nuclear space propulsion engine was being developed. Fission in this engine occurred within a uranium plasma, and severe heat-transfer problems were expected to be encountered. It was essential to solve these problems using a nonnuclear energy source so that failure of the test hardware would not result in loss of radioactive material. The oscillator was intended to produce a plasma simulating the uranium plasma during the development of the engine. It was built at AEDC because a suitable d-c power source and other utilities were available and because personnel at AEDC had gained considerable expertise in induction heating of gases. Although work on the nuclear engine was discontinued, the oscillator was completed and is now being used as a power source for plasma experiments at AEDC.

Direct-current plate supply power for the oscillator is obtained from an ignitron rectifier, which also powers several arc-heated test facilities in the area. The supply consists of a load-tap-changing transformer and six ignitron tubes in a three-phase, full wave bridge circuit. The d-c output is unfiltered and contains the normal 360-Hz ripple. The output voltage can be varied under load in steps of about 1,000 v from zero to full-rated output by changing the transformer tap setting. Phase control of the output voltage is also available but is seldom used because of the poor output voltage waveform it produces. The supply is normally rated at 19,000 v at 900 amp. However, the maximum voltage rating can be exceeded somewhat at the low current required by the oscillator (232 amp).

Design of the oscillator was begun in January 1971, with a six-month study sponsored by NASA. The study resulted in the selection of the basic circuit and the type of vacuum tube to be used; it also produced a cost estimate. The final design and construction were begun in January 1972, again under NASA sponsorship. Shakedown of the oscillator was begun in late 1973 and was completed in July 1974.

This report is not intended as an operating manual. Rather, it is intended to acquaint the reader sufficiently with the capabilities and limitations of the oscillator so that he can interface it with experimental hardware and write his own operating procedures. Section 2.0 discusses the reasons for the selection of the particular circuit and tube type and the problem of choosing component values. Section 3.0 describes the computer program which was used to verify (and in some cases to change) the oscillator circuit and component values. Section 4.0 describes the limitation imposed on the oscillator power output and frequency range by the tank capacitor and feedback capacitor ratings. Section 5.0 describes the physical arrangement of the oscillator components and the cooling water and air supplies. Section 6.0 describes protective devices and instrumentation. Finally, Section 7.0 describes the present state of the oscillator and operating experience to date.

One deviation from standard nomenclature has been adopted. The symbol V is used to represent the reactive power handled by a capacitor ("vars"). Voltages are represented exclusively by the symbol E. The subscript b refers to one of the two tank capacitor banks, and the subscript f refers to one of the two feedback capacitor banks. The subscript t refers to the plate-to-plate tank capacitance (two C_b's and two C_f's in series). The additional subscript r refers to the rated value of the variable; for example, V_{br} is the rated var handling capacity of a tank capacitor bank.

2.0 CIRCUIT CONFIGURATION AND COMPONENT VALUES

During the initial study, it was determined that NASA required a supply with a power input of 4 MW or greater which could be operated at any frequency in the range from 10 to 50 kHz. Consideration was given to rotating machinery, to semiconductors, and to vacuum tubes. It was found that rotating machinery could not be purchased for frequencies greater than 10 kHz and was very expensive, costing about $200/kw (installed). Variable frequency operation would have increased the cost

still further. Whereas small silicon-controlled rectifiers (SCR's) could be operated above 10 kHz, larger units were restricted to about 3 kHz by dI/dt and turnoff time limitations. Transistors which could operate at 50 kHz were so small that paralleling problems would have been severe. Thus, vacuum tubes became the only practical choice for the supply.

2.1 VACUUM TUBES

It was found that the variety of tubes which were suitable for this application was not large. Tubes which were thought to be suitable are described below. All are designed to operate at a plate voltage of 20 kv.

7482 and 7560. These are large triodes which are identical, except for the method of cooling. The 7482 is vapor cooled (that is, the anode is immersed in water and is cooled by convective boiling) and has a plate dissipation rating of 200 kw. The 7560 is of conventional water-cooled design (no boiling takes place) with a plate dissipation rating of 175 kw. Each is capable of 580 kw input. These tubes are available from at least two manufacturers, at a cost of about $5.40/kw input. The 7560 is an established "workhorse" in the field of induction heating and is also used in LORAN transmitters. The 7482 is used in a number of international broadcast transmitters.

1142. This tube is essentially a lengthened version of the 7560. Power capability and price are roughly 1.66 times the corresponding figures for the 7560. However, at the time of the study, the tube had just completed development and had had no application.

4CW 250,000A. This is a water-cooled tetrode with a plate dissipation rating of 250 kw and a plate input capability of 615 kw. The cost is about $8.10/kw input. It is a well-established tube, used in international broadcast and VLF Navy transmitters.

X2159. This is a water-cooled tetrode with power ratings three to four times as large as the corresponding figures for the 4CW 250,000A. The cost is about $5.00/kw input. The tube was in development at the time of the initial study (1971) but would have been available in time for this application. It was being developed for international broadcast.

The 7482 and the 4CW 250,000A were the tubes considered in the comparison of triodes and tetrodes (see below). The 1142 and the

X2159 were eliminated because they were new designs. It was felt that an induction heater was a rather rough application for an unproven tube. The choice of the 7482 over the 7560 was merely a matter of convenience. The 7482 requires less than one-tenth as much cooling water as the 7560; however, piping for exhausting the steam complicates design.

2.2 CIRCUIT SELECTION

A wide variety of circuits could potentially be used to generate the power required in this application, and some effort was devoted to selecting the best circuit configuration. In the selection the following choices had to be made:

1. Should the tubes be triodes or tetrodes?
2. Should the load be tuned or untuned?
3. Should the tubes be operated single-ended or push-pull?
4. Should the tubes be self-excited (oscillator) or separately excited (amplifier)?

The considerations which entered into each choice are discussed below and are summarized in Table 1.

1. The primary advantages of a tetrode over a triode are considerably lower driving power and far smaller feedback capacity. These are important points if the tube is operated as an amplifier, but they lose most of their significance if it is operated as an oscillator. On the other hand, a tetrode requires an additional power supply, and the screen is susceptible to damage under light load. The efficiency is lower, because the plate cannot be driven to a low voltage without overheating the screen. Finally, a tetrode is more expensive than the equivalent triode.
2. The primary reason for using an untuned load is that a nonsinusoidal voltage may be applied to the load. If the load voltage were a square wave, then plate current could be allowed to flow in pulses up to one-half cycle long. Peak plate currents would be

greatly reduced, efficiency would be very high, and the power a tube could handle might be doubled, as compared to conventionally tuned Class C operation. Also, untuned operation would require no tuning capacitor, an expensive component. Unfortunately, one could not build an untuned oscillator, nor could one build a single-ended circuit with an untuned load (unless the inefficiency of Class A operation were tolerated). Furthermore, the tubes would have to be shunted by diodes to carry the lagging current of the reactive load. It did not appear to be practical to use these diodes, because of the large current and voltage ratings and the small charge storage they would have to have.

3. The only advantage of single-ended operation seems to be that the load voltage is lower. Other considerations favor push-pull operation. The most important reason for using a push-pull circuit is that only half of the tubes conduct at one time, so the problem of current sharing between the tubes is eased. A push-pull circuit will also tolerate a loaded Q lower by a factor of two. As will be seen, this cuts the cost of the tuning capacitor by a factor of two.

4. The primary advantage of the oscillator configuration is that grid driving power need not be generated separately, but can be taken from the plate circuit. The primary advantage of the amplifier configuration is that the load voltage can be easily controlled. Another consideration is that with an amplifier one must manage to keep the load tuned to the driving frequency (or vice versa).

Table 1. Considerations Entering into Choice of Circuit Configuration

1. Triode versus Tetrode:

Triode	Tetrode
More difficult to damage.	Lower driving power.
Better operation at low voltages.	Much lower feedback capacitance.
No screen supply.	
Lower cost per kilowatt.	

2. Tuned versus Untuned:

Tuned	Untuned
No shunt diode needed.	Load voltage can be nonsinusoidal.
Can operate single-ended.	No tuning capacitor required.
Can operate as oscillator.	

3. Push-pull versus Single-ended:

Push-pull	Single-ended
Half as many tubes to parallel.	Lower load voltage.
Tolerate lower load Q.	

4. Amplifier versus Oscillator:

Amplifier	Oscillator
Load voltage easily controlled.	Need not generate driving power.
	Tolerates large feedback capacity.
	Load automatically tuned to operating frequency.

These four possible choices result in the 16 possible configurations, which are depicted in Fig. 1. Since neither a single-ended, untuned circuit nor an untuned oscillator can be built, and since an untuned amplifier would require diodes which are difficult to supply, all untuned configurations have been eliminated. It has already been mentioned that there is no advantage to using tetrodes in an oscillator, nor to using triodes in an amplifier; therefore, only the four white blocks in

Fig. 1 remain. Since there are several good reasons for using a push-pull circuit, the final choice must be made between a tuned, push-pull, triode oscillator, and a tuned, push-pull tetrode amplifier.

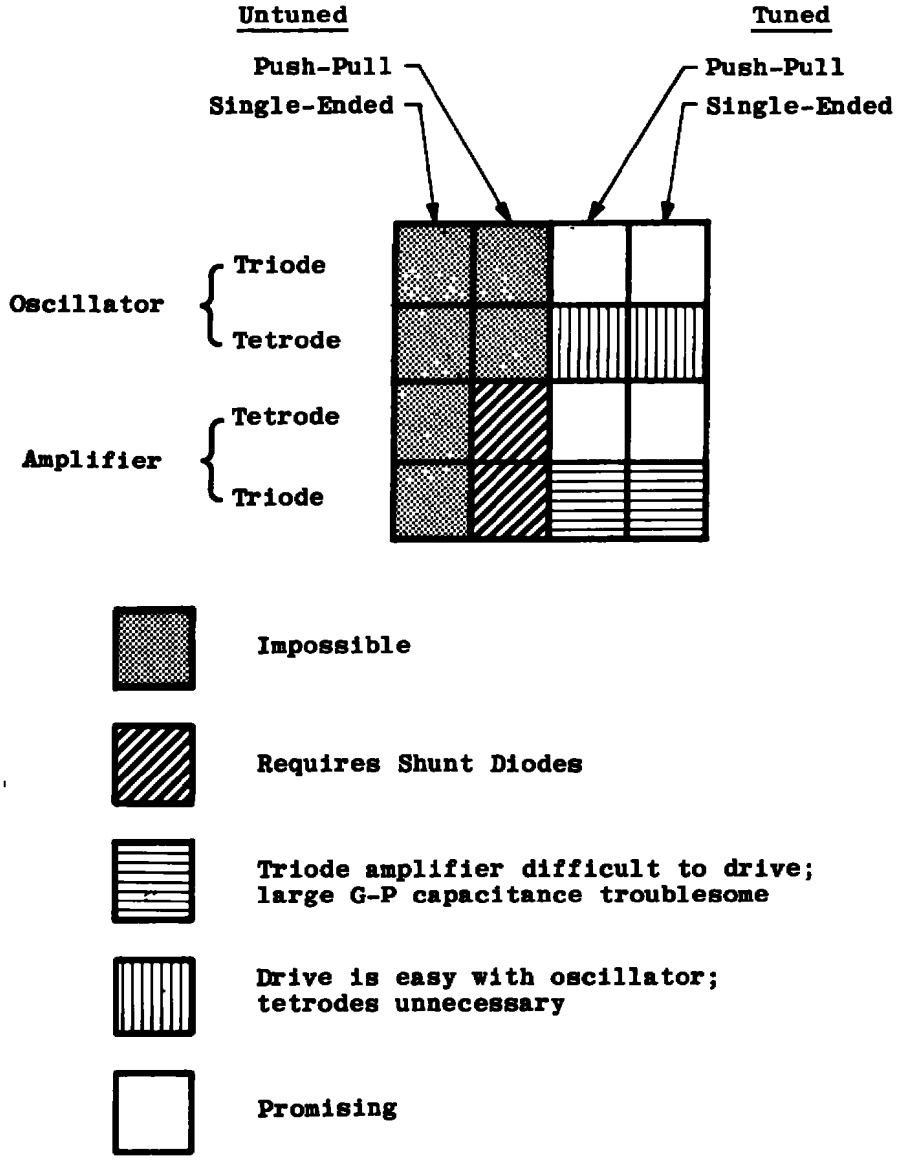

Figure 1. Summary of the possible circuit configurations.

The most important advantages of the oscillator are as follows:

1. It is somewhat cheaper, since driving circuitry need not be provided.
2. The problem of keeping the driver and the load tuned to the same frequency is eliminated.

The only advantage of the amplifier seems to be:

3. The load voltage can be more easily controlled.

Point 2 is quite significant, in view of the rather large changes in coil inductance and Q which take place when the plasma is established or extinguished. Point 3 loses most of its significance, since the d-c power supply which was to power the oscillator (or amplifier) included a tap-changing transformer which allowed control of the plate supply voltage under load. The choice was therefore made in favor of the tuned, push-pull, triode oscillator.

The type of feedback for the oscillator was next chosen. Most induction heaters use some form of inductive feedback, either a small coil coupled to the plate tank coil (tickler circuit) or a tap on the plate tank coil (Hartley circuit). Inductive feedback was not used in this application for two reasons. First, the plate tank coil is difficult to build at best, considering the voltage and current it must handle and the size restrictions placed on it by the necessity of coupling into the plasma experiment. It seemed best not to complicate the tank coil design by requiring taps or tickler windings to be placed on it. Second, it was probable that the amount of feedback would be difficult to control because of the variable influence of the plasma on the tank coil. For these reasons, capacitive feedback (the Colpitts circuit) was selected.

The basic circuit of the oscillator is shown in Fig. 2. Shunt feed was used in the plate circuit (even though it required the purchase of a plate choke) so that the plate supply voltage would not appear on the tank coil, thus easing the design of this component somewhat. The individual grids were shunt fed to allow measurement of individual grid currents, and also to allow selection of individual grid resistors. (Individual biasing was provided as an aid in balancing the loading of the tubes, but this was not entirely successful; see Section 7.2). Protective bias from a variable bias supply was applied through a diode to each grid. This allowed the non-oscillating plate current of the tubes to be controlled. In oscillation, bias is determined by the grid current and the bias resistor, not by the protective bias supply.

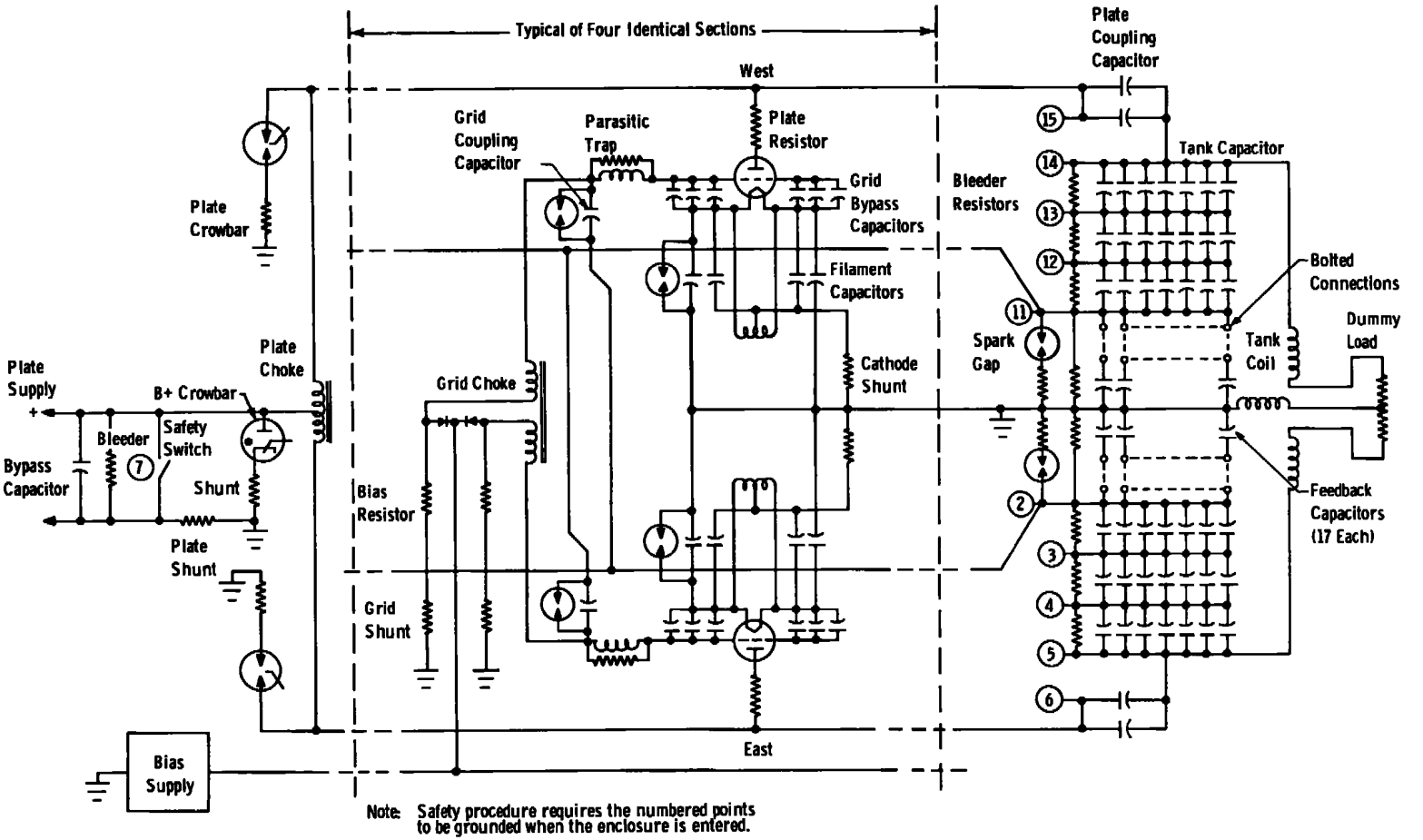

Figure 2. Elementary circuit diagram of the oscillator.

The tank capacitor and the feedback capacitor each consists of a series-parallel capacitor bank, and both are described in Section 4.0. For shakedown, the entire tank coil was placed within the oscillator enclosure, and the load consisted of a water-cooled resistor placed outside the enclosure. When the oscillator is used to drive a plasma experiment, all or part of the tank coil surrounds the plasma, and the load represents the resistance coupled into the tank coil by the plasma. The choke grounding the load center-tap serves no function in the basic oscillator circuit, but prevents a bias instability which was found in running the computer simulator program (Section 3.4).

The parasitic choke and resistor and the grid bypass capacitors operate together to prevent feedback at frequencies above the highest operating frequency and thus prevent parasitic oscillations. The exact function of these components is discussed later in this section. The plate resistors provide essential protection for the tubes in the event of a grid-plate flashover (Section 6.1).

2.3 COMPONENT VALUES

The first task in selecting component values is to determine the tank circuit components. In doing so, one can assume that the tank circuit Q is much larger than one. If this is the case, the sinusoidal circulating current in the tank will be much larger than the nonsinusoidal current injected into the tank by the tubes. Neglecting the latter leads to sinusoidal voltages and currents, and a very simple, yet accurate analysis results. Errors introduced by the approximation are difficult to handle analytically, and are better resolved by use of the computer simulation (Section 3.0).

A simplified diagram of the tank circuit is shown in Fig. 3. The frequency of oscillation is immediately given by

$$\omega_o = (L\,C_t)^{-0.5} \tag{1}$$

The circuit Q is defined as

$$Q = \frac{\omega_o L}{R} \tag{2}$$

Since the Q is much larger than 1, the impedance presented to the voltage E_t by L and R in series is nearly equal to $\omega_o L$, and the circulating current in the tank is then given by

$$I_t = \frac{E_t}{\omega_o L} = E_t\left(\frac{C_t}{L}\right)^{0.5} \tag{3}$$

The power output is then

$$P = I_t^2 R = E_t^2 \frac{C_t R}{L} \tag{4}$$

Equations (3) and (4) can be combined to obtain

$$I_t = \frac{PQ}{E_t} \tag{5}$$

The reactive power which must be handled by the tank capacitor is the product of the rms current through it (I_t) and the rms voltage across it (E_t). From Eq. (5), this is

$$V_t = PQ \tag{6}$$

(The reactive power handled by the coil is nearly identical.) The power output can also be written as

$$P = \frac{E_t^2}{Z_t} \tag{7}$$

where Z_t is the plate-to-plate impedance (resistive) presented to the tubes by the tank at resonance. From Eqs. (4) and (7), Z_t is given by

$$Z_t = \frac{L}{C_t R} = \frac{Q}{\omega_o C_t} \tag{8}$$

Then, in terms of ω_o, Z_t, and Q, from Eq. (8) one obtains

$$C_t = \frac{Q}{\omega_o Z_t} \tag{9}$$

and from Eqs. (1) and (8),

$$L = \frac{Z_t}{\omega_o Q} \tag{10}$$

Tube tables for the 7482 give the peak radio frequency (rf) plate voltages as 17,400 v, and the power output as 440 kw for a single tube.

The rf voltage, plate to plate, is then 34,800 v peak, or 24,600 v rms (E_t). Power output for eight tubes is 3.52 MW (P). Then from Eq. (7), the impedance which the tank must present to the tubes is Z_t = 172 ohms.

The nature of the compromise which must be made in selecting tank Q is clearly indicated by Eq. (6). Although increasing Q will increase the stability of the oscillator and decrease the harmonic content of voltage and current waveforms, it will also increase the required var handling capability of the tank capacitor and make it proportionately more expensive (and bulkier). On the basis of the computer simulation of the oscillator, a nominal Q of 10 was selected. The circulating tank current is then, by Eq. (5), 1430 amp rms, and the range of tank component values is given below.

Frequency, kHz	L, μh	C_t, μf
10	274	0.925
50	55	0.185

The component C_t in Fig. 3 is actually composed of two "tank" capacitors and two "feedback" capacitors in series. Further details on the selection of these components are given in Section 4.0.

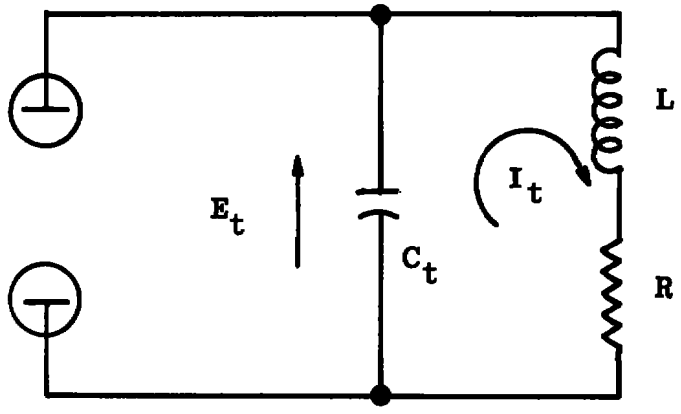

Figure 3. Simplified diagram of the plate tank circuit.

The Q chosen influences the design of experiments which will utilize the oscillator in the following manner. It is useful to take the view that the tubes supply the power to the load but that the tank capacitor supplies the reactive vars required by the load coupling coil. If the coupling between the load coupling coil and the plasma is tight, then the coupling coil will have a Q of less than 10, and it can easily be padded with series inductance within the oscillator enclosure, so that the effective Q of the tank coil is 10. On the other hand, if the coupling is loose, the coil will have a Q greater than 10. There are then two alternatives. One is to reduce the power output of the oscillator to avoid exceeding the var or current rating of the tank capacitors. The other is to supply the extra vars required by using an external capacitor bank across the load coupling coil. More details on this problem are given in Section 4.0.

Not all of the power generated by the tubes reaches the load. Estimated circuit losses are as follows:

Power input to tubes	-	4,640 kw
Power output of tubes	-	3,520 kw
Efficiency of tubes	-	0.759
Losses in plate resistors	-	109 kw
Driving power	-	48 kw
Losses in tank coil	-	38 kw
Losses in plate choke	-	26 kw
Losses in transmission line	-	15 kw
Losses in tank coil shield	-	7 kw
Losses in tank capacitors	-	7 kw
		250 kw
Circuit efficiency	-	0.929
Power output of circuit	-	3,270 kw
Overall efficiency	-	0.705

Having selected the values of tank circuit components, one is now in a position to select values for the shunt feed capacitors and chokes. The plate shunt feed choke is directly in parallel with the tank coil at the operating frequency. Its value is not at all critical, but it must be large enough so that it does not carry excessive a-c current. A value of 27 mH plate-to-plate (100 times the largest tank inductance) was arbitrarily selected. The maximum a-c current through the choke was then 14.3 amp rms. The choke must be insulated for 20 kv from center-tap to ground, and for 40 kv plate-to-plate, and from each plate to ground.

The computer program showed that the coupling between the two halves of the choke had some effect on the transient response of the oscillator but was otherwise unimportant. The choke finally purchased was of an iron core design, and the coupling between halves is probably greater than 0.99, although it has not been measured. It was difficult to find a manufacturer for the choke, primarily, it seems, because of the high voltages involved and because the iron losses are difficult to estimate.

The plate-coupling capacitors must meet two requirements. First, they must have sufficient current-carrying capacity, and second, they must have sufficiently low impedance. The computer program showed the current through each coupling capacitor to be 185 amp rms (highly nonsinusoidal). Since the capacitor style available had bushings rated at only 100 amp, it became necessary to use two capacitors in parallel. Each package of this style could hold a capacitance of 2.5 μf, so a total of 5 μf was used for each coupling capacitor. This value easily meets the second requirement (impedance), as can be verified in two ways. First, the impedance of 5 μf at 10 kHz is only 3.18 Ω, as compared to the tank impedance of 172 Ω. Second, the total plate current of four tubes is 116 amp DC. Then in one conduction period at 10 kHz, a coupling capacitor will pass a total charge of 0.0116 coulombs. This charge will change the voltage across the coupling capacitor by 2320 v. This is the peak-to-peak a-c voltage across the capacitor and is sufficiently low compared to the 17,400-v peak rf voltage on each plate, especially since the two voltages add in quadrature. The computer program showed little change in waveform when the coupling capacitor was changed from 5 μf to infinity. The coupling capacitors are rated at 20 kv DC.

There are four grid chokes, one for each pair of tubes. The inductance of these chokes must be large enough so that the current carried by each choke is small compared to the grid current of a tube. An inductance of 100 mH was chosen arbitrarily. This results in a current through the choke of 0.38 amp rms, or 0.53 amp peak, as compared to the d-c grid current of 3.4 amp and peak grid current of about 28 amp. The chokes were fabricated locally, using C-cores wound with 4-mil silicon steel.

The grid-coupling capacitors must be large enough so that the voltage developed across the capacitor by the flow of grid current will be small compared to the rf voltage on the grid. The design grid current is 3.4 amp DC per tube, or 3.4×10^{-4} coulombs per conduction period at 10 kHz. As a 2.5-μf, 1500-v capacitor was readily available, this value was selected. The peak-to-peak voltage across the capacitor

was then 136 v, sufficiently small compared to the peak rf grid voltage of 1680 v. The computer program again verified that the effect on waveforms of changing the grid coupling capacitor from 2.5 μf to infinity was small.

Filament bypass capacitors may not be strictly necessary, but they were inexpensive and were included as a precaution. The a-c cathode current of the tube should divide evenly between the two filament legs and should flow to the filament transformer center-tap through the leakage inductance of the two halves of the transformer secondary winding (which will not be perfectly coupled). However, since the leakage inductance of the secondary was unknown, bypass capacitors were included which were large enough to handle the entire cathode current of the tube. A current of 5 μf was used from each filament leg to the top of the cathode current shunt. The peak-to-peak rf voltage across the capacitors calculates (by the same methods used with the plate- and grid-coupling capacitor) to be 324 v, which is small compared to the peak grid voltage of 1680 v. The capacitors were returned to the shunt and not to ground, so that the instantaneous cathode current could be measured by the shunt. This was not entirely successful (see Sections 6.4 and 7.3). The filament bypass capacitors are physically large and are self-resonant at several hundred kHz. To prevent the impedance from filament to ground from becoming uncontrolled at high frequencies, small 0.05-μf mica capacitors were also connected from filament to ground. The largest, lowest inductance leads practical were used from the filament connectors on the tubes to these capacitors.

Although the oscillator is not required to operate at frequencies above 50 kHz, the tubes used have gain at frequencies up to perhaps 100 MHz. Unless precautions were taken, it seemed likely that parasitic oscillations would occur at some frequencies in this range. Two sources of parasitic feedback were identified. First, the tank capacitors themselves became self-resonant at about 500 kHz. To avoid aggravating this problem, the largest, lowest inductance connections possible were used to interconnect tank capacitors (see Section 5.1). Then, a low-pass, critically damped LC network, consisting of the parasitic choke and resistor and the grid bypass capacitors, was inserted in series with each grid. This network essentially disconnects the grids from the tank circuit for frequencies above 300 kHz and prevents feedback from the tank for frequencies for which the tank impedance is uncontrolled.

The second feedback path is through the tube grid-plate capacitance. Feedback through this path could be caused by the inductance of the plate resistors and interconnecting conductors, and transmission line effects. This feedback is prevented by connecting capacitors with the lowest possible inductance between grid and filament. These capacitors form a voltage divider in conjunction with the grid-plate and grid-filament capacitances, with a division ratio of 44 to 1. Since the amplification factor of the tube is only 45, parasitic oscillation through this path is impossible. Six 500-pf, 5-kv ceramic capacitors were mounted directly on the grid connector ring of each tube and were connected by short, heavy straps to the filament connectors. These capacitors also form a component of the low-pass parasitic network. At the operating frequency, they are in parallel with the feedback capacitors, although they are small enough to be neglected.

The dummy load, while not a component of the oscillator itself, was required for shakedown. It was constructed of water-cooled stainless steel tubes and was provided with sliding clamps, so that the total resistance could be varied. Total water flow and temperature rise were measured and were used to calculate the power output of the oscillator. For shakedown, the dummy load was connected in series with the tank coil.

3.0 DIGITAL COMPUTER SIMULATION PROGRAM

If the design of a class C oscillator is carried out analytically using the usual classical techniques (Refs. 1 and 2), several idealizations must be made. The tank Q must be assumed to be infinite and the phase shifting effects of shunt feed components must be neglected, because the procedure requires the grid and plate voltages to be sinusoidal and in phase. It is thus not possible to study the effect of finite tank Q and of grid circuit driving impedance on waveforms. Furthermore, only steady-state solutions can be obtained, and it is not possible to study transient response and stability. The classical technique also requires a graphical integration to be carried out by hand, which limits the accuracy of the technique.

Analog computer simulation of the circuit is not generally possible because of the highly nonlinear nature of vacuum tubes. Although function generators are available which can produce a nonlinear function of a single variable, a tube must be described by two functions (grid current and plate current), each a function of two variables (grid voltage and plate voltage).

It is now economically possible, however, to simulate the operation of a vacuum tube circuit digitally, because of the general availability of fast digital computers with large memories. The tubes can be described with arbitrary accuracy by two-dimensional tables. The circuit equations can be integrated by any of several numerical techniques, again with arbitrary accuracy. The technique has been used extensively to study the behavior of guided missiles and other complex nonlinear dynamic systems. The circuit of the oscillator was studied by this technique, and the results were felt to be well worth the time spent. Because many of the components of the oscillator were expensive and required long lead times, unexpected circuit difficulties which resulted in damage to components or required changing component values would have had serious consequences.

3.1 STATE VARIABLE EQUATIONS

Because of the favorable results which were obtained with this method of simulation, it seems appropriate to include in the following paragraphs a brief description of the method and of our experience with it.

The circuit to be studied is drawn, and the energy storage elements (in this case capacitors and inductors) are identified. (In a more general case, energy storage elements would include masses, springs, pressure vessels, etc.). A variable is chosen which will determine the energy stored in each such component (for example, the voltage across each capacitor and the current through each inductor). These are known as the system "state variables." They completely describe the present state of the system in the sense that if the values of the state variables are known at $t = 0$, and if the values of all inputs to the system after $t = 0$ are known, then the response of the system is uniquely determined. (In the present case there are no external inputs; the problem is essentially to determine the response of an isolated system to its initial conditions.)

Having selected the system state variables, one must next express all of the interesting voltages and currents in the system in terms of the state variables. In doing this, one can describe nonlinear passive elements in the system either by analytical expressions (in simple cases) or by tables (in more complicated cases). Certain troublesome conditions can occur at this step if, for example, every path from a particular node contains an inductance, or if the network contains

loops composed entirely of capacitors. To resolve these difficulties the reader is referred to texts on network theory (Ref. 3).

Finally, one writes a single first-order differential equation for each state variable which expresses the rate of change of that variable in terms of the values of the state variables at that instant. These equations are known as the system state variable equations.

As an example, consider the series LCR circuit shown in Fig. 4, in which the resistor is nonlinear and is characterized by $e_R = R\, i_L^3$. The energy storage elements are L and C, and as state variables, e_C and i_L are selected. In terms of the state variables, the important voltages and currents are given by

$$e_R = R\, i_L^3$$

$$e_L = e_C - e_R = e_C - R\, i_L^3$$

$$i_C = i_L$$

The rates of change of state variables are given by

$$\dot{e}_C = \frac{1}{C}\, i_C = -\frac{1}{C}\, i_L$$

$$\dot{i}_L = \frac{1}{L}\, e_L = \frac{1}{L}\left(e_C - R\, i_L^3\right)$$

These last two equations are the state variable equations for the circuit.

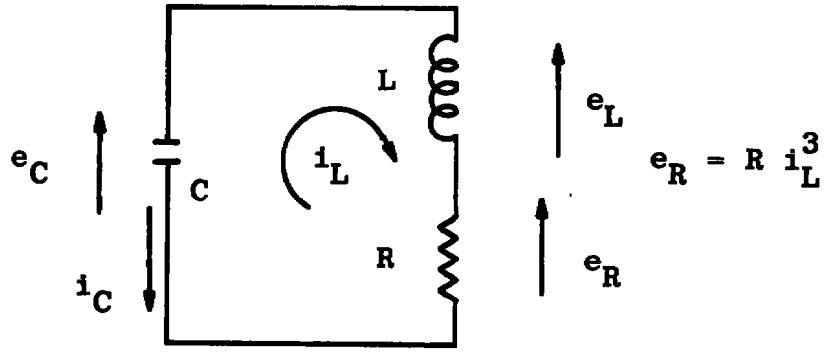

Figure 4. Circuit with nonlinear resistor used as an example in writing state variable equations.

The state variable equations are integrated step by step, beginning with the initial conditions, to obtain a time history of the performance of the system. The simplest way of doing this, known as Euler's method, is to approximate the value of a variable at time t + Δt by

$$x(t + \Delta t) \cong x(t) + \Delta t \cdot \dot{x}(t)$$

(see Fig. 5). Since the state variable equations give the rates of change of all of the state variables at time t, their values can be estimated at time t + Δt. The rates of change at time t + Δt can then be evaluated, the values of the state variables at time t + 2Δt can be estimated, and so forth. Euler's method is never used in practice, because its accuracy is inadequate unless Δt is very small. Other methods are available which can use a much larger step size with acceptable accuracy and thus conserve computer time (Refs. 4 and 5). The fourth-order Runge-Kutta method was used in studying the oscillator.

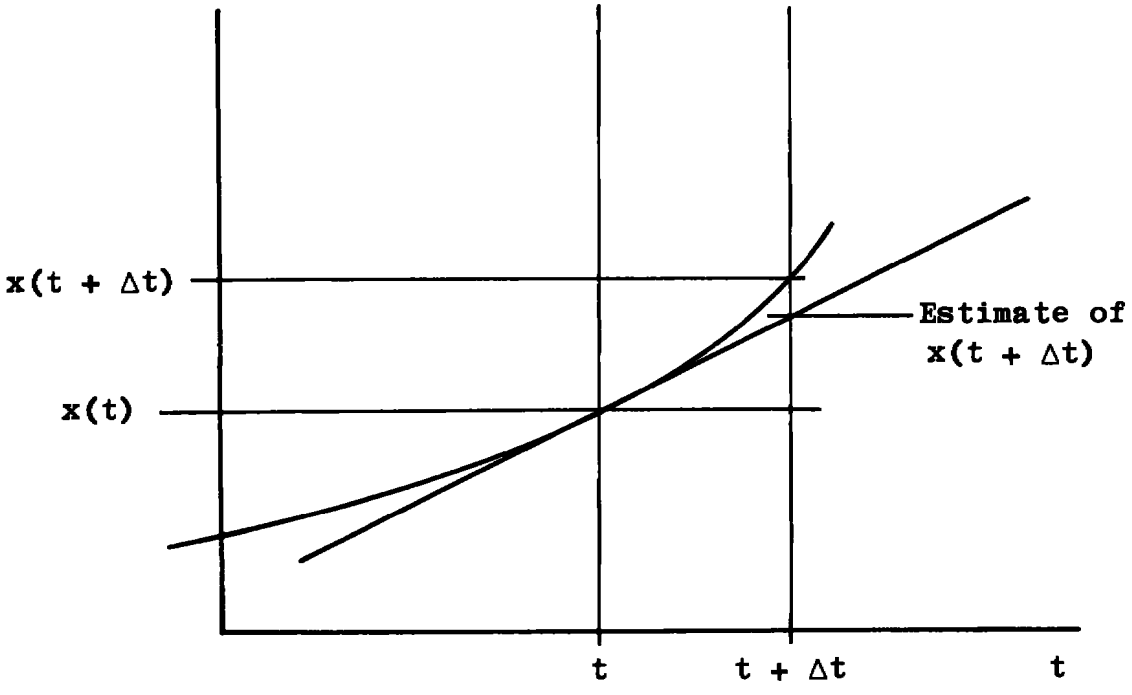

Figure 5. Euler's method for integrating state variable equations.

3.2 LIMITATIONS OF SIMULATION TECHNIQUES

Although digital computer simulation has advantages which have been mentioned, limitations of the technique were also encountered. Some circuits are difficult to handle. When an attempt was made to include the plate resistors (Fig. 2) in the computer model, it was

found that the plate current could not be calculated until plate voltage was known (since plate voltage is a table argument), and plate voltage could not be calculated until plate current was known (because of the presence of the plate resistor). There were two ways out of the difficulty. One was to recalculate the plate current table to, in effect, include the resistor as part of the tube. This approach was deemed too tedious. The other was to iterate to find a plate voltage which resulted in a plate current which resulted in the assumed plate voltage. This course was successfully taken, but extreme measures were necessary to obtain convergence at low plate voltages and high grid voltages.

Another limitation is caused by the relationship between Δt and error. Because the sampling error varies approximately as $(\Delta t)^5$, there is almost a threshold effect. Below a certain step size, accuracy is very good and is limited only by the computational accuracy of the computer (six decimal digits in this case). Above this step size, errors rapidly become intolerable, and the numerical solution may become unstable. The limiting step size is, roughly speaking, a fraction of a period at the highest natural frequency in the system. This means that it is not economical to incorporate all of the known high frequency components into the computer model of the circuit. In particular, the tube grid-plate capacitance and the parasitic suppression network were not included in the computer model. In one computer run, the numerical solution became unstable when the coefficient of coupling between plate choke halves was increased from 0.8 to 0.99. The resulting decrease in the leakage inductance of the choke caused the problem.

The problem can be viewed from another angle. If it is desired to run a solution from an initial condition until steady state is reached, then the solution must be run until t equals several periods at the lowest natural frequency in the system. However, Δt must be no more than a fraction of a period at the highest natural frequency in the system. Therefore, the number of steps which must be computed (as well as the amount of computer time used) is proportional to the ratio of the highest to the lowest natural frequency in the system. Thus, economic considerations must be included in the decision as to how much high frequency detail to include in the circuit model.

It was somewhat of a surprise to realize then when the circuit being simulated misbehaved, the simulator program might offer no more indication to the designer as to the cause of the problem than the actual hardware would. The designer still derives two advantages from the program, however. First, he can experiment with no fear of damaging expensive equipment; second, he can measure virtually

any variable with the program, whereas many measurements are impossible with the hardware.

3.3 DESCRIPTION OF THE COMPUTER PROGRAM

Some brief comments will be made on the computer program which was used. It is written in FORTRAN IV. The program consists of a MAIN routine and seven subroutines. MAIN initializes the program and calls subroutines as necessary. Subroutine INPUT reads from cards component values, initial conditions, and control information such as total run time, Δt, plotter setup information, etc. After each run, another set of cards is read which changes component values or initial conditions, and another run is made. Subroutine DIFFER performs the Runge-Kutta integration. Four times during each step of Δt, it calls subroutine DERIV, which calculates the rates of change of state variables.

Subroutine DERIV is really the heart of the program, as it contains the state variable description of the circuit. One version of subroutine DERIV, shown in Fig. 6, can be compared with the corresponding circuit model in Fig. 7. Most of the features of the circuit can easily be identified among the equations. The only complication occurs in the equations describing the coupled inductors and the choke in the plate supply lead (one of the troublesome cases mentioned earlier). The program assumes eight identical tubes. Some consideration was given to including eight separate tubes in the circuit and investigating the manner in which they divided the load. Unfortunately, no one knew enough about the differences between individual tubes to make such an investigation possible.

Functions IPLATE and IGRID are actually two calls to a single function subroutine which calculates the currents by linear interpolation in two 2-dimensional tables. These tables occupy a large amount of memory, and indications are that the interpolation required consumes over half of the computer time used. However, no attempt was made to simplify the tables at the expense of accuracy. Initially the tables covered only the region of the tube characteristic in the vicinity of the steady-state load line. Invariably, a starting transient would get out of this area in one direction or another, and the tables were extended in several stages, until now they cover the entire published tube characteristic. The plate actually becomes negative for part of the cycle with very light loads. In this region the grid current is calculated analytically by a method derived from Ref. 6. Figures 8 and 9 show the extent of the plate and grid current tables, respectively.

```
FORTRAN IV G LEVEL  21                DERIV                DATE = 75078          12/26/56

0001                SUBROUTINE DERIV
                C
0002                IMPLICIT REAL * 4 (I), INTEGER * 2 (O), REAL * 4 (L, M)
0003                INTEGER * 4 METHOD, METHOX
0004                COMMON A(510), N(280), C(1110)
0005                EQUIVALENCE (A(  1), EC    ), (A( 21), IL    ), (A( 41), ECD   ),
                   *            (A( 61), ILD   ), (A( 81), EL    ), (A(101), IC    ),
                   *            (A(121), LP    ), (A(131), IP    ), (A(141), EG    ),
                   *            (A(151), IG    ), (A(161), E     ), (A(181), I     ),
                   *            (A(201), X     ), (A(231), T     ), (A(241), C     ),
                   *            (A(261), L     ), (A(281), M     ), (A(291), R     ),
                   *            (A(311), V     ), (N(  11), KRASH ), (N(  13), KDERIV)
0006                EQUIVALENCE (N(231), NLIST ), (N(271), METHOD), (N(272), NO    ),
                   *            (N(273), NEW   )
0007                DIMENSION    EC (20), IL (20), ECD(20), ILD(20), EL (20), IC (20),
                   *    EP (10), IP (10), EG (10), IG (10), E  (20), I  (20), X  (30),
                   *    C  (20), L  (20), M  (10), R  (20), V  (10),
                   *    NLIST(40), NLISTX(40)
                C
                C     CALCULATE DERIVATIVES.
                C     CIRCUIT NO 5.
                C
0008                DATA NLISTX / 1, 2, 3, 4, 5, 6, 7, 8, 21, 22, 23, 24, 27,28,26*0/,
                   *     NEQX   / 14 /
0009                DATA METHOX / 0 /, NDX / 40 /
0010                EP(1) = EC(3) + EC(5) + EC(7)
0011                EP(2) = EC(4) + EC(6) + EC(8)
0012                EG(1) = EC(1) + EC(8)
0013                EG(2) = EC(2) + EC(7)
0014                IP(1) = 4. * IPLATE(EP(1), EG(1))
0015                IP(2) = 4. * IPLATE(EP(2), EG(2))
0016                IG(1) = 4. * IGRID (EP(1), EG(1))
0017                IG(2) = 4. * IGRID (EP(2), EG(2))
0018                IF (KRASH .EQ. 1) GO TO 10
                C
0019                IC(1) = IL(1) - IG(1)
0020                IC(2) = IL(2) - IG(2)
0021                IC(3) = IL(3) - IP(1)
0022                IC(4) = IL(4) - IP(2)
0023                IC(5) = IC(3) - IL(7)
0024                IC(6) = IC(4) - IL(8)
0025                IC(7) = IC(2) + IC(5)
0026                IC(8) = IC(1) + IC(6)
                C
0027                I(3) = IL(7) + IL(8)
0028                E(1) = - IL(1) * R(1)
0029                E(2) = - IL(2) * R(2)
0030                IF (E(1) .GT. V(2))  E(1) = V(2)
0031                IF (E(2) .GT. V(2))  E(2) = V(2)
0032                EL(1) = E(1) - EG(1)
0033                EL(2) = E(2) - EG(2)
0034                E(3) = V(1) - EP(1)
0035                E(4) = V(1) - EP(2)
0036                E(5) = EC(5) + EC(7) - IL(7) * R(7) - I(3) * R(3)
0037                E(6) = EC(6) + EC(8) - IL(8) * R(8) - I(3) * R(5)
                C
```

Figure 6. Subroutine DERIV, containing the state variable equations for the circuit shown in Fig. 7.

```
FORTRAN IV G LEVEL  21                DERIV                DATE = 75078        12/28/56

0038              ELD(1) = IC(1) / C(1)
0039              ELD(2) = IC(2) / C(2)
0040              ELD(3) = IC(3) / C(3)
0041              ELD(4) = IC(4) / C(4)
0042              ELD(5) = IC(5) / C(5)
0043              ELD(6) = IC(6) / C(6)
0044              ELD(7) = IC(7) / C(7)
0045              ELD(8) = IC(8) / L(8)
                  C
0046              DENOM1 = L(1) * L(2) - M(1) ** 2
0047              DENOM2 = (L(3) + L(9)) * (L(4) + L(9)) - (M(2) - L(9)) **2
0048              DENOM3 = (L(7) + L(10)) * (L(8) + L(10)) - (M(3) - L(10)) ** 2
0049              ILD(1) = (L(2) * EL(1) + M(1) * EL(2)) / DENOM1
0050              ILD(2) = (L(1) * EL(2) + M(1) * EL(1)) / DENOM1
0051              ILD(3) = ((L(4) + L(9)) * E(3) + (M(2) - L(9)) * E(4)) / DENOM2
0052              ILD(4) = ((L(3) + L(9)) * E(4) + (M(2) - L(9)) * E(3)) / DENOM2
0053              ILD(7) = ((L(8) + L(10)) * E(5) + (M(3) - L(10)) * E(6)) / DENOM3
0054              ILD(8) = ((L(7) + L(10)) * E(6) + (M(3) - L(10)) * E(5)) / DENOM3
                  C
0055              IF (KDERIV .EQ. 0) RETURN
                  C
0056              E(7) = 0.5 * (EP(1) + EP(2))
0057              E(8) = 0.5 * (EG(1) + EG(2))
0058              E(9) = 0.5 * (EC(7) + EC(8))
0059              I(1) = IL(3) + IL(4)
0060              I(2) = IL(1) + IL(2)
0061              I(4) = IP(1) + IP(2)
0062              I(5) = IG(1) + IG(2)
0063              I(6) = IC(3) + IC(4)
0064              ILD(3) = ILD(3) + ILD(4)
0065              ILD(10) = ILD(7) + ILD(8)
0066              EL(9) = ILD(9) * L(9)
0067              EL(10) = ILD(10) * L(10)
0068              EL(3) = E(3) - EL(9)
0069              EL(4) = E(4) - EL(9)
0070              E(10) = EL(10) + I(3) * R(3)
0071              X(1) = EP(1) * IP(1)
0072              X(2) = EP(2) * IP(2)
0073              X(3) = EG(1) * IG(1)
0074              X(4) = EG(2) * IG(2)
0075              X(5) = IL(7) ** 2 * R(7) + IL(8) ** 2 * R(8)
0076              X(6) = IP(1) + IG(1)
0077              X(7) = IP(2) + IG(2)
0078              X(8) = I(1) * V(1)
0079              X(30) = 0.5 * (IL(7) - IL(8))
0080              RETURN
                  C
0081           10 WRITE (6, 501) EP(1), EG(1), EP(2), EG(2)
0082          501 FORMAT (/' OUT OF RANGE OF TUBE TABLES.  EP1 = ', F9.1, ' ,    EG1
                  * = ', F8.1, ' ,          EP2 = ', F9.1, ' ,    EG2 = ', F8.1)
0083              RETURN
                  C
                  C     INITIALIZE NLIST
0084              ENTRY LIST
0085              NEQ = NEQX
0086              METHOD = METHOX
```

Figure 6. Concluded.

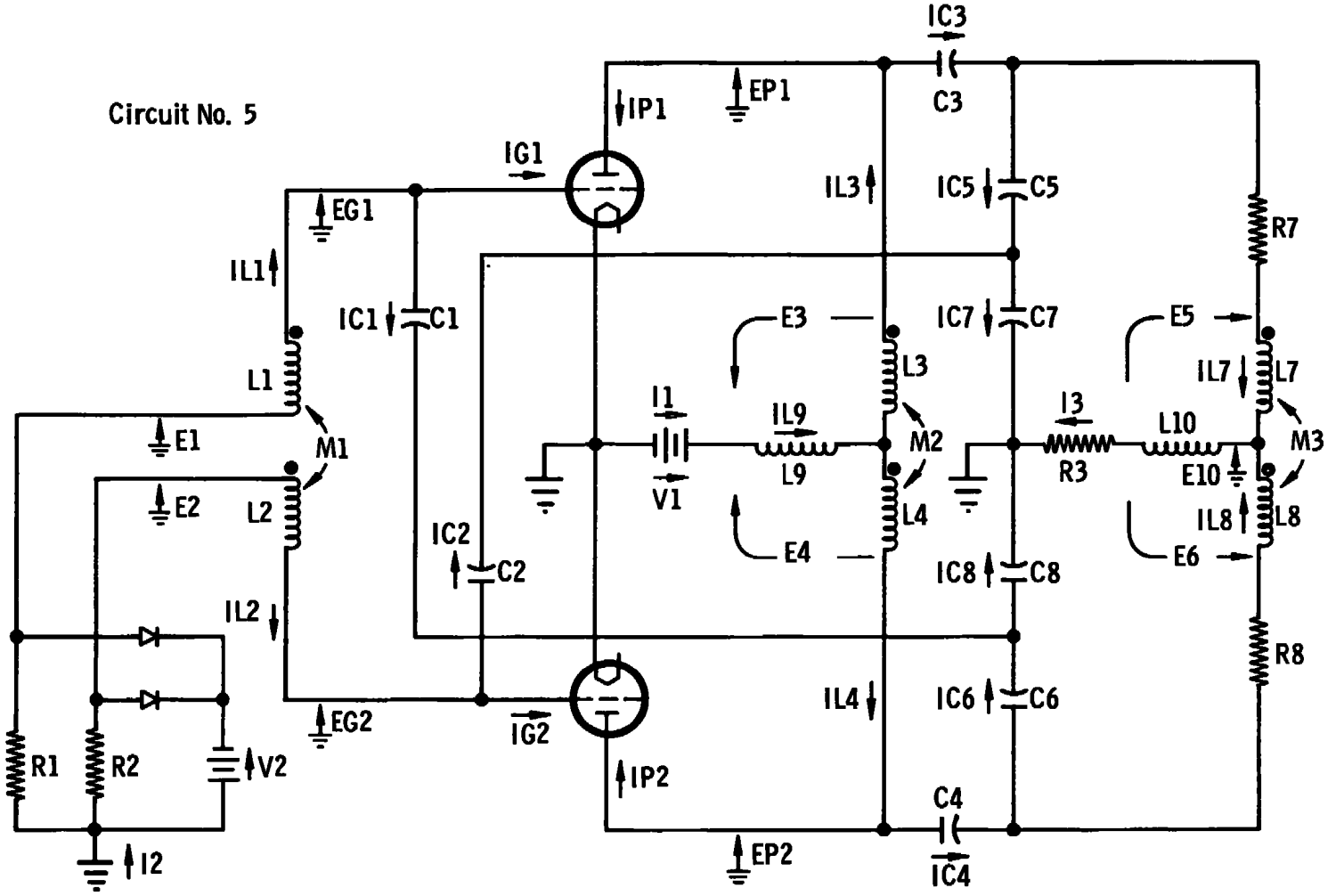

Figure 7. Computer model of the oscillator circuit.

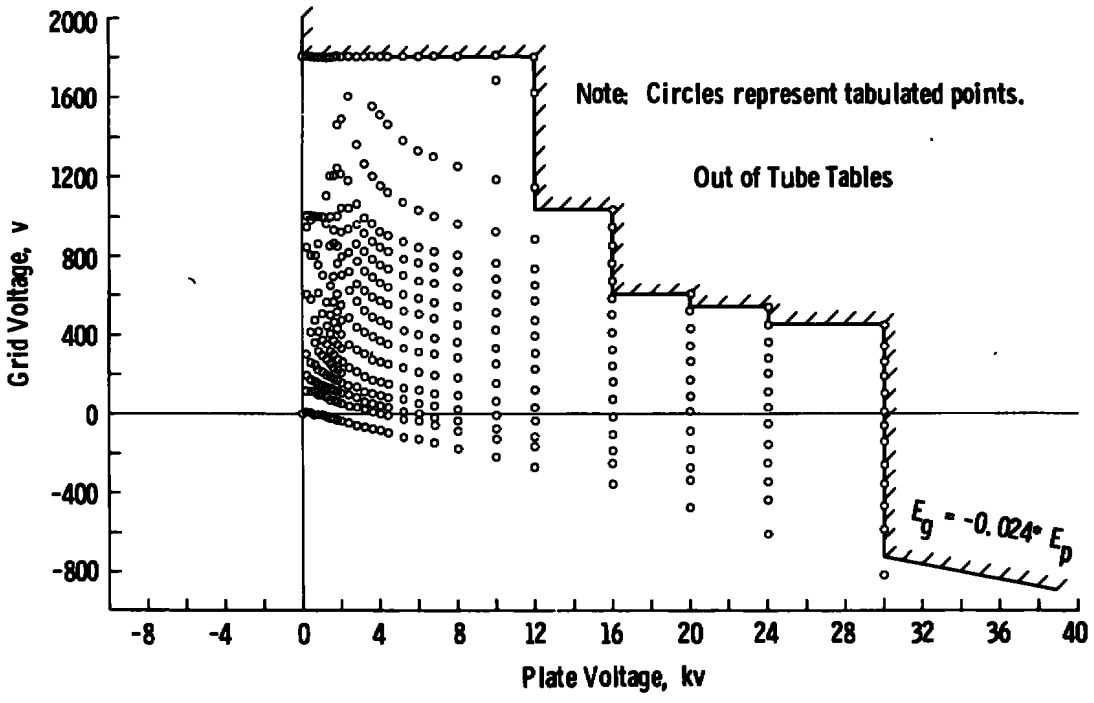

Figure 8. Extent of plate current table.

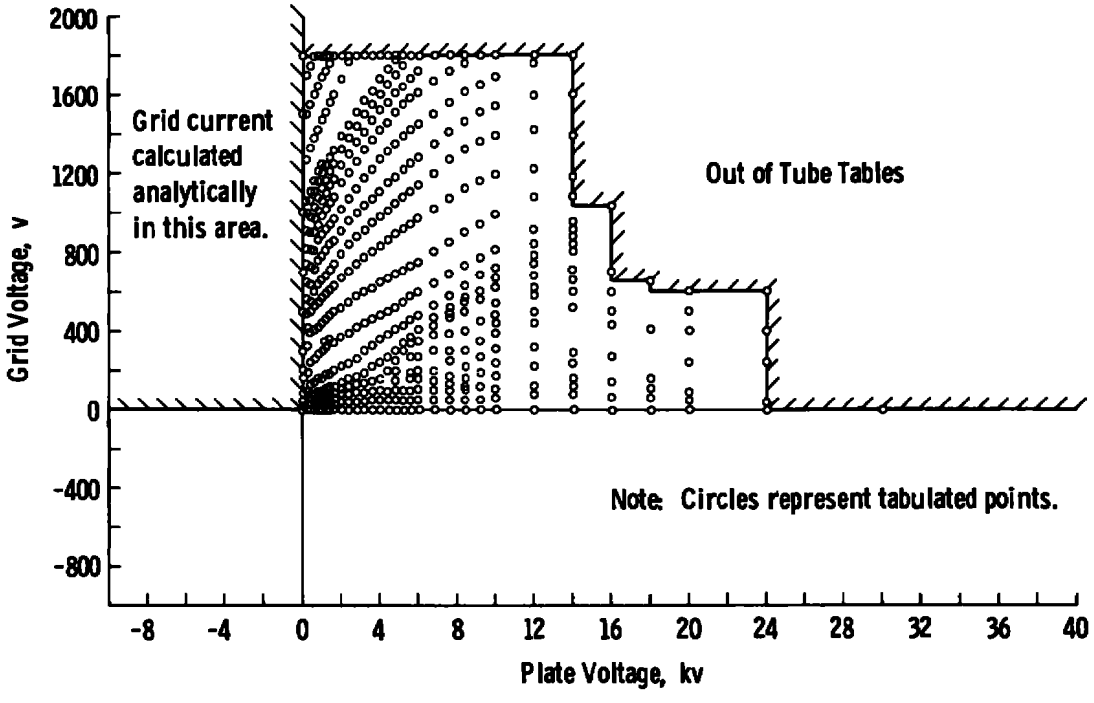

Figure 9. Extent of grid current table.

Subroutine PRINT prints the time history of any desired variables. A sample output is shown in Fig. 10. Subroutine PLOT stores values of any desired variables during the calculation and then plots them against time or each other. Several examples will be discussed later. Subroutine AVERAG is inactive until time TAVE, which is read from an input card. Presumably, by this time the circuit is in a steady-state condition. It looks for a zero crossing of the tank current. It then averages any desired variable for exactly one cycle of output. It can calculate average value, rms value (with or without d-c component), or mean squared value. After a second zero crossing in the same direction is found, the run is terminated and the averages are printed. This subroutine is used to calculate power output, plate dissipation, supply current, electrode current, etc. Figure 11 shows an example.

```
RUN NO 12.  CKT NO 5.  STAFT, AS BUILT, EB = 20,000.  WITHOUT COIL MUTUAL IND.
27 SEPTEMBER, 1974.

SET       N(  8)  NOPLOT                             0
PLOT          0        0       0    0.     100.          0.       5.
PLOT         12        1      16    0.     100.E-06      0.    5000.
PLOT         12        2      10    0.     100.E-06      0.    5000.
PLOT         12        3      10    0.     100.E-06      0.    5000.
PLOT          0        0       0    0.     100.        -2.4      .4
PLOT         12        4      16    0.     100.E-06-2400.       400.
PLOT         12        5      10    0.     100.E-06-2400.       400.
PLOT         12        6      10    0.     100.E-06-2400.       400.
PLOT          0        0       0    0.     100.          0.     100.
PLOT         12        7      16    0.     100.E-06      0.     100.
PLOT         12        8      10    0.     100.E-06      0.     100.
PLOT         12        9      10    0.     100.E-06      0.     100.
PLOT          0        0       0    0.     100.          0.      20.
PLOT         12       10      16    0.     100.E-06      0.      20.
PLOT         12       11      10    0.     100.E-06      0.      20.
PLOT          0        0       0    0.       2.        -2.4      .4
PLOT          1        4      16    0.    2000.     -2400.      400.
PLOT          2        5      10    0.    2000.     -2400.      400.
PLOT          0        0       0    0.     100.          0.     100.
PLOT         12       13      16    0.     100.E-06      0.     100.
PLOT         12       14      10    0.     100.E-06      0.     100.
SET       A(311)  V1                           20000.
SET       A(312)  V2                            -180.
SET       A(  1)  EC1                           -180.
SET       A(  2)  EC2                           -180.
SET       A(  3)  EC3                          20000.
SET       A(  4)  EC4                          20000.
SET       A(  5)  EC5                              5.
SET       A(  6)  EC6                             -5.
SET       A(  7)  EC7                              0.
SET       A(  8)  EC8                              0.
SET       A( 21)  IL1                              0.
SET       A( 22)  IL2                              0.
SET       A( 23)  IL3                             80.
SET       A( 24)  IL4                             80.
SET       A( 27)  IL7                              0.
SET       A( 28)  IL8                              0.
SET       A(232)  TDELTA                           0.5     E-06
SET       A(233)  TAVE                          1250.      E-06
SET       A(234)  TMAX                          1500.      E-06
SET       N(  1)  NPRINT                           5
SET       N(  2)  NPLOT                            3
GO
```

a. Printout of input cards

Figure 10. Sample printout produced by subroutine PRINT.

TIME MICROSEC	EP1 VOLTS	EG1 VOLTS	IP1 AMPERES	IG1 AMPERES	E1 VOLTS	IL3 AMPERES	IB AMPERES	ECT VOLTS	ECMP VOLTS	ECMG VOLTS	ICT AMPERES	ILT AMPERES
	EP2 VOLTS	EG2 VOLTS	IP2 AMPERES	IG2 AMPERES	E2 VOLTS	IL4 AMPERES	IC AMPERES					
1259.766	31680.602	-1840.015	0.0	0.0	-734.371	111.443	209.402	0.0	21359.887	-786.177	58.139	-1382.093
	11039.176	267.660	355.048	-3.067	-838.338	97.959	21.325					
1262.266	34913.648	-2257.518	0.0	0.0	-786.266	69.284	129.666	0.0	20704.313	-837.736	134.042	-800.241
	6494.977	582.045	570.999	32.035	-849.554	60.382	22.181					
1264.765	36187.063	-2537.498	0.0	0.0	-894.235	58.246	113.328	0.0	19744.063	-931.589	142.577	-113.457
	3301.067	674.319	527.627	95.684	-908.669	55.082	24.446					
BEGIN LAST CYCLE. TIME = 1265.163 MICROSECONDS.												
1267.264	35541.590	-2584.559	0.0	0.0	-1004.763	78.628	160.260	0.0	19051.711	-1008.760	87.385	591.580
	2561.837	567.040	380.818	81.117	-968.678	81.632	26.759					
1269.764	33229.793	-2399.241	0.0	0.0	-1073.652	117.477	243.753	0.0	18751.610	-1039.207	-3.336	1223.798
	4274.027	320.827	291.746	14.239	-991.803	126.276	28.006					
1272.263	29626.465	-1991.677	0.0	0.0	-1083.073	158.699	330.900	0.0	18998.688	-1011.934	-94.114	1705.259
	8370.914	-32.192	51.560	0.0	-965.510	172.201	27.777					
1274.763	25176.480	-1414.442	0.0	0.0	-1033.538	180.968	378.438	0.0	19747.270	-940.873	-141.183	1973.321
	14318.059	-467.303	0.0	0.0	-894.904	197.470	26.148					
1277.262	20362.445	-789.543	0.0	0.0	-959.568	174.582	366.635	0.0	20566.203	-864.148	-126.182	1999.661
	20769.961	-938.753	0.0	0.0	-816.868	192.053	24.087					
1279.762	15662.004	-202.179	34.605	0.0	-884.004	140.946	298.274	0.0	21246.578	-800.278	-54.398	1789.800
	26831.152	-1398.376	0.0	0.0	-754.216	157.328	22.213					
1282.261	10962.055	274.145	360.430	-3.348	-837.175	91.921	197.249	0.0	21347.738	-786.466	47.447	1372.777
	31733.422	-1847.078	0.0	0.0	-735.542	105.328	21.325					
1284.760	6432.094	585.312	572.571	33.218	-849.084	55.000	118.805	0.0	20682.754	-838.713	122.621	788.910
	34933.418	-2262.737	0.0	0.0	-788.269	63.804	22.201					
1287.260	3272.971	674.110	525.632	96.061	-908.412	50.520	104.096	0.0	19723.211	-932.495	130.729	101.432
	36173.453	-2539.099	0.0	0.0	-896.491	53.576	24.473					
1289.760	2575.667	564.308	380.192	80.154	-967.798	77.721	152.334	0.0	19037.051	-1008.815	74.878	-602.761
	35498.438	-2581.947	0.0	0.0	-1006.324	74.613	26.768					
1292.259	4324.492	316.512	289.919	13.410	-990.012	122.784	236.683	0.0	18743.687	-1038.206	-15.432	-1232.795
	33163.285	-2392.924	0.0	0.0	-1074.137	113.899	27.988					
1294.758	8457.668	-37.798	48.950	0.0	-962.716	168.809	324.056	0.0	19000.785	-1009.808	-104.980	-1710.975
	29543.902	-1981.819	0.0	0.0	-1082.314	155.247	27.729					
1297.258	14420.133	-473.559	0.0	0.0	-891.544	193.895	371.262	0.0	19752.918	-938.264	-150.127	-1975.067
	25085.707	-1402.969	0.0	0.0	-1031.918	177.368	26.081					
1299.757	20870.133	-944.884	0.0	0.0	-813.487	188.262	359.062	0.0	20570.734	-861.486	-133.052	-1997.368
	20271.336	-778.089	0.0	0.0	-957.621	170.801	24.015					
1302.257	26915.207	-1403.821	0.0	0.0	-751.176	153.433	290.528	0.0	21245.566	-797.969	-59.364	-1783.876
	15575.926	-192.118	37.309	0.0	-882.116	137.094	22.146					
1304.756	31790.141	-1852.609	0.0	0.0	-733.661	101.752	190.171	0.0	21330.223	-785.429	43.582	-1363.843
	10870.305	281.751	366.716	-3.674	-836.201	88.419	21.286					
1307.255	34956.539	-2266.962	0.0	0.0	-787.621	61.108	113.509	0.0	20653.402	-838.764	118.802	-777.803
	6350.270	589.434	574.523	34.736	-849.157	52.401	22.194					
1309.755	36162.129	-2539.927	0.0	0.0	-896.502	51.997	101.049	0.0	19693.813	-932.822	126.572	-89.445
	3225.498	674.282	522.684	96.823	-909.058	49.052	24.482					
END LAST CYCLE. TIME = 1310.069 MICROSECONDS. FREQUENCY = 22268.828 HERTZ.												

b. Printout of program output
Figure 10. Concluded.

```
AVERAGE VALUES COMPUTED OVER LAST CYCLE.

PLATE INPUT POWER     =   4829.348  KILOWATTS
OUTPUT POWER TO LOAD  =   3521.330  KILOWATTS
PLATE SUPPLY CURRENT  =    241.467  AMPERES
BIAS  SUPPLY CURRENT  =     24.764  AMPERES
TANK CURRENT (RMS)    =   1429.858  AMPERES
PLATE 1 DISSIPATION   =    177.329  KILOWATTS*
PLATE 2 DISSIPATION   =    177.000  KILOWATTS*
PLATE 1 CURRENT       =     31.042  AMPERES  *
PLATE 2 CURRENT       =     31.019  AMPERES  *
GRID  1 CURRENT       =      3.068  AMPERES  *
GRID  2 CURRENT       =      3.076  AMPERES  *
PLATE 1 CURRENT(RMS)  =     58.007  AMPERES  *
PLATE 2 CURRENT(RMS)  =     57.991  AMPERES  *
GRID  1 CURRENT(RMS)  =      7.748  AMPERES  *
GRID  2 CURRENT(RMS)  =      7.760  AMPERES  *
CATH  1 CURRENT(RMS)  =     64.328  AMPERES  *
CATH  2 CURRENT(RMS)  =     64.327  AMPERES  *
C1 CURRENT (RMS)      =     28.399  AMPERES
C3 CURRENT (RMS)      =    227.278  AMPERES
C5 CURRENT (RMS)      =   1475.029  AMPERES
C7 CURRENT (RMS)      =   1477.291  AMPERES
L1 CURRENT            =     12.377  AMPERES
L3 CURRENT            =    120.732  AMPERES
COIL CT CURRENT(RMS)  =    101.018  AMPERES

                                    * VALUES ARE PER TUBE
```

Figure 11. Sample printout produced by subroutine AVERAG.

3.4 RESULTS OF SIMULATION

The computer simulation of the oscillator was initially undertaken in order to answer the following questions:

1. Will dangerous conditions exist during the initial starting transient as oscillations build up?
2. Have the values of shunt feed components been properly chosen (that is, do they adversely influence waveforms)?
3. What tank Q is necessary to achieve adequate stability and purity of waveforms?
4. Will grid dissipation become excessive if the oscillator is lightly loaded (that is, if the plasma is suddenly extinguished)?
5. How much power output will be lost due to the presence of the plate resistors?

A sixth question was originally considered: will the use of shunt feed in both grid and plate result in low frequency parasitic oscillations? On reflection, it was decided that this question could not be answered by the simulation program, since the grid-plate capacitance was not included in the circuit model. These oscillations did not in fact materialize, perhaps because of the damping effect of the bias resistors in the grid circuit.

The earliest circuit model used did not include a center tap on the tank circuit (R3 and L10 in Fig. 7), and the resulting behavior of the oscillator was completely unexpected. Figure 12 shows the plate voltage waveforms which were obtained. There is evidently a blocking oscillation superimposed on the normal oscillation. At first it was suspected that the trouble was caused by a resonance between the shunt feed components. However, a number of runs were made in which the grid and plate choke inductances were varied over a wide range, with little change in the behavior of the circuit. The oscillation was evidently of a relaxation type, rather than a resonant type. It was then theorized that changes in common mode plate voltage were forcing current through the plate coupling capacitors, the tank capacitors, and the grid coupling capacitors, and were causing changes

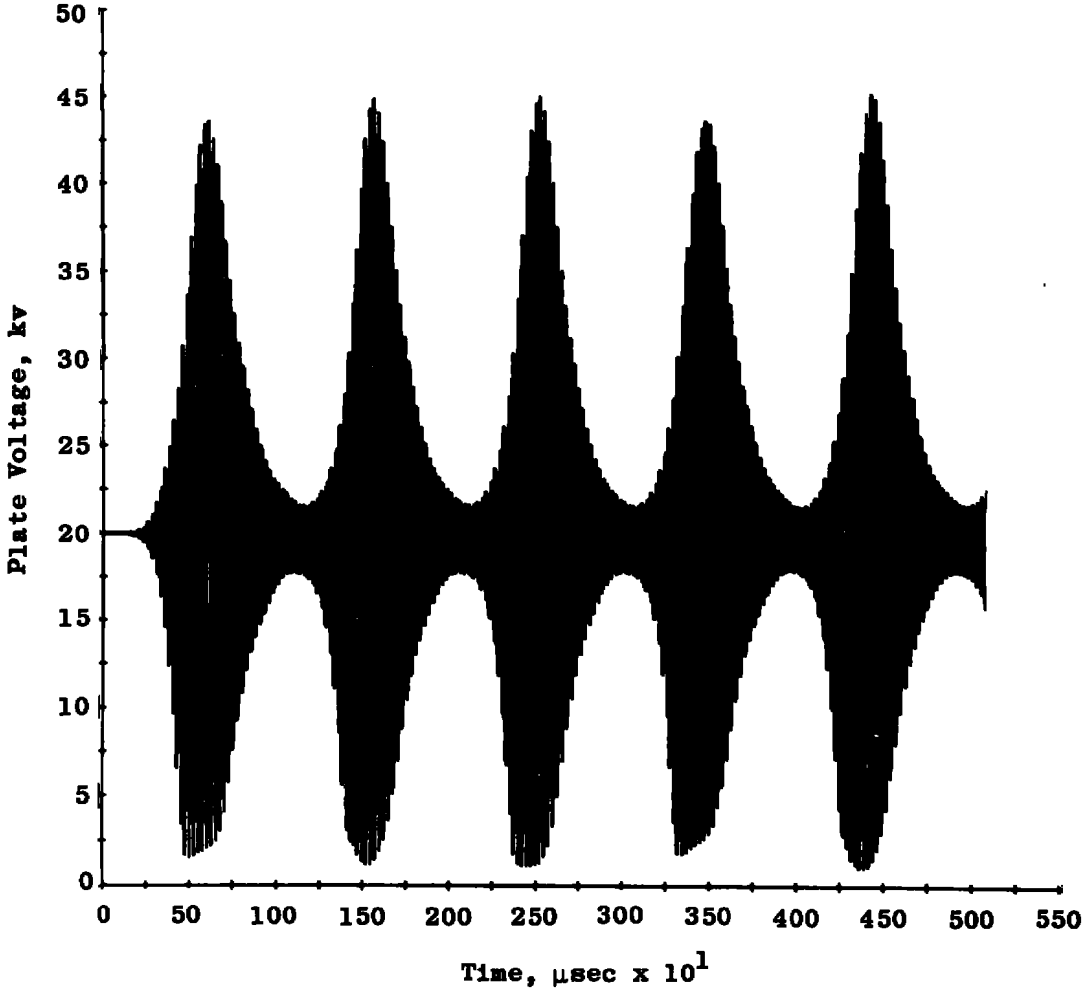

Figure 12. Plate voltage waveform showing the blocking oscillation.

in the bias voltage. This proved to be correct. The circuit was modified by grounding the center tap on the tank coil, so that low frequency current forced through the plate coupling capacitors could flow to ground, rather than being forced to flow through the tank capacitors. The resulting waveforms are shown in Fig. 13.

The poorly damped envelope was found to be caused by a resonance between the leakage reactance of the plate choke and the plate coupling capacitors. It was adequately damped by placing a small resistance (R3 in Fig. 7) in series with the ground connection (Fig. 14). L10 was placed in series with R3 to prevent R3 from dissipating an inconveniently large amount of power because of the second harmonic voltage on the coil center tap (and, practically, due to the fundamental voltage on the center tap if it is not perfectly centered). (L10 has been incorporated into the oscillator, but R3 has not, as yet. The nature of the startup transient is not especially important at the present time, as long as it is not violent.)

These computer runs also answered Question 1. Even with the most unstable circuit, the peak instantaneous plate voltage never exceeded 45 kv. In the unstable condition, the load line repeatedly entered the high grid dissipation region (low plate voltage, high grid voltage), but it stayed there only a small fraction of the time, and there appeared to be no danger of overheating the grid. With the stable circuit, plate supply current reached a peak of more than twice the rated value, and grid current went through a similar peak. However, the entire starting transient is over in less than 1 msec, and the tubes can easily withstand this minor overload.

In practice, the oscillator is not subjected to even this much of a transient. It is always energized at a low plate voltage, and then plate voltage is increased in steps until the desired conditions are reached.

With the instability disposed of, it became possible to investigate the other questions originally posed. The effect of coupling capacitors on waveform (Question 2) was determined by making four complete runs, as shown below.

	Grid Coupling Cap	Plate Coupling Cap
Circuit No. 3, Run 14	Infinite*	Infinite*
Circuit No. 3, Run 16	10 μF	Infinite*
Circuit No. 3, Run 17	Infinite*	5 μF
Circuit No. 3, Run 18	10 μF	5 μF

*Infinite = 10×10^6 F

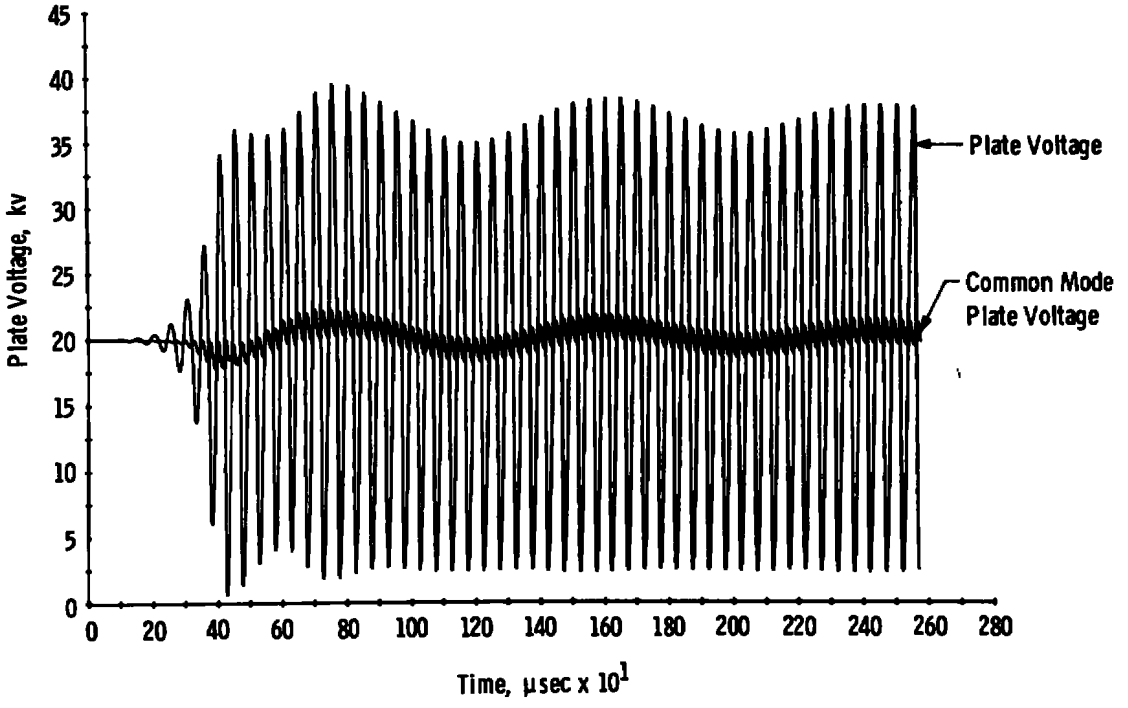

Figure 13. Plate voltage waveform obtained with the center tap of the load grounded.

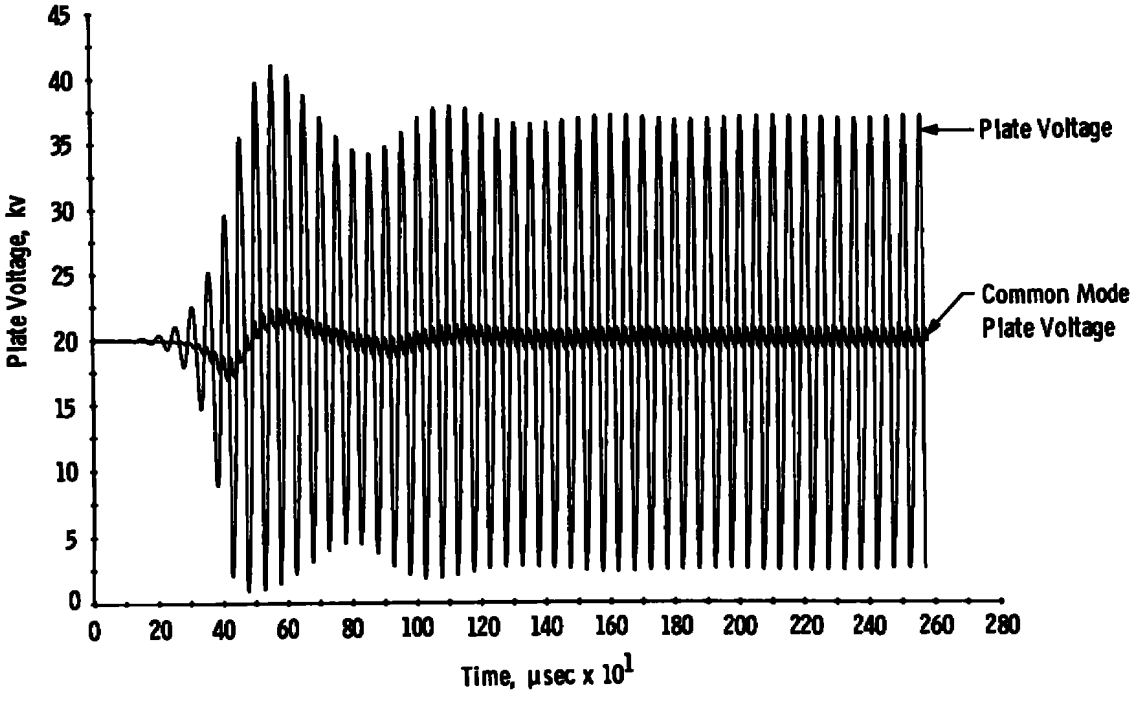

Figure 14. Plate voltage waveform obtained with the center tap of the load grounded through a resistor.

The circuit was operated at a frequency of 10 kHz, with a tank Q of 10, and initial conditions were chosen as close as possible to steady state. The plate voltage waveforms were nearly indistinguishable in the four cases, and a typical waveform is shown in Fig. 15. A slight relaxation to the true steady-state conditions is evident at the beginning of the run. The clearest picture of the effect of the coupling capacitors was obtained by plotting grid voltage versus plate voltage (that is, by plotting the load line). Figures 16a and b show the load lines which were obtained with infinite and design value coupling capacitors, respectively. Load lines obtained for the other two runs, with only one coupling capacitor infinite, were about intermediate between the two shown. The classical design technique requires that the load line be assumed to be a straight line. However, it can be seen that the load line has actually opened into a figure eight.

There are two effects operating. First, the coupling capacitors cause some phase shift at the fundamental frequency. This by itself would cause the load line to become an ellipse, but it would not explain the figure eight. The second effect is that of finite grid driving impedance. The grid current drawn by the tube must flow

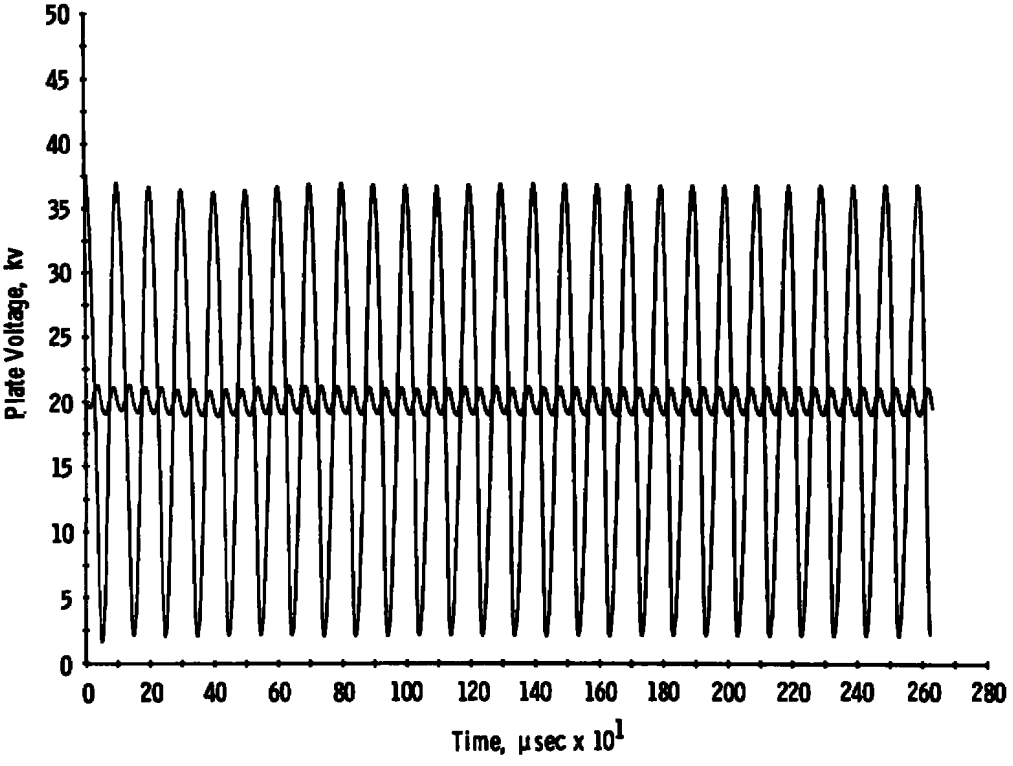

Figure 15. Steady-state plate voltage waveform obtained with the coupling capacitors set at their design values.

through the grid coupling capacitor and the feedback capacitor. Thus, when grid current begins to flow, the grid voltage becomes more negative by the voltage drop in this source impedance. The voltage on the other grid becomes more negative at the same time because of the coupling through the tank circuit. The grid voltage then contains a second harmonic component which is not present in the plate voltage, and the load line becomes a figure eight.

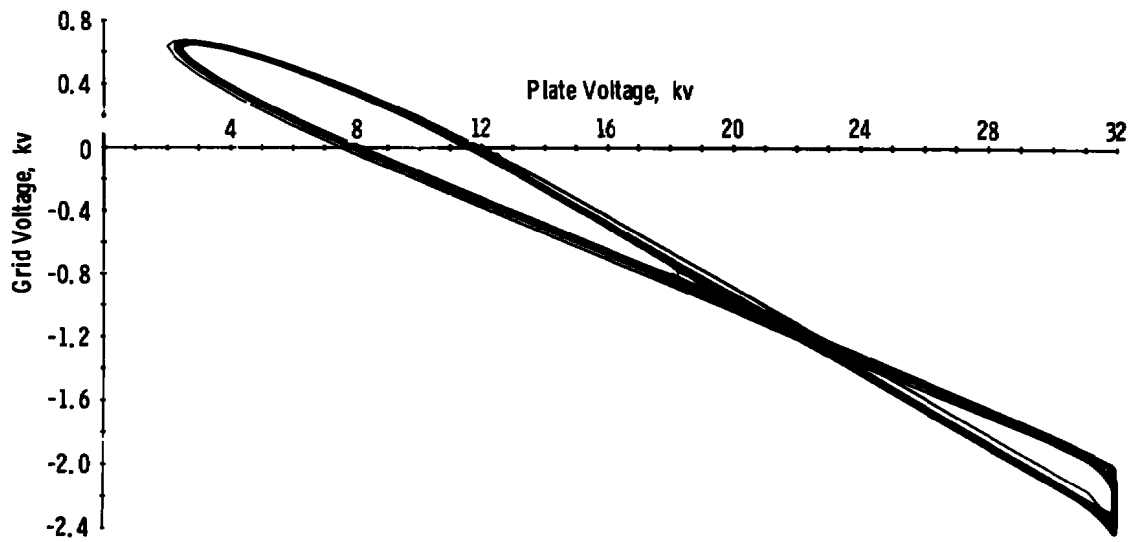

a. Obtained with Q = 10 and infinite coupling capacitors

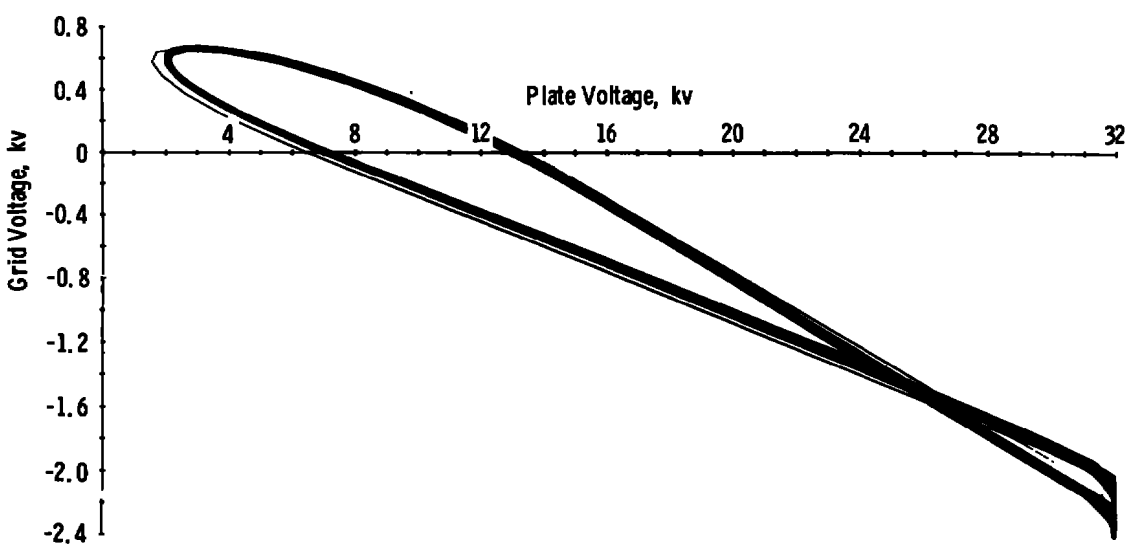

b. Obtained with Q = 10 and design value coupling capacitors

Figure 16. Load line.

The effect of the grid circuit driving impedance in distorting the grid voltage is also clearly evident in the plate current waveform. The plate voltage is nearly sinusoidal, while the grid voltage contains a second harmonic component. This causes the plate current waveform to be skewed, as in Fig. 17.

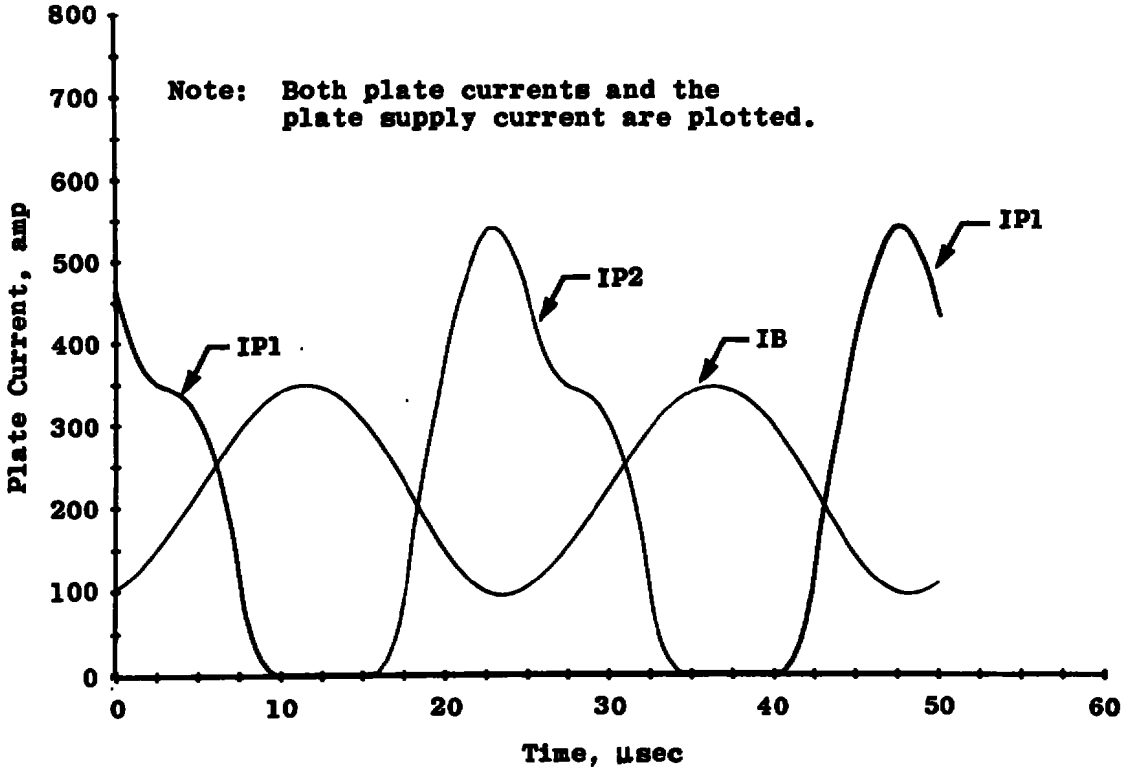

Figure 17. Skewing of the plate current waveform caused by grid circuit driving impedance.

As a final test of the hypothesis that the distortion of the load line was caused by grid circuit driving impedance, a run was made with infinite coupling capacitors and a tank Q of 100. Since the feedback capacitor is proportional to tank Q [Eqs. (9), (22), and (23)], increasing the tank Q decreases the grid driving impedance attributable to this component. The resulting load line (Fig. 18) shows nearly no distortion.

It was decided (rather arbitrarily) that the degree of distortion shown in Figs. 16b and 17 was acceptable. These waveforms were made at 10 kHz. At higher frequencies, the coupling capacitors would have even less influence, and the distortion would approach that shown in Fig. 16a. Thus, the values of the coupling capacitors chosen

in Section 2.0 are acceptable. A design Q of 10 was also deemed acceptable (Question 3). Lower Q was ruled out by increased distortion and by the fact that such a tight coupling to the load might be difficult to obtain. Computer runs made at a lower Q showed no difficulty in starting, even at a Q of 5.

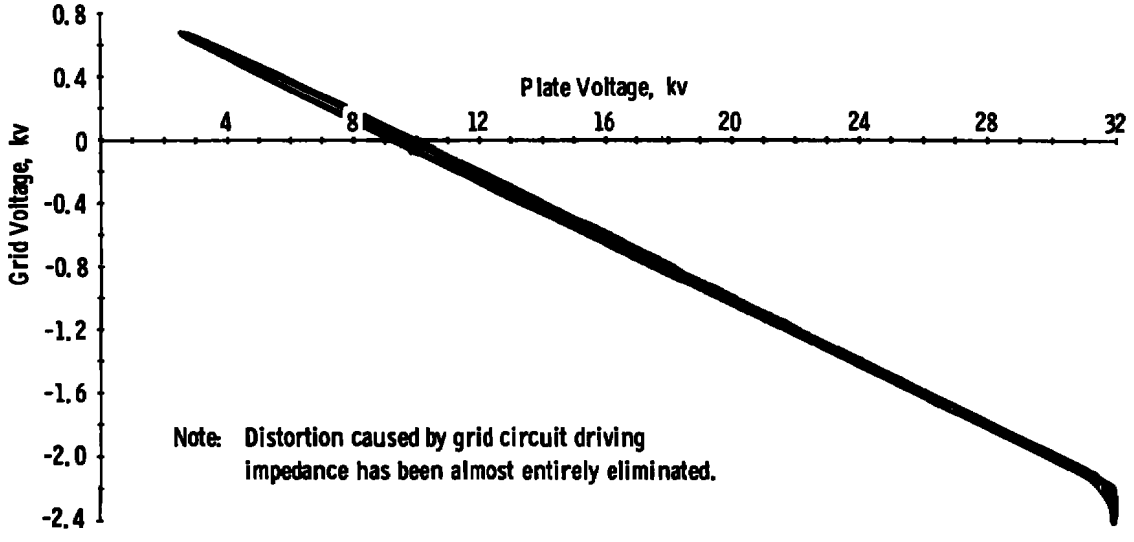

Figure 18. Load line obtained with infinite coupling capacitors and a tank Q of 100.

To investigate the effect of light loading (Question 4), a run was made at full load conditions and was allowed to proceed until steady state was reached. The tank Q was then increased to 200 (a rough estimate of the unloaded Q of the tank), and a second run was made, using as initial conditions the final conditions from the previous run. It was found that only a mild transient occurred and that the oscillator settled down quickly into an unloaded steady-state condition. In this condition the rf plate voltage is increased, so that the plate actually becomes negative for a small portion of the cycle (Fig. 19). Peak plate voltage never exceeded 43 kv, even during the transient. The peak positive grid voltage is decreased from 680 v loaded to about 400 v unloaded. The steady-state grid current increased from 3.4 amp loaded to about 5.4 amp unloaded, which is not dangerously large. The small increase is undoubtedly attributable to the use of grid resistor bias, which inherently protects the tubes from excessive grid current.

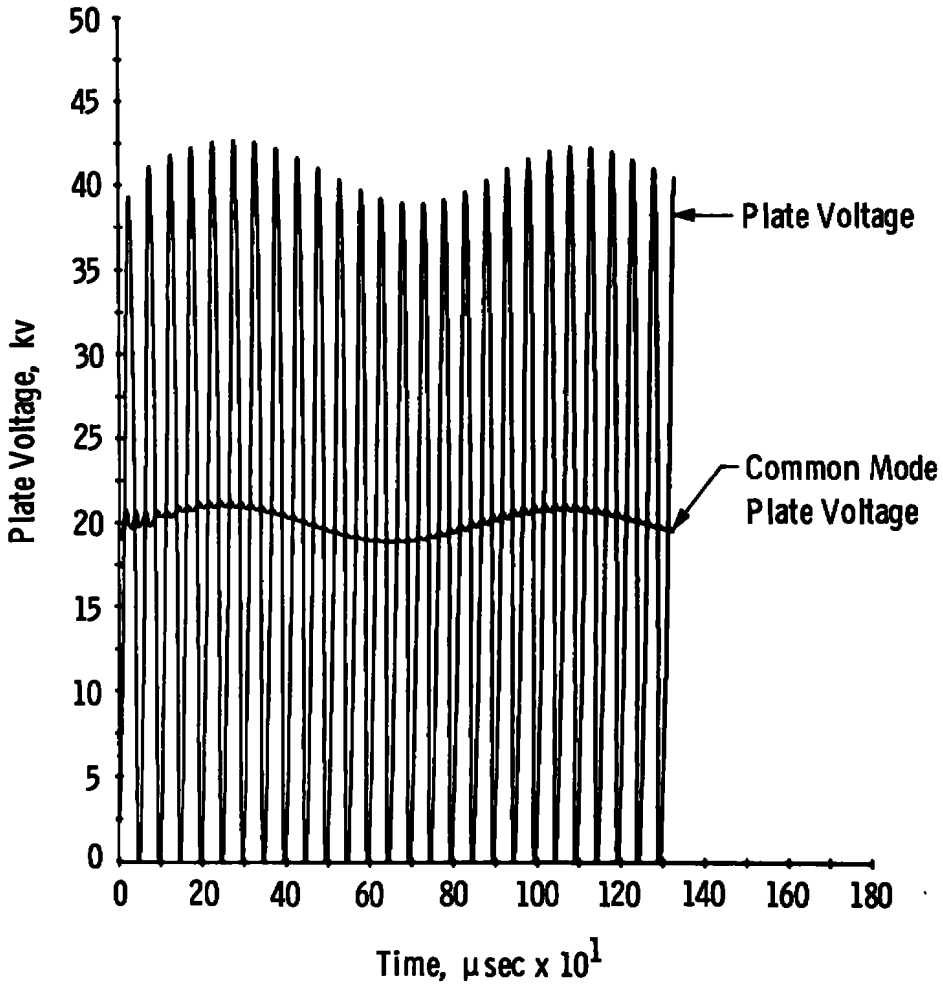

Figure 19. Plate voltage waveform obtained with very light load.

The last question (Question 5) was answered by incorporating the plate resistors into the circuit. This necessitated the use of the iterative technique mentioned in Section 3.2. Because of the uncertainty of convergence and the extra computer time used, only a few runs were made with this circuit. It was found that the general behavior of the circuit was not altered by the resistors. In particular, the rms plate current of the tubes did not change significantly, so that the power output lost in the resistors could be calculated by I^2R, where I is the rms plate current predicted by the computer program for the circuit model without the resistors. This amounts to about 13.6 kw per tube under design conditions, or a power loss of 3.1 percent.

4.0 TANK AND FEEDBACK CAPACITOR CONFIGURATION

One of the most difficult and expensive components of the oscillator to obtain was the tank capacitor. The difficulty is caused primarily by the wide frequency range which must be covered: five to one. For comparison, the standard broadcast band covers a range of less than three to one. The expense is caused by the fact that the capacitors must handle 10 vars (Q = 10) for each watt of output from the oscillator.

4.1 TANK CAPACITOR RATINGS

Early discussions with manufacturers showed that the use of any form of variable capacitor was completely out of the question, because of the large capacitance required. The tank capacitor would therefore have to consist of a bank of many capacitors which could be connected in various series-parallel configurations, in order to achieve a range of total capacitances. It was also learned that the price of such a capacitor depended primarily upon its var-handling capability and was influenced very little by its voltage rating or capacitance. The most suitable capacitor for the application was found to be a water-cooled unit with a capacitance of 0.425 μF, a voltage rating of 6 kv rms, a current rating of 400 amp rms, and a var rating of 1200 kvar. It is packaged in a metal can 6.25 by 13.5 by 23 in.

As the tank capacitor is required to handle 35.2 Mvar under design conditions, the bank would have to consist of at least 30 capacitors. Some spare capability is desirable to handle the rise in rf plate voltage which accompanies unloaded operation and other off-design conditions. The most desirable configurations are those which load all capacitors in the bank equally. The entire var capability of the bank is then available. Unfortunately, in order to achieve a sufficient number of capacitance values within the required range, less desirable configurations had to be used. As result, the bank finally selected contained 42 capacitors.

The task of selecting tank capacitor configurations was handled largely by trial and error. A proposed configuration was analyzed to determine its power handling capability as a function of frequency and tank Q. If it fell in the desired range, it was included in the catalog of useful configurations. The methods by which the power-handling capability of a configuration can be determined are discussed next.

4.2 RATINGS OF A CAPACITOR BANK

It is found that the power lost in the dielectric of a capacitor as a result of dielectric heating is a fixed fraction of the reactive power (var) being handled by the capacitor over a wide range of frequency. It is the necessity of removing this heat which limits the var rating of the capacitor. In addition, the capacitor has a voltage rating determined by the breakdown strength of the dielectric used, and a current rating determined by the current-carrying capability of the foil and other conductors.

The rms current through a capacitor is given by

$$I = \omega CE \tag{11}$$

and the var loading of the capacitor is given by

$$V = I \cdot E = \omega CE^2 \tag{12}$$

where E is the rms voltage across the capacitor. Figure 20 shows the maximum voltage which can be applied at any frequency to the particular tank capacitor selected for the oscillator, without exceeding any of its ratings. (For smaller capacitors, the var limit is not effective; rated voltage at rated current will not overheat the capacitor.) The two break frequencies can easily be calculated, as follows:

$$\omega_\ell = \frac{V_r}{C E_r^2} \tag{13}$$

$$\omega_h = \frac{I_r^2}{C V_r} \tag{14}$$

In the case of the capacitor chosen, ω_ℓ is 78,431 rad/sec (12,483 Hz), and ω_h is 313,725 rad/sec (49,931 Hz).

In order to determine the voltage, current, and var ratings of a bank of capacitors, an rms voltage, E_b, is applied at some frequency across the bank. The rms current into the bank is denoted by I_b, and the total capacitance of the bank is designated by C_b. By elementary circuit analysis each capacitor in the bank is examined and the one (or ones) carrying the highest voltage is found. Since every capacitor in the bank has the same capacitance, this will also be the capacitor carrying the highest current (by Eq. 11). The ratios of the voltage

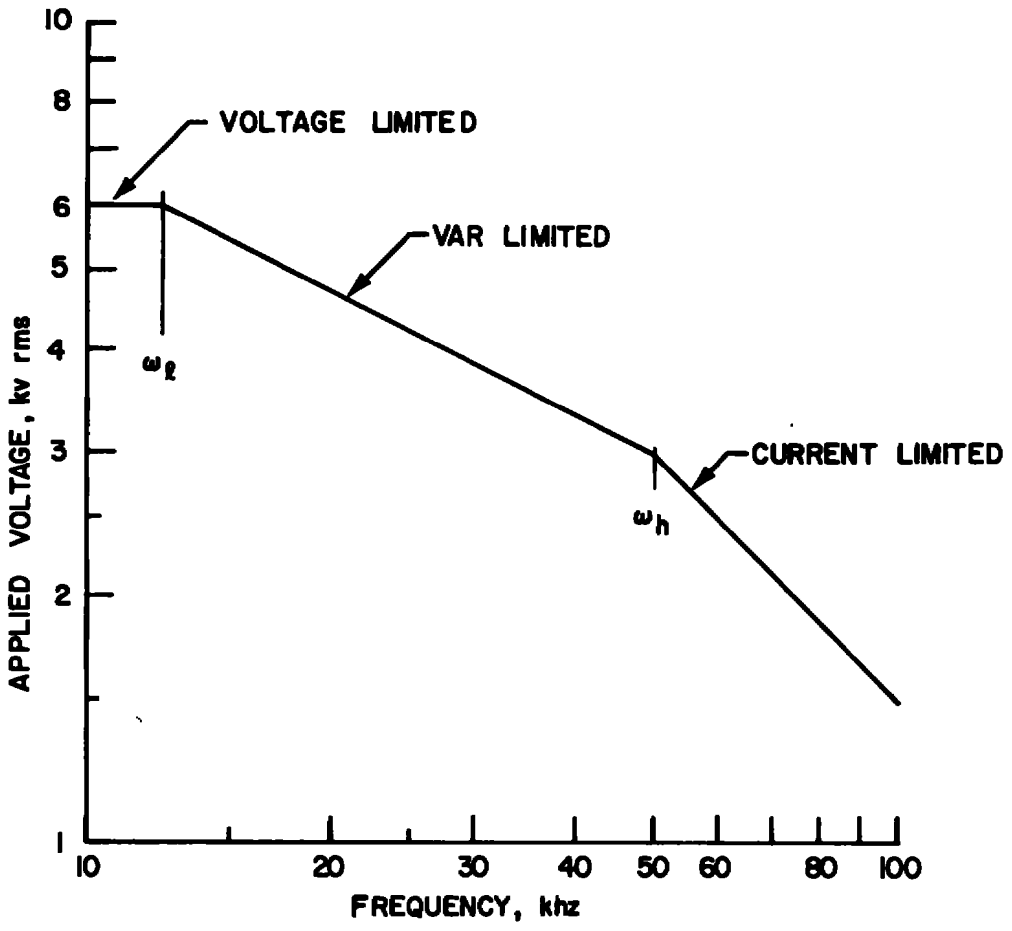

Figure 20. Maximum rms voltage which may be applied to a tank capacitor at any frequency without exceeding its voltage, current, or var ratings.

and current in the limiting capacitor to the voltage and current in the entire bank are then denoted by ℓ and m:

$$E = \ell E_b \tag{15}$$

$$I = m I_b \tag{16}$$

Substituting Eqs. (15) and (16) in Eq. (11),

$$m I_b = \omega C \ell E_b$$

$$I_b = \omega\left(\frac{\ell}{m} C\right) E_b \tag{17}$$

or, applying Eq. (11) to the entire bank,

$$C_b = \frac{\ell}{m} C \tag{18}$$

The bank is then considered to be at its rated voltage, current, or var limit when the limiting capacitor is at its corresponding limit:

$$E_{br} = \frac{1}{\ell} E_r \tag{19}$$

$$I_{br} = \frac{1}{m} I_r \tag{20}$$

$$V_{br} = \frac{1}{\ell m} V_r \tag{21}$$

Substituting Eqs. (18) through (21) into Eqs. (13) and (14) one finds that ω_ℓ and ω_h have the same values for the bank as a whole as they have for the individual capacitors. Thus it is found that any configuration is completely characterized by the two numbers ℓ and m. If every capacitor in the bank is equally loaded, the var rating of the bank will be $V_{br} = n V_r$, where n is the number of capacitors in the bank. It is therefore necessary that $(\ell m)^{-1} \leq n$, and $(\ell mn)^{-1}$ can be considered to be the efficiency with which the configuration utilizes the capacitors in it.

In addition to the three limits on power output imposed by the capacitor, there are two more imposed by the tubes: the plate voltage and plate current of the tubes cannot exceed rated values.

After selecting a tank capacitor configuration, an experimenter has the following freedom:

1. He can select any value of tank inductance and is therefore free to choose ω.
2. He can couple to the load as closely as desired and therefore is free to choose Q.
3. He can increase plate voltage (and power output) until one of the five limits is reached.

The maximum power output capability of a given configuration is therefore a function of the ω and Q at which it is operated.

In Section 2.3 most of the equations have been derived which are needed to relate power output to the five limiting ratings. However,

there the tank capacitor is considered to be a single capacitor, denoted by C_t. In reality, this capacitor is composed of two "tank" capacitors, C_b, and two "feedback" capacitors, C_f, in series (Fig. 2). Conditions as seen by C_t must now be related to conditions as seen by C_b. C_f is determined by the ratio of the rf grid voltage to the rf plate voltage, denoted by k:

$$C_f = \left(\frac{1-k}{k}\right) C_b \tag{22}$$

It is then easily shown that the following relationships hold true:

$$C_t = \left(\frac{1-k}{2}\right) C_b \tag{23}$$

$$I_t = I_b \tag{24}$$

$$E_t = \left(\frac{2}{1-k}\right) E_b \tag{25}$$

$$V_t = \left(\frac{2}{1-k}\right) V_b \tag{26}$$

Each of the limiting ratings must now be expressed in terms of P, Q, and ω. This will give five inequalities which will bound the operating region of the configuration in the Q, ω plane.

Bank voltage [from Eqs. (2), (4), and (25)]:

$$E_{br} \geq P^{0.5} Q^{0.5} (\omega C_b)^{-0.5} \left(\frac{1-k}{2}\right)^{0.5} \tag{27}$$

Bank current [from Eqs. (1), (2), (4), and (24)]:

$$I_{br} \geq P^{0.5} Q^{0.5} (\omega C_b)^{0.5} \left(\frac{1-k}{2}\right)^{0.5} \tag{28}$$

Bank var rating [from Eqs. (6) and (26)]:

$$V_{br} \geq P\ Q \left(\frac{1-k}{2}\right) \tag{29}$$

Plate Voltage: Limiting the d-c plate supply voltage to 20 kv is essentially the same as limiting the peak rf plate voltage to 17,400 v, or the tank voltage to 24,600 v rms. There is thus a second limit on bank voltage. From Eqs. (27) and (25),

$$E_{pr}\left(\frac{1-k}{2}\right) \geq P^{0.5} Q^{0.5} (\omega C_b)^{-0.5} \left(\frac{1-k}{2}\right)^{0.5} \tag{30}$$

This relationship is not exact, because the peak rf plate voltage will also vary somewhat with loading and drive conditions, but it is probably accurate within 10 percent and should be sufficiently good to prevent damage to tubes or capacitors.

Plate Current: If it is assumed that the efficiency of the tubes is constant under all operating conditions and that the rf plate voltage is proportional to the d-c plate supply voltage (as was assumed above), then

$$\frac{P}{P_r} = \frac{E_t}{E_{pr}} \cdot \frac{I_{bb}}{I_{bbr}} \tag{31}$$

To obtain the desired inequality, Eq. (31) is solved for I_{bb}/I_{bbr}, and the result is set ≤ 1, with Eqs. (25) and (27) substituted for E_t. The result is

$$\frac{P_r}{E_{pr}} \geq P^{0.5} Q^{-0.5} (\omega C_b)^{0.5} \left(\frac{1-k}{2}\right)^{0.5} \tag{32}$$

Once the configuration is selected, ℓ and m will be known and C_b, E_{br}, I_{br}, and V_{br} can be calculated. In terms of ℓ and m and the individual capacitor ratings, the five inequalities become

Capacitor voltage limit:

$$\left(\frac{1-k}{2}\right)^{-1} (\ell m)^{-1} C E_r^2 \geq P Q \omega^{-1} \tag{33}$$

Capacitor current limit:

$$\left(\frac{1-k}{2}\right)^{-1} (\ell m)^{-1} C^{-1} I_r^2 \geq P Q \omega \tag{34}$$

Capacitor var limit:

$$\left(\frac{1-k}{2}\right)^{-1} (\ell m)^{-1} V_r \geq P Q \tag{35}$$

Plate voltage limit:

$$\left(\frac{1-k}{2}\right)\left(\frac{\ell}{m}\right) C E_{pr}^2 \geq P Q \omega^{-1} \tag{36}$$

Plate current limit:

$$\left(\frac{1-k}{2}\right)\left(\frac{\ell}{m}\right) C \frac{E_{Pr}^2}{P_r^2} \leq P^{-1} Q \omega^{-1} \tag{37}$$

Here constants are on the left, variables are on the right, and the most symmetrical forms of the equations possible have been used.

The performance of a given configuration can now be mapped. A value of P can be chosen, and one can then plot each of the inequalities in the Q, ω plane. The region not excluded encloses those operating conditions at which the chosen value of power can be obtained. Figure 21 is an example. The hatched regions are those excluded by the inequalities. For low powers, the capacitor current limit is a boundary (for example, curve P_1 in Fig. 21); for higher powers, it may not be (for example, curve P_2, Fig. 21). Either plate voltage or capacitor voltage (but not both) will be a limit. Comparison of Eqs. (33) and (36) shows that whichever equation is dominant for a particular configuration will be dominant for all values of P. As P increases, the plate current and plate voltage (or capacitor voltage) boundaries eventually merge, and the operating region degenerates into a line terminated at either the capacitor current or var boundary (see curve P_3, Fig. 21).

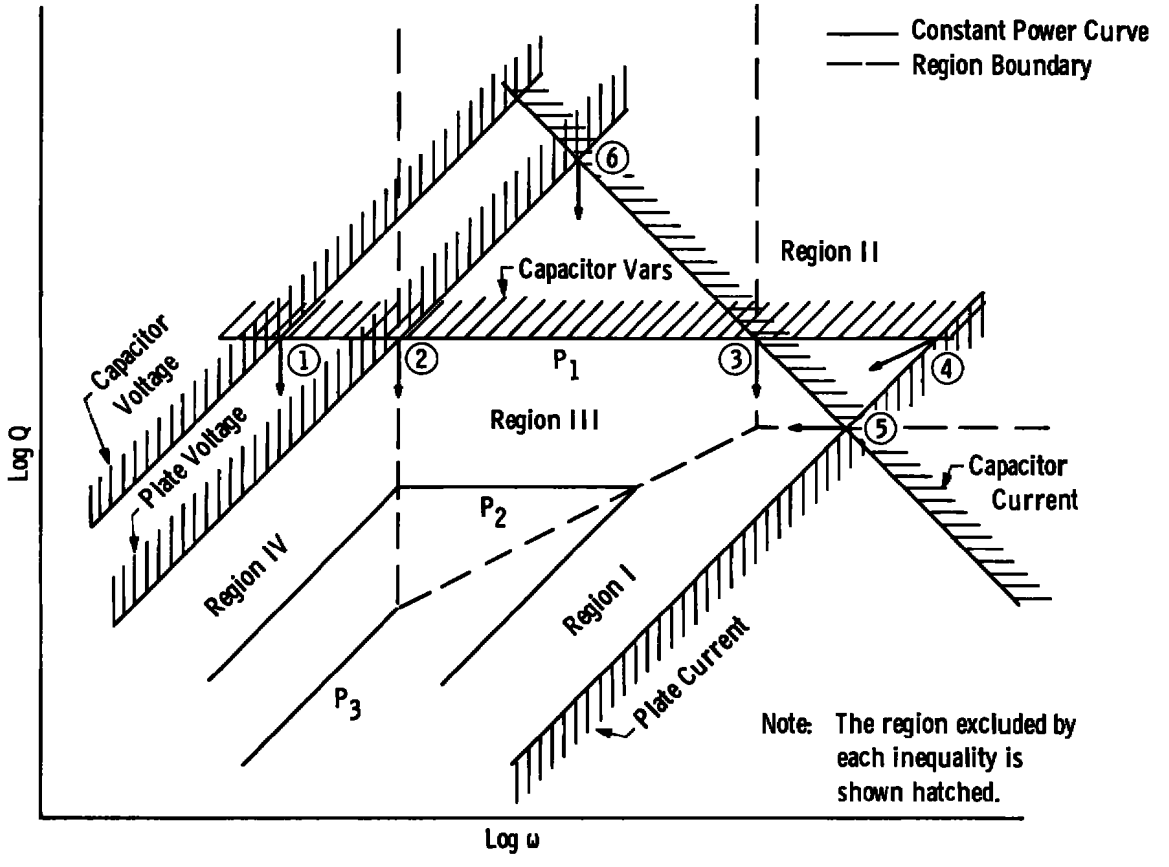

Figure 21. Plot on the Q, ω plane of the five inequalities which limit power output.

It is possible to calculate the points of intersection of the several boundaries, as identified in Fig. 21. In doing so, it is convenient to express the results in terms of ω_h and four dimensionless quantities: P_r/P, and

$$Q_o = \frac{E_{pr} I_r}{P_r} \cdot \frac{1}{m} \tag{38}$$

$$A = \left(\frac{1-k}{2}\right)^{-1} \frac{V_r}{E_{pr} I_r} \cdot \frac{1}{\ell} \tag{39}$$

and

$$B = \left(\frac{\omega \ell}{\omega_h}\right)^{1/2} = \frac{V_r}{E_r I_r} \tag{40}$$

Then for the points of intersection (Fig. 21) the following quantities are obtained:

$$Q_1 = A\left(\frac{P_r}{P}\right) Q_o \tag{41}$$

$$\omega_1 = B^2 \omega_h \tag{42}$$

$$Q_2 = A\left(\frac{P_r}{P}\right) Q_o \tag{43}$$

$$\omega_2 = A^2 \omega_h \tag{44}$$

$$Q_3 = A\left(\frac{P_r}{P}\right) Q_o \tag{45}$$

$$\omega_3 = \omega_h \tag{46}$$

$$Q_4 = A\left(\frac{P_r}{P}\right) Q_o \tag{47}$$

$$\omega_4 = A^2\left(\frac{P_r}{P}\right)^2 \omega_h \tag{48}$$

$$Q_5 = Q_o \tag{49}$$

$$\omega_5 = A\left(\frac{P_r}{P}\right) \omega_h \tag{50}$$

$$Q_6 = \left(\frac{P_r}{P}\right) Q_o \tag{51}$$

and

$$\omega_6 = A\,\omega_h \tag{52}$$

The loci of these points as P is increased are shown in Fig. 21. It is easily verified that points 3, 4, and 5 coalesce at $\frac{P_r}{P} = A^{-1}$. Thereafter, points 3 and 5 are of no interest, because the capacitor current rating no longer forms a boundary of the operating region. Points 2 and 4 coalesce at $\frac{P_r}{P} = 1$, and the operating region closes to a line.

These loci and the $P = P_r$ contour divide the plane into four regions (Fig. 21). In each region, operating power is limited by a different rating:

Region I:	Plate current
Region II:	Capacitor current
Region III:	var rating
Region IV:	Plate (or capacitor) voltage

Although the situation depicted in Fig. 21 is the usual case, two other situations can occur, depending on whether plate voltage or capacitor voltage limits output, and on whether plate voltage and capacitor current ratings will allow the var rating to be exceeded.

Case I: $\omega_1 < \omega_2 < \omega_3$; $B < A < 1$, Fig. 22a. In this case, plate voltage rating is more restrictive than capacitor voltage rating, and the var rating is a boundary. Capacitor current rating is a boundary at low power, but not at high power. At $P = P_r$, the operating region shrinks to a line terminating at point 7:

$$Q_7 = A\,Q_o \tag{53}$$

$$\omega_7 = A^2\,\omega_h \tag{54}$$

Case II: $\omega_2 < \omega_1 < \omega_3$; $A < B < 1$, Fig. 22b. In this case, capacitor voltage rating is more restrictive than plate voltage rating, and the var rating is a boundary. Rated power output cannot be obtained, because rated plate voltage would destroy the capacitor. Capacitor current is a boundary at low, but not at high power. The operating region shrinks to a line at a power of P_m:

$$P_m = AB^{-1}\,P_r \tag{55}$$

The line terminates at point 8:

$$Q_8 = B\,Q_o \tag{56}$$

$$\omega_8 = B^2\,\omega_h \tag{57}$$

Case III: $\omega_1 < \omega_3 < \omega_2$; $B < 1 < A$, Fig. 22c. In this case, plate voltage rating is more restrictive than capacitor voltage rating. In fact, it is so restrictive that rated plate voltage and rated capacitor current applied together will not exceed the capacitor var rating. There are three boundaries at all power levels: plate voltage, plate current, and capacitor current. At $P = P_r$, the operating region becomes a line terminating at point 9:

$$Q_9 = Q_o \tag{58}$$

$$\omega_9 = A\,\omega_h \tag{59}$$

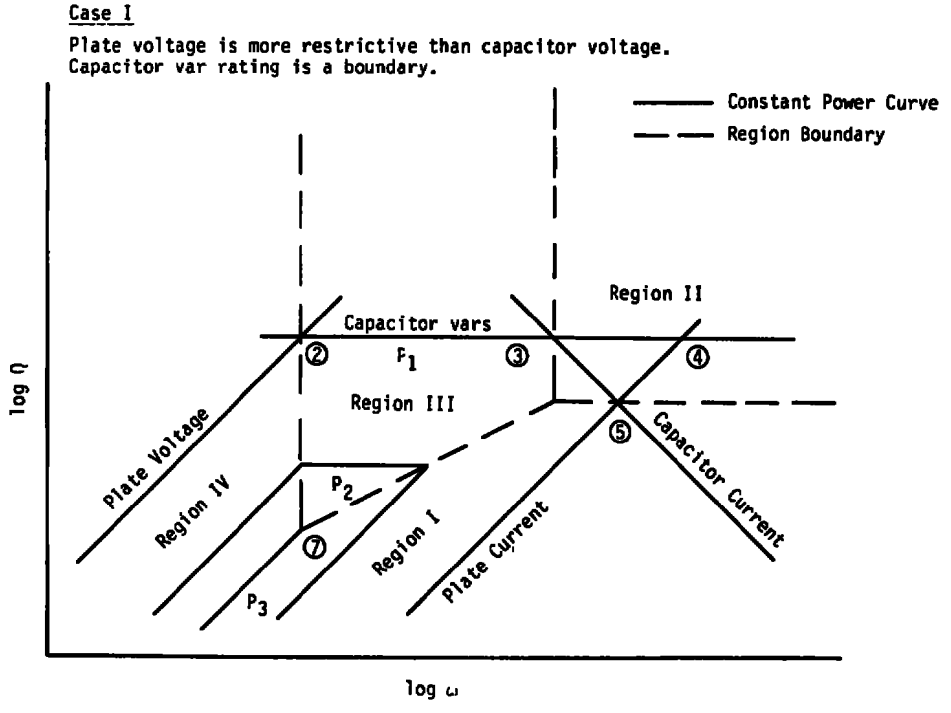

a. Case I

Figure 22. Form of the Q, ω plane.

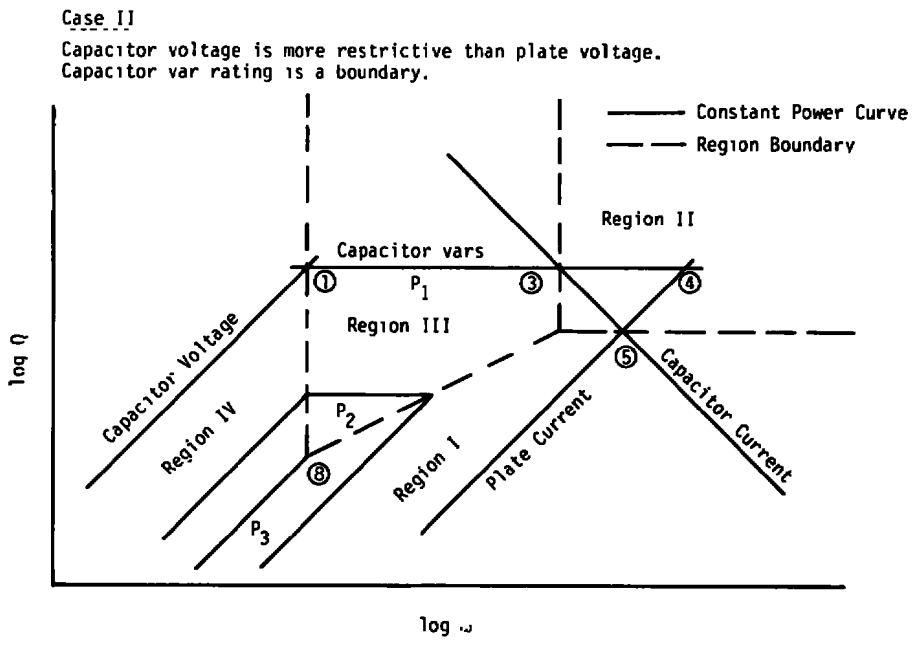

b. Case II

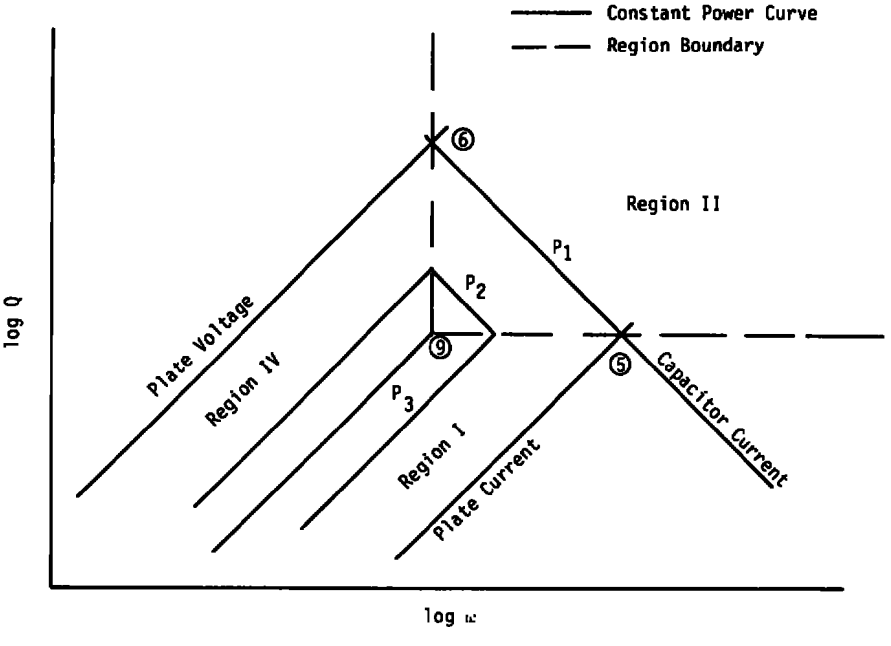

c. Case III

Figure 22. Concluded.

Three additional cases can theoretically be encountered: $\omega_2 < \omega_3 < \omega_1$, $\omega_3 < \omega_2 < \omega_1$, and $\omega_3 < \omega_1 < \omega_2$. However, each of these requires that ω_3 be less than ω_1; that is, that ω_h be less than ω_ℓ. This implies that the capacitor var rating cannot be exceeded at rated voltage and current, and such a capacitor is not likely to be encountered in this application.

It is interesting to find the loci of the points in Fig. 21 as the parameters ℓ and m are changed, but P is held constant. Of course, ℓ changes only A, and m changes only Q_o. These loci are shown in Figs. 23 and 24, for ℓ and m, respectively. A change in ℓ moves the points in different directions and therefore changes the shape of the contour. However, a change in m moves all of the points in the same direction, and will not change the shape of a contour on a log-log plot, but will merely shift it along the Q axis. The shape of the contours in thus a function of ℓ alone.

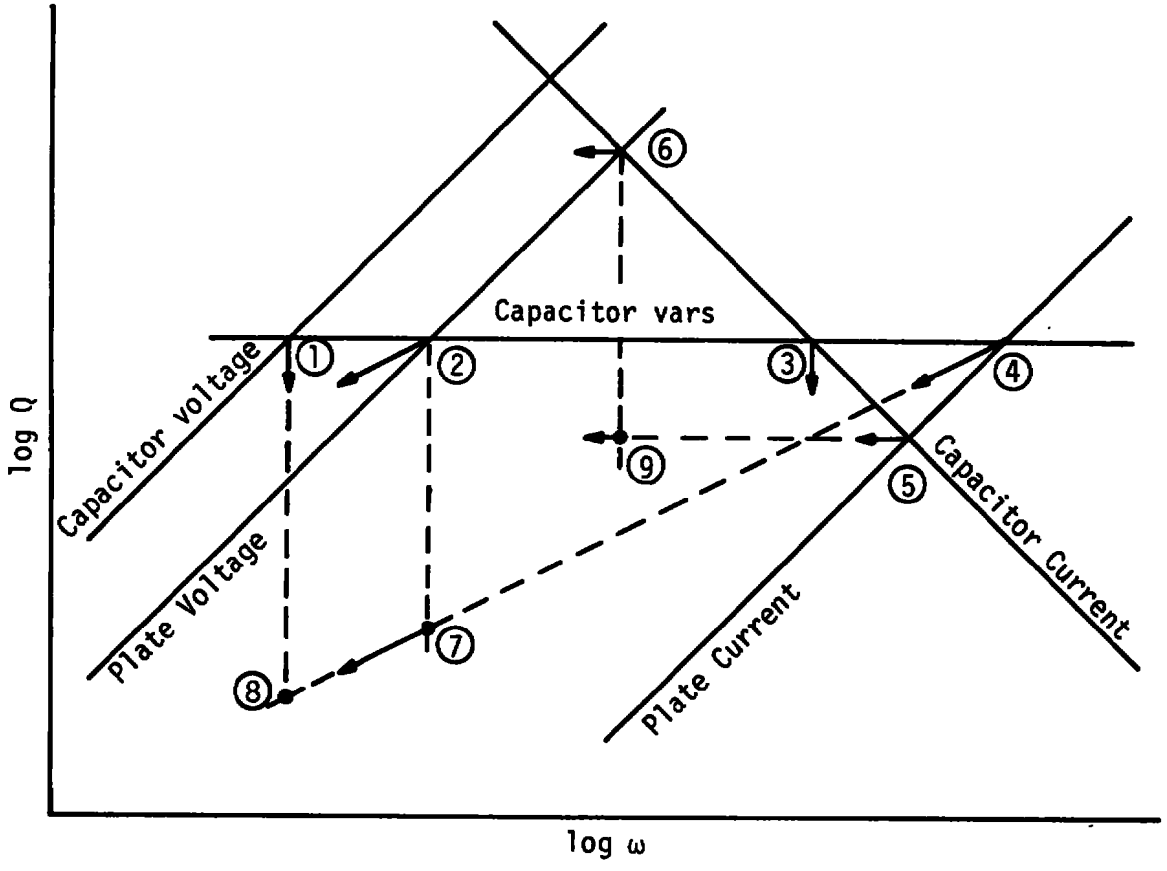

Figure 23. Loci of points of intersection as ℓ is increased.

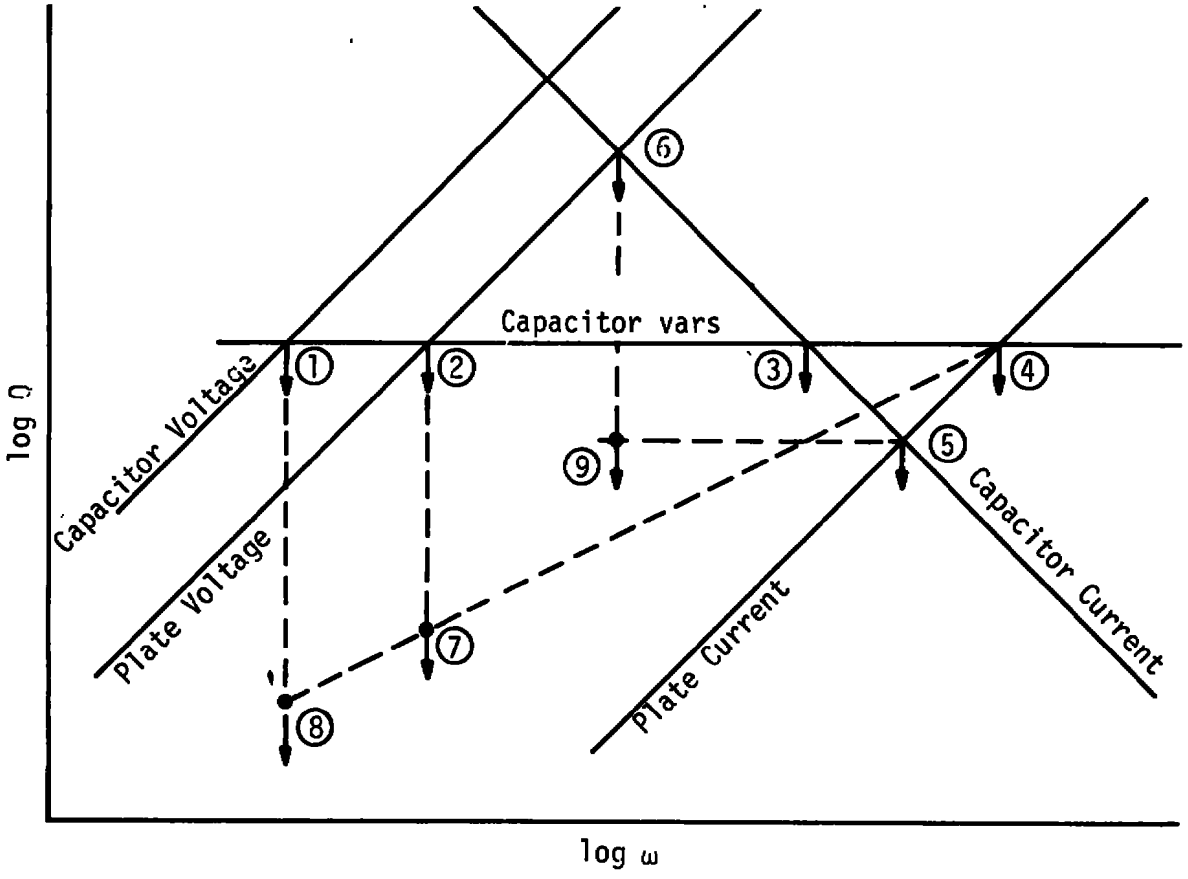

Figure 24. Loci of points of intersection as m is increased.

Table 2 summarizes the performance of some of the more useful configurations which have been found. With these, a power output of 3 MW or more can be obtained at any frequency between 10 and 50 kHz, and full power operation can be achieved at eight frequencies in this range. Other configurations probably can be found if needed. Figure 25 is a composite map of these configurations.

4.3 PRACTICAL CONSIDERATIONS

As a practical matter, one must realize that although panel meters indicate directly when plate voltage and plate current limits are being exceeded, no such instruments protect the capacitors. Furthermore, with a plasma load, it may be very difficult to control Q (and, to a certain extent, ω). The best course to follow as an operating procedure is probably to calculate the operating frequency, ω, with the coil fully loaded by the plasma. The ratings of the capacitor configuration will be known, and by Eqs. (11) and (12) one can calculate the

maximum voltage which can be applied to the bank (call it E_{br}) at this frequency. The plate supply voltage which will produce this capacitor voltage is given approximately by

$$E_{bb} = \frac{E_{br}\ \frac{2}{1-k}}{24{,}600} \cdot 20{,}000 \qquad (60)$$

Equation (60) is plotted in Fig. 26 for each of the catalogued configurations. If this plate supply voltage is not exceeded, there should be little danger to the capacitor bank. Even if the plasma should be extinguished, the capacitor voltage could not rise more than about 15 percent, and this might be partially compensated by a small decrease in ω.

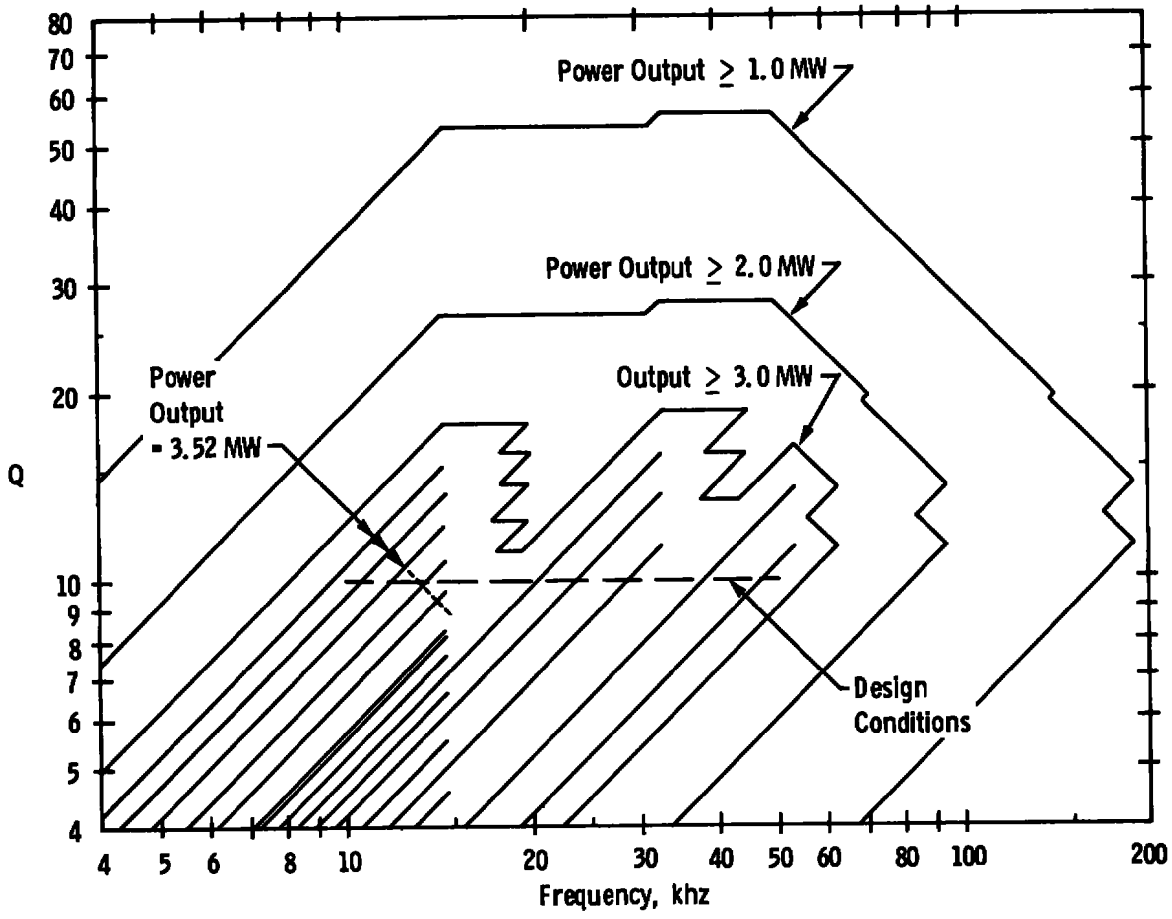

Note: A power of 1.0, 2.0, or 3.0 MW may be obtained at any point within the corresponding contour. The rated power of the tubes, 3.52 MW, may be obtained only along the lines within the inner contour.

Figure 25. Composite Q, ω map for all tank capacitor configurations.

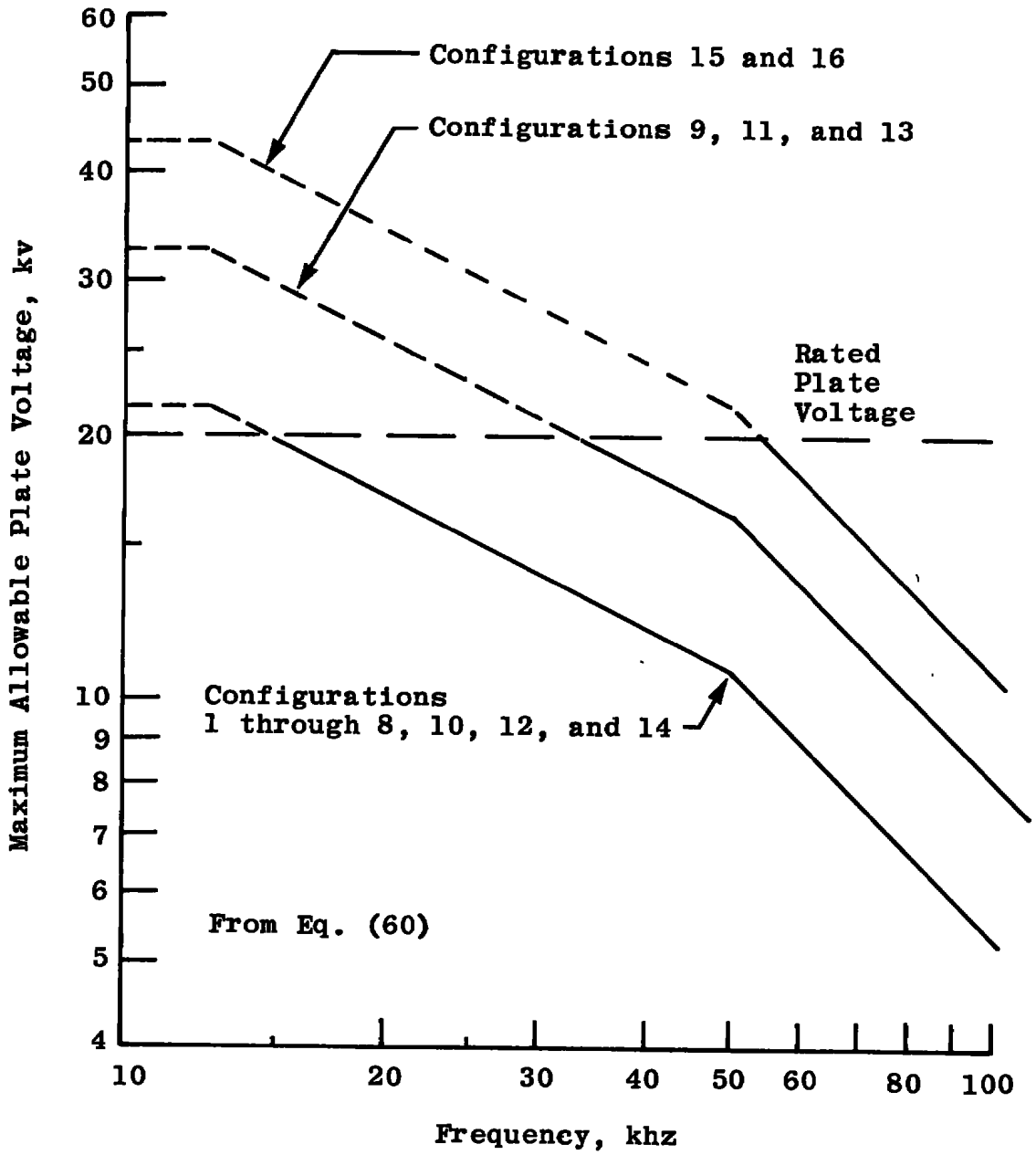

Figure 26. Maximum allowable plate supply voltage for any tank capacitor configuration, as a function of frequency.

Table 2. Tank Capacitor Configurations
a. Catalog

B = 0.5 f_3 = 49931 Hz

Config.	ℓ	m	A	Case	f_7, Hz	Q_7	f_2, Hz	Q_o	P, MW	Q_1
1	1/2	1/10	0.540	I	14556	15.09	14556	27.95	1.0 2.0 3.0	53.13 26.56 17.71
2	1/2	1/9	0.540	I	14556	13.58	14556	25.16	1.0 2.0 3.0	47.82 23.91 15.94
3	1/2	1/8	0.540	I	14556	12.07	14556	22.36	1.0 2.0 3.0	42.50 21.25 14.17
4	1/2	1/7	0.540	I	14556	10.57	14556	19.57	1.0 2.0 3.0	37.19 18.60 12.40
5	1/2	3/19	0.540	I	14556	9.56	14556	17.70	1.0 2.0 3.0	33.65 16.82 11.21
6	1/2	2/11	0.540	I	14556	8.30	14556	15.38	1.0 2.0 3.0	29.22 14.62 9.74
7	1/2	3/16	0.540	I	14556	8.05	14556	14.91	1.0 2.0 3.0	28.34 14.17 9.44
8	1/2	1/5	0.540	I	14556	7.55	14556	13.98	1.0 2.0 3.0	26.56 13.29 8.86
10	1/2	3/13	0.540	I	14556	6.54	14556	12.11	1.0 2.0 3.0	23.02 11.51 7.67
12	1/2	3/11	0.540	I	14556	5.53	14556	10.25	1.0 2.0 3.0	19.48 9.74 6.49
14	1/2	1/3	0.540	I	14556	4.53	14556	8.39	1.0 2.0 3.0	15.94 7.97 5.32
Config.	ℓ	m	A	Case	f_7, Hz	Q_7	f_2, Hz	Q_o	P, MW	Q_6
9	1/3	1/7	0.810	I	32752	15.87	32752	19.59	1.0 2.0 3.0	55.85 27.92 18.62
11	1/3	1/6	0.810	I	32752	13.58	32752	16.77	1.0 2.0 3.0	47.81 23.90 15.94
13	1/3	1/5	0.810	I	32752	11.32	32752	13.98	1.0 2.0 3.0	39.86 19.93 13.29
Config.	ℓ	m	A	Case	f_9, Hz	Q_9	f_6, Hz	Q_o	P, MW	Q_6
15	1/4	1/5	1.080	III	53919	13.98	53919	13.98	1.0 2.0 3.0	49.21 24.60 16.40
16	1/4	1/4	1.080	III	53919	11.18	53919	11.18	1.0 2.0 3.0	39.35 19.68 13.12

Table 2. Concluded
b. Diagrams

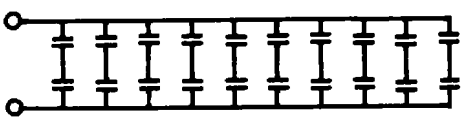
1

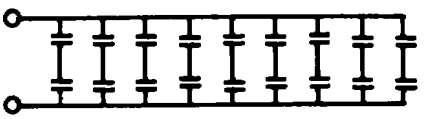
2

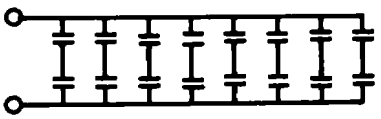
3

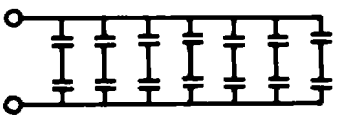
4

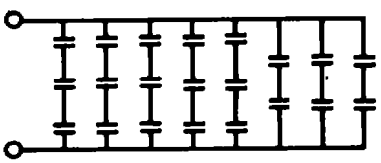
5

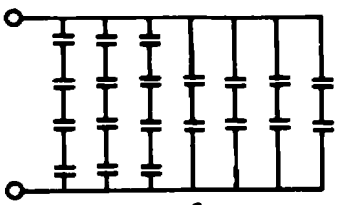
6

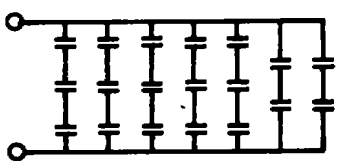
7

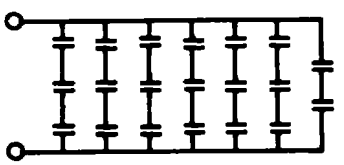
8

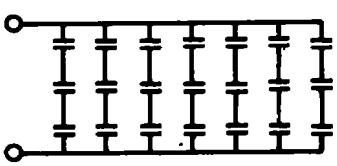
9

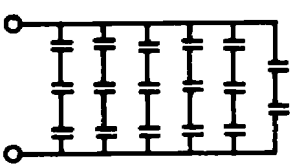
10

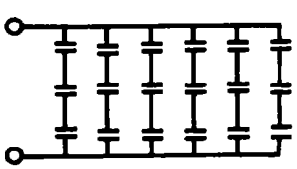
11

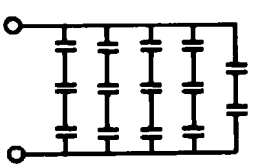
12

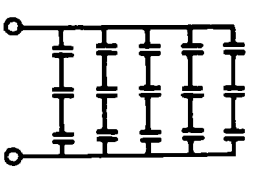
13

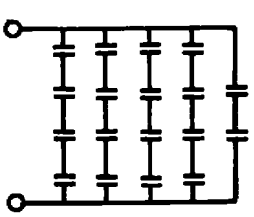
14

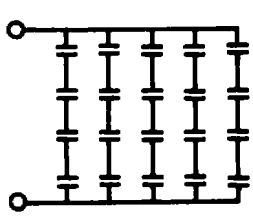
15

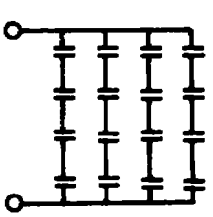
16

4.4 SELECTION OF FEEDBACK CAPACITOR

Since the feedback capacitors handle only about one-tenth of the var load of the tank capacitors, and since they are used to adjust the grid drive voltage, it seemed that ease of adjustment was more important than efficient use of their var capability. Accordingly, the capacitors in the feedback capacitor banks are used only in parallel. Each capacitor has a voltage rating sufficient to withstand the rf grid voltage, and var loading is not high enough to be a limitation, so the only limitation is the current rating of the capacitors. This is established by the bushings used at 400 amp per capacitor section.

The approach taken in selecting the capacitors was as follows. The value of the feedback capacitor required at the nominal design grid voltage is 19.2 μF at 10 kHz and 3.83 μF at 50 kHz. In order to cover this range and to allow the grid voltage to be adjusted ±20 percent, a feedbank capacitor is required which can be adjusted from 3.1 to 23.0 μF. The smallest capacitor in the bank is arbitrarily chosen to be 0.1 μF. This is 3.3 percent of the smallest feedback capacitor which will ever be required (3.1 μF), which is a sufficiently small increment. The capacitors in the bank will be given values of 0.1, 0.2, 0.4, 0.8, ..., μF.

The number of capacitors of each value which is required is determined by the current rating of the capacitors (400 amp). The highest frequency at which each capacitor can be used at the design rf grid voltage of 1,680 v peak is given by Eq. (11) and is shown below.

Capacitance, μF	Maximum Frequency, kHz
0.1	535.9
0.2	268.0
0.4	134.0
0.8	67.0
1.6	33.5
3.2	16.7

The next question is, given a value, C_f, of the feedback capacitor bank, what is the highest frequency at which this value will ever be used? This is obtained from Eq. (11), using the nominal voltage and the nominal tank current:

$$f = \frac{1430\sqrt{2}}{2\pi C_f \cdot 1{,}680} = \frac{0.192}{C_f} \qquad (61)$$

Then, for example, if one considers a bank capacitance of 5.0 μF, Eq. (61) shows that it might be used at a frequency as high as 38.4 kHz; therefore, it cannot include any capacitors larger than 0.8 μF.

Building the bank is begun with a total capacity of 3.1 μF. Since this value may be used at 50 kHz, and thus can use no capacitors larger than 0.8 μF, one each 0.1-, 0.2-, and 0.4-μF, and three 0.8-μF capacitors are selected. To obtain 3.2 μF, another capacitor must be added. Equation (61) shows that 3.2 μF might be used at 50 kHz, so another 0.8-μF capacitor must be added. The bank now totals 3.9 μF. To obtain 4.0 μF, a capacitor must be added which Eq. (61) tells us will be used at 48 kHz and so must be 0.8 μF. Repetition of this procedure generates the capacitor bank shown below.

Bank Capacitance, μF	Highest Frequency of Use,* kHz	Capacitance Added, μF	New Total Bank Capacitance, μF
	50.0	0.1	0.1
	50.0	0.2	0.3
	50.0	0.4	0.7
	50.0	0.8	1.5
	50.0	0.8	2.3
	50.0	0.8	3.1
3.2	50.0	0.8	3.9
4.0	48.0	0.8	4.7
4.8	40.0	0.8	5.5
5.6	34.3	0.8	6.3
6.4	30.0	1.6	7.9
8.0	24.0	1.6	9.5
9.6	20.0	1.6	11.1
11.2	17.1*	3.2*	14.3
14.4	13.3	3.2	17.5
17.6	10.9	3.2	20.7
20.8	9.2	3.2	23.9

*Criterion violated by 2.3 percent for ease of packaging.

These seventeen capacitors were arranged in one package containing five values: 0.1, 0.2, 0.4, 0.8, and 3.2 μF, and three packages containing four values: 0.8, 0.8, 1.6, and 3.2 μF.

In general, in selecting the capacitors to be used to obtain a given total capacitance, one should use the smallest values possible

(i.e., two 0.8's should be used, instead of one 1.6). The capacitance used should be spread out equally over the four packages if possible, and not concentrated in a single package. This will minimize the power to be dissipated in a package and will also reduce the stray inductance of the capacitor leads.

5.0 PHYSICAL ARRANGEMENT AND COOLING

The physical arrangement of the oscillator was strongly influenced by the decision to use vapor cooling of the tubes in place of conventional water cooling. Vapor cooling was chosen because it allowed the total water flow required by the oscillator to be reduced to about 60 gal/min, from the 350 gal/min which would have been required for water cooling. A supply of demineralized water was available which could maintain this rate almost indefinitely. Had water cooling been used, it would have been necessary either to limit the lengths of runs and to schedule the use of water closely, or to have used a closed water system with a bulky and expensive heat exchanger.

The use of vapor cooling was not without penalities, however. The vessels and ducts which dispose of the steam are bulkier than the piping for water cooling would have been. As a result, it is very difficult to gain access to certain components in the plate circuit. Also, with vapor cooling, there is no way to run a heat balance on the anode of a tube, and thus no way to measure plate dissipation directly. It is therefore difficult to determine how much power is being supplied to a plasma load.

5.1 PHYSICAL ARRANGEMENT OF COMPONENTS

The vacuum tubes are mounted in two groups of four tubes. The tubes in each group are mounted as shown in Fig. 27, with their anodes projecting down into a vat, which contains the steam generated by the tubes. Each anode is immersed in a separate water-filled jar. All four anodes are normally at the same potential. However, if a flash-over occurs within a tube, its anode voltage may differ from the other three anode voltages by as much as 40 kv. It was for this reason that separate jars were used, rather than an inner water-filled vat enclosing all of the tubes. The vat and the covers are made of fiberglass-covered plywood. The jars are made of molded fiberglass. The steam and the

excess water which spills out of the jars are conducted away by an 8-in. -diam polyvinyl chloride (PVC) pipe connected to the center of the bottom of the vat. The vat is supported by an aluminum-angle framework, which is mounted on ceramic stand-off insulators.

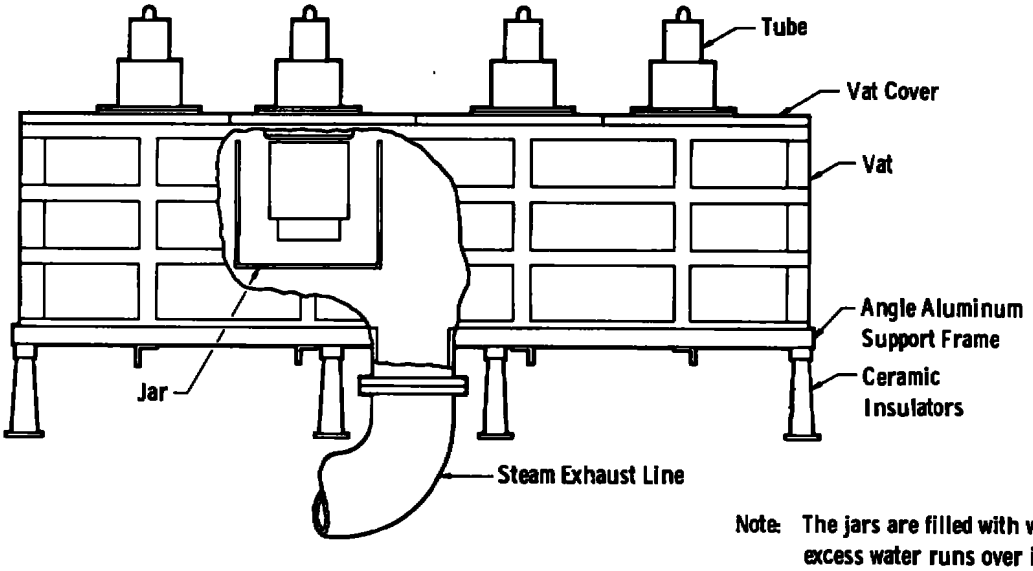

Figure 27. Arrangement for mounting and cooling the tubes.

The arrangement of the remaining oscillator components, which is shown in Figs. 28 and 29, was arrived at as a compromise between conflicting requirements, some of which were as follows:

1. The desire to keep components as accessible as possible.
2. The need to keep the inductance of interconnections as low as possible.
3. The need to maintain adequate spacing between high voltage components in order to prevent arcing.
4. The need to minimize stray coupling between grid and plate circuits.

Unfortunately, the desire for accessibility was usually in direct conflict with the other three requirements, and as insufficient attention to the other three could have led to failure of the oscillator, accessibility was often sacrificed. As a result, some of the plate circuit components are very difficult to reach. Nevertheless, there is scarcely a component which has not been serviced in place since construction was completed.

Inductance of leads is minimized by keeping conductors short and of large diameter, and by placing them as close as possible to the return current paths. In most cases this means placing the conductor as close as possible to the grounded structure, which conflicts with the requirement for maintaining adequate spacing.

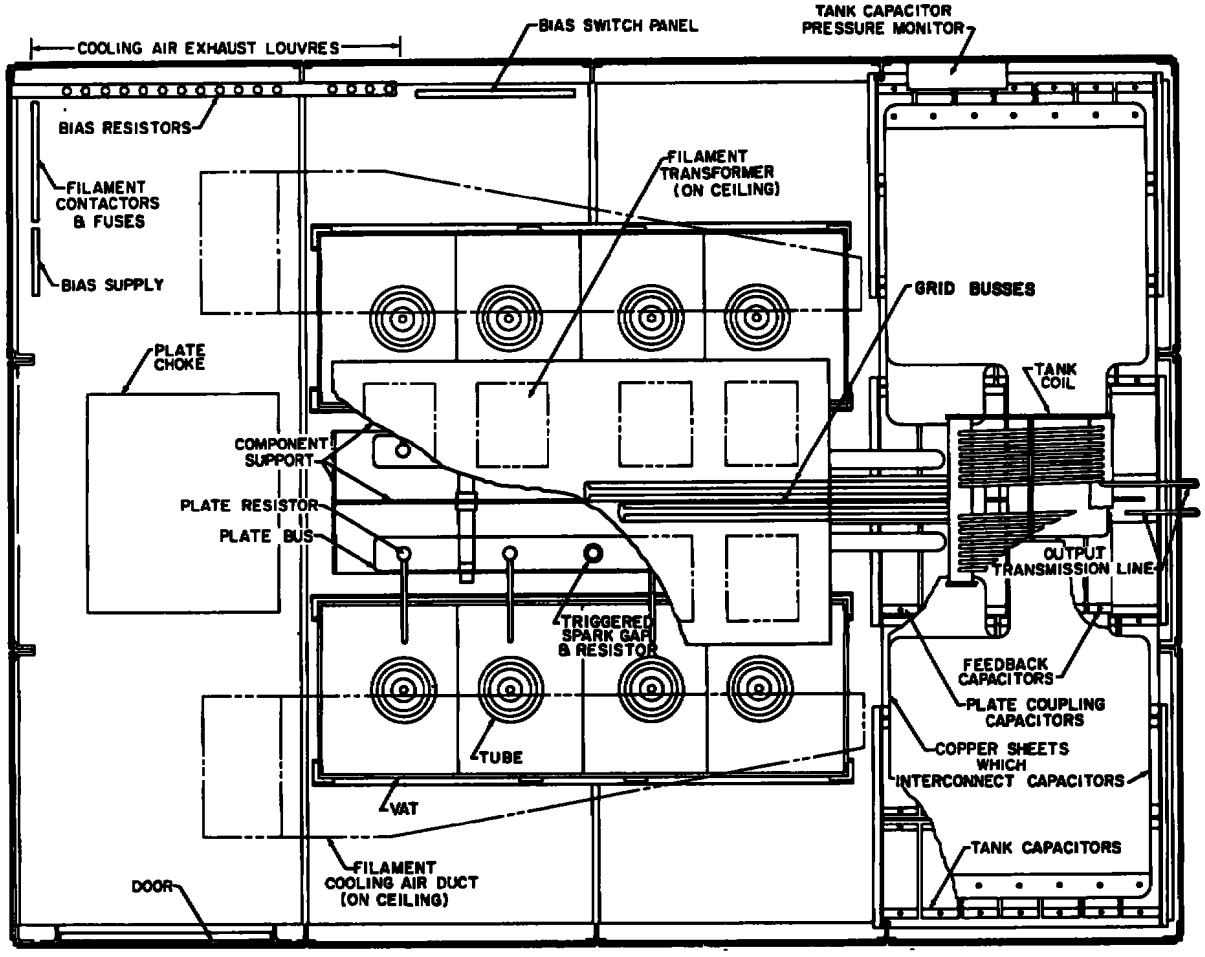

NOTE: THE LAYOUT OF THE TOP OF THE COMPONENT SUPPORT IS SHOWN IN FIG. 29.

Figure 28. Plan view of the oscillator showing the locations of the major components.

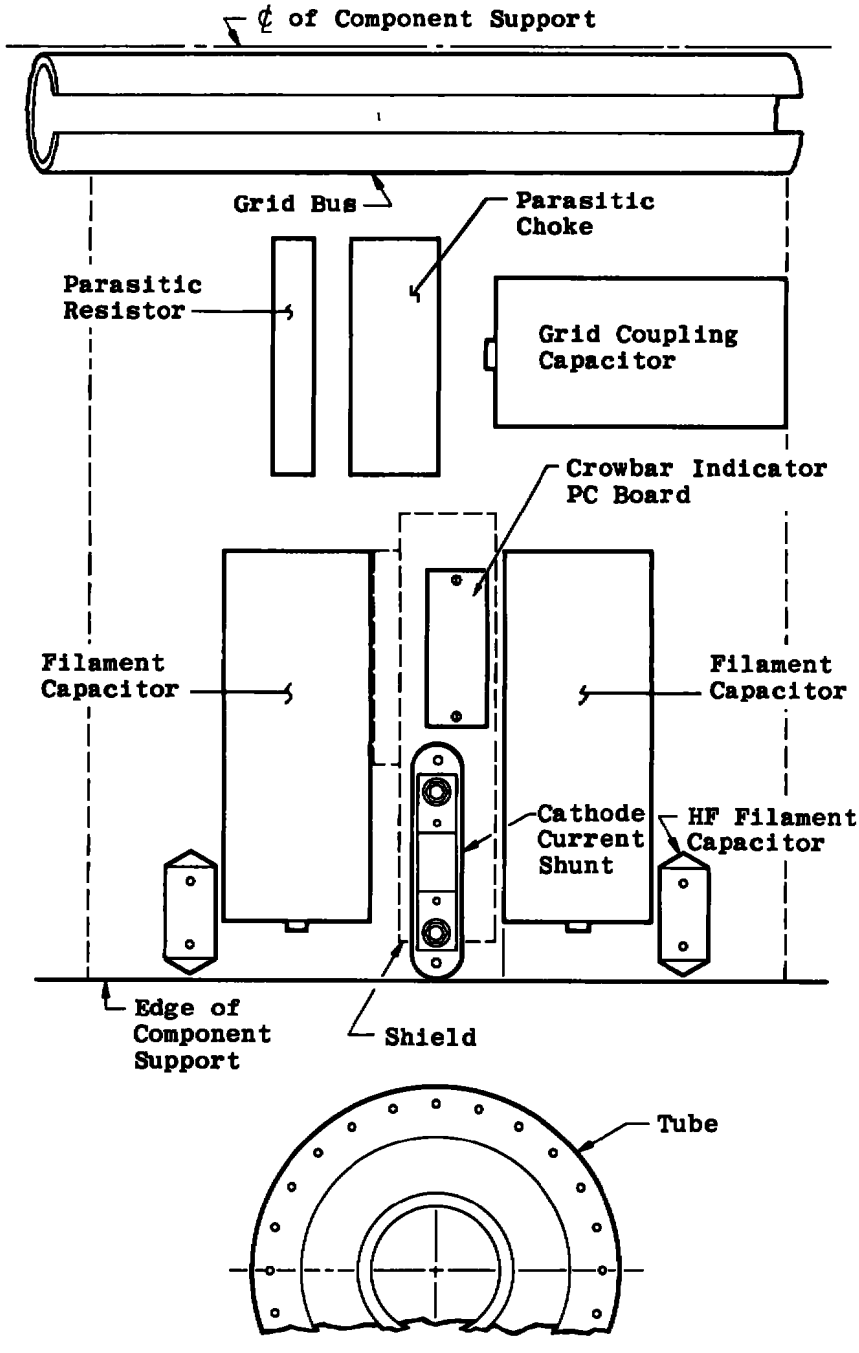

Note: Typical of eight such areas, one for each tube.

Figure 29. Arrangement of grid and filament circuit components on top of the component support.

The general rule used for spacing of high voltage components was to use 10 in. along the surface of an insulator, or 6 in. through air, between components with a peak voltage difference of 40 kv. For lower voltages, proportionately smaller spacings were used. (At a few points, spacings slightly smaller than this rule required were used an an expedient.) In addition, conductors at high potentials were kept well rounded, and projecting wires, screws, etc. were avoided. This rule is apparently a good compromise between the requirements for low inductance and high voltage insulation, because neither parasitic oscillations nor arc-overs have been experienced.

Stray coupling between the grid and plate circuits was minimized by keeping grid and cathode circuit components above the component support, and plate circuit components below.

The grid and plate busses were mounted as close as insulation requirements would permit to the grounded component support so that at very high frequencies they would look like low impedance transmission lines. This was done as an aid in preventing parasitic oscillations and may have had a beneficial effect. The plate busses were made quite large, as they enclose and protect from corona a number of water connections and protective components. The plate busses support the plate resistors and the crowbar resistors.

The tank and feedback capacitors are arranged in the most compact manner possible at the output end of the oscillator and are interconnected by wide copper sheets, in order to avoid introducing stray inductance. The individual capacitors are self-resonant at about 500 kHz with their terminals shorted, a margin of 10 to 1 over the highest operating frequency, and it was felt to be important not to reduce this margin by adding high inductance interconnections. A large area of copper is also required to carry the design tank current of 1,430 amp without overheating. The tank capacitor configuration is changed by installing a new set of copper sheets. Feedback capacitor sections are added or removed by installing or removing silicon-bronze bolts, as shown in Fig. 30.

Careful consideration was given to identifying and localizing the currents which flow in the component support and in the shielding enclosure. The tank current is carried from one set of feedback capacitors to the other by a copper sheet which is grounded to the component support as it passes over it. Thus, no tank current flows in the component support. Only the cathode current of the tubes flows

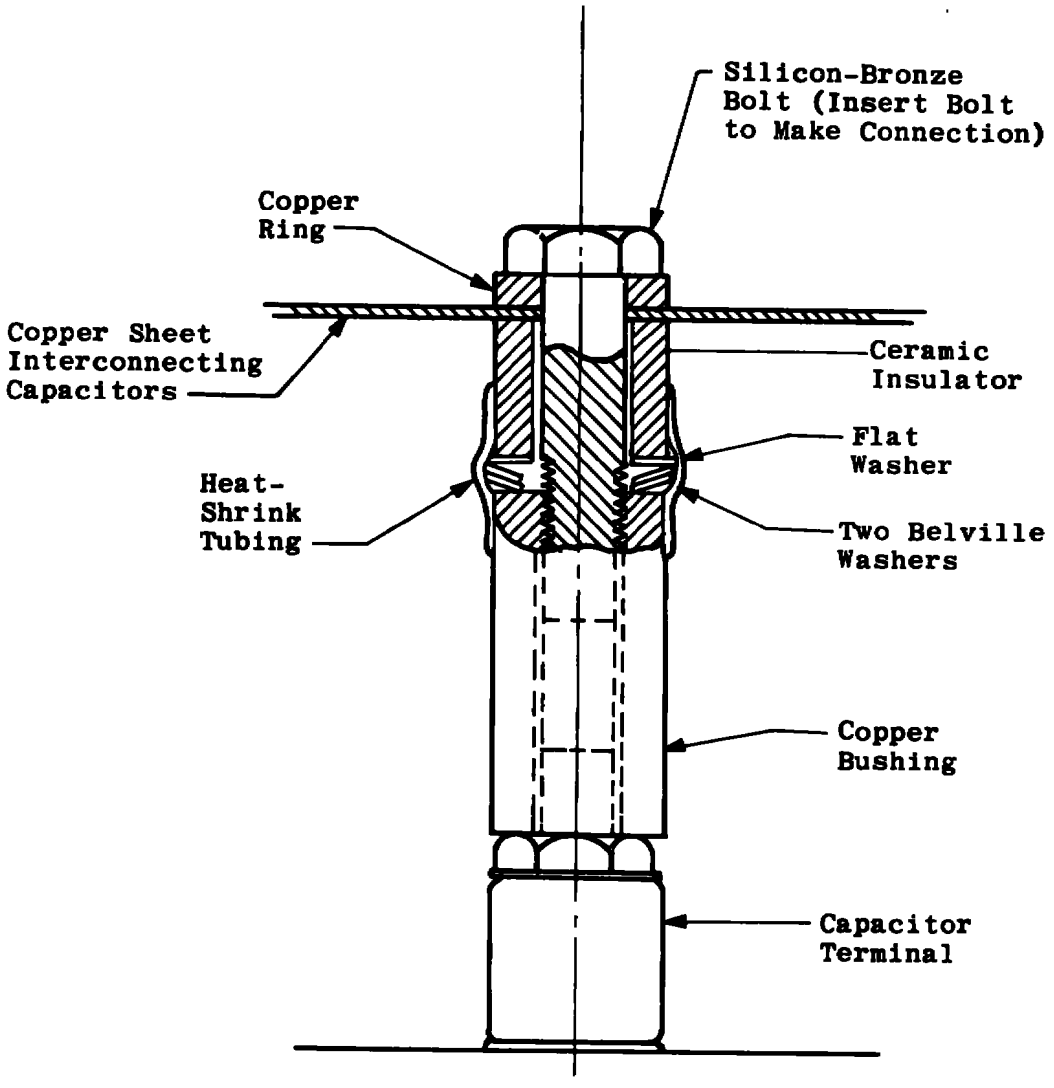

Note: The desired sections are selected by inserting bolts as required.

Figure 30. Detail of the connection to a feedback capacitor section.

in the component support. An attempt was made to localize this current by mounting the grid and plate busses as close as adequate insulation would permit to the surface of the component support. The component support is insulated from the enclosure, except at one point located between the feedback capacitors, where it is welded to the floor of the enclosure. It was hoped that this would eliminate all a-c currents in the enclosure walls, which would minimize radiation of joints, and would also eliminate common mode voltage problems and assist in making accurate measurements. It was later found that

the tank coil induced some current in the enclosure walls, but this has not led to serious problems.

The entire oscillator is housed within an aluminum enclosure 16 ft long by 12 ft wide by 8 ft high. The structure of the enclosure is made of aluminum H-beams, and the walls and ceiling are covered with 1/8-in. aluminum sheet. The floor is of 1/4-in. plate. The structure is of sufficient strength that the oscillator can be lifted and moved as a unit (except that the 3,500-lb plate choke must be removed first). Two Plexiglas®-covered windows were installed in one sidewall of the enclosure, but it was later necessary to cover them with aluminum sheeting to prevent exposure of personnel to X-rays generated by the tubes.

All of the electrical power and instrumentation leads penetrate the end of the enclosure opposite the tank circuit. Power wiring is carried in aluminum conduit which is routed to avoid high-field areas. Instrumentation wiring is carried in a separate conduit system, which is grounded only where it penetrates the enclosure and is isolated elsewhere. The least possible lead length is exposed outside of the conduit.

5.2 COOLING

The cooling-water circuitry for the oscillator is shown in Fig. 31. The tank and feedback capacitors are divided into eight groups. Originally, one group of capacitors, one plate resistor, and one tube were cooled by each of eight similar cooling-water circuits. During shakedown it was found that additional water for the tubes was needed, so the return water from the plate choke was divided into eight equal parts and was also routed to the tubes. Where high voltage insulation is necessary, it is provided by a length of 1/2-in.-OD polyethylene tubing. Four feet is a sufficient length, even for the leads to the tube anodes. The conductivity of the demineralized water supply is maintained at less than 20 μmhos/cm.

Cooling-water requirements were arrived at by the following reasoning:

Tank and Feedback capacitors: As these capacitors are rated at 1,200 kvar and have a nominal dissipation factor of 0.0002, the maximum power loss in a capacitor is 240 w. At the nominal flow rate of 2 gal/min, the temperature rise is less than 1°F.

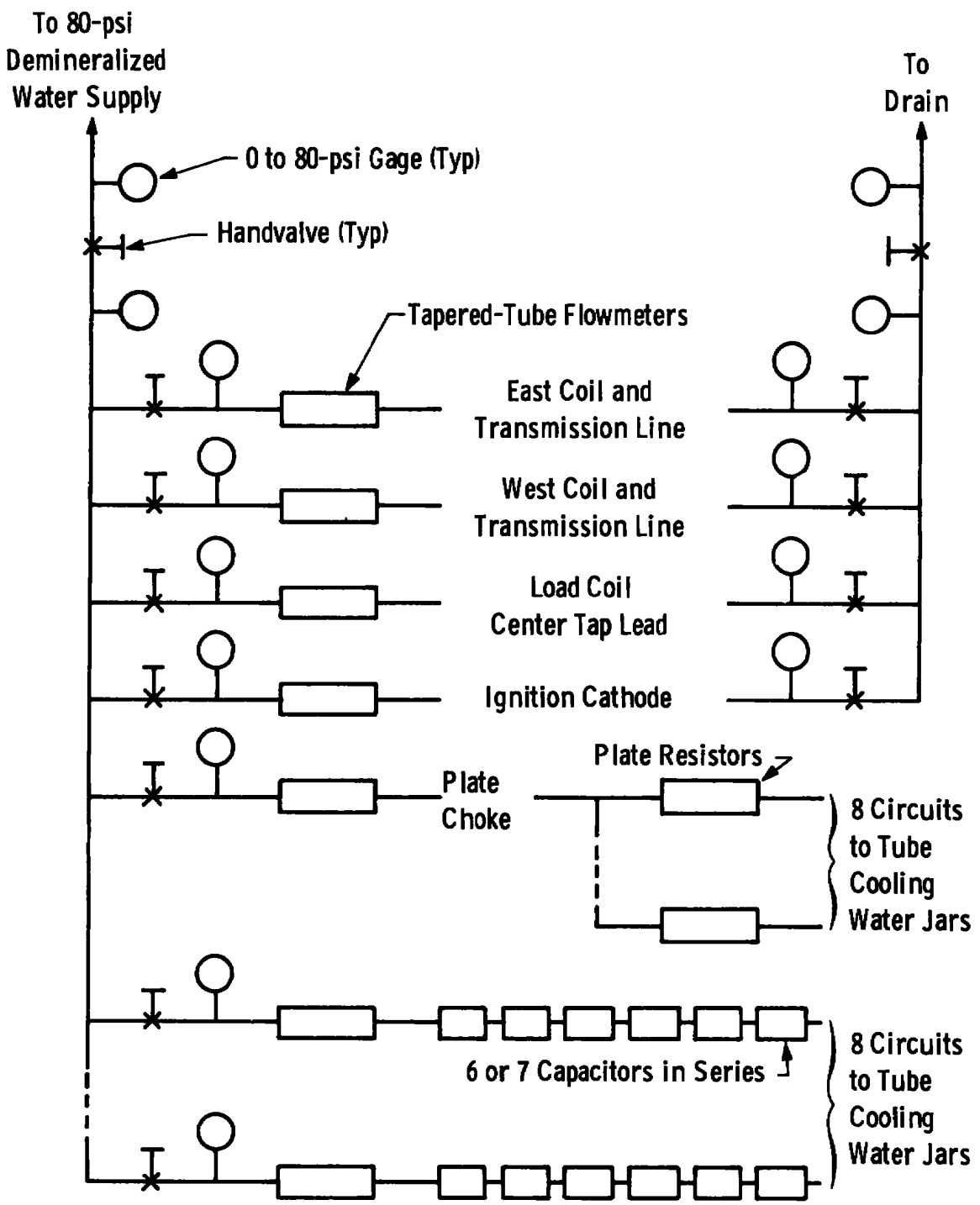

Figure 31. Schematic diagram of cooling water circuitry, after modifications.

Plate Resistors: The computer program showed the rms plate current (including the d-c component) to be 55 amp. Since the nominal value of the resistor is 4.5 Ω, the power loss is 13,600 w per resistor, and at a flow of 2 gal/min, the temperature rise is 46°F. The pressure drop through the resistors is large, and it limits the flow of water to the tubes by this path to a little over 2 gal/min at the full supply pressure.

Tubes: Since the water supply to the tubes has been heated by losses in the plate resistors, the flow rate required by the tubes was calculated assuming that only the latent heat of vaporization, 972 Btu/lb, removes heat from the anode. Then at 200 kw plate dissipation, it should be possible to boil 1.40 gal/min. However, at a flow rate of 2 gal/min and a plate dissipation of roughly 120 kw, the water level in the jars slowly fell, probably because the violent boiling at the surface of the anode splashes additional water out of the jars. As has been mentioned, the water flow was increased by routing the return flow from the plate choke to the tubes, and by increasing the flow through the original circuit to the maximum allowed by the pressure drop in the plate resistors. The total flow is now about 4.5 gal/min, and this amount has been sufficient for all conditions which have been encountered to date. Frequent inspection of the tube anodes has shown no areas of bright copper, which would indicate film boiling and inadequate cooling.

Tank Coil and Transmission Line: The flow in each coil was chosen at 10 gal/min, as this gave a velocity of 10 ft/sec in the 0.75-in.-OD tubing, which was sufficient for good heat transfer. Using a skin depth of 0.012 in. at 50 kHz and a current of 1,430 amp, one finds that the loss in the copper tubing is 589 w/ft. The actual loss in the coil might be perhaps twice this figure because of eddy currents and distortion of the current profile in the tubing by the magnetic field of adjacent turns. Total loss in each coil and line is estimated at 26,500 w, which results in a temperature rise of 18°F.

Plate Choke: The total losses in the choke are estimated by the manufacturer to be 26 kw. The manufacturer's specifications require a flow rate of 10 gal/min.

Ignitron Cathode: In order for the ignitron to hold off an anode voltage of 20 kv, it is necessary to keep the condensed mercury temperature below 80°F. This is accomplished by flowing about 0.5 gal/min to a 0.25-in.-OD copper coil in contact with the body of the ignitron and is only necessary because the ambient air temperature within the enclosure can exceed 80°F.

Transmission Line Center Tap: The 0.25-in.-OD copper tube which grounds the center tap of the load coupling coil is supplied with 0.5 gal/min. This is probably not absolutely necessary, since L10 (Fig. 7) prevents significant current in this lead.

In addition to the water cooling, which removes most of the losses in the oscillator, some air cooling is also necessary. Air flow to cool the filament terminals of the tubes is supplied by two 3,500 ft^3/min blowers through a duct arrangement which can be seen in Fig. 32. The entire enclosure is washed by air from two 6,700 ft^3/min blowers. This air passes over the grid resistors (which are operated somewhat above their convection-cooled power rating) as it leaves the enclosure. The blowers, filters, and associated ducting are mounted on the second floor of the building, directly above the enclosure.

Several photographs of the oscillator are shown in Figs. 32 through 36. The major components can easily be identified.

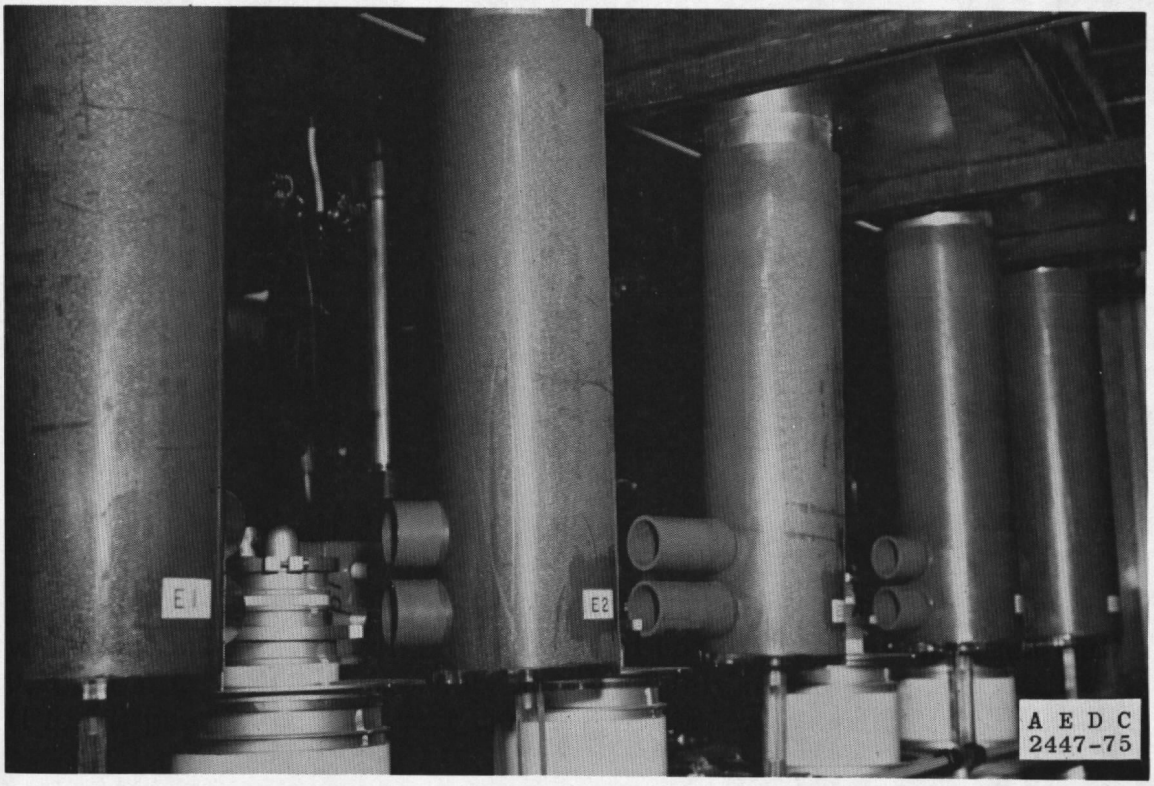

Figure 32. Cooling air ducts for the tube filament terminals.

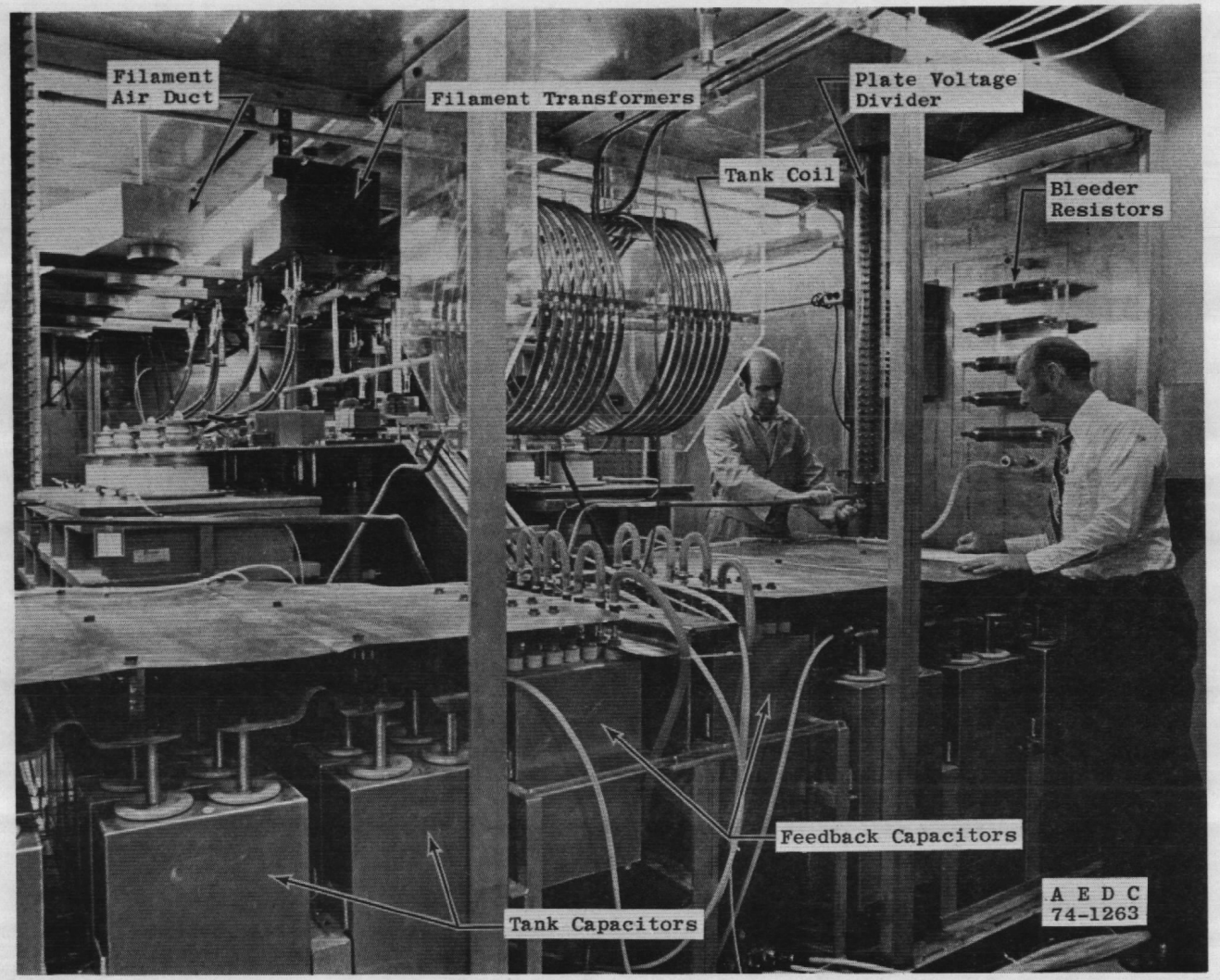

Figure 33. View of tank circuit end of the oscillator.

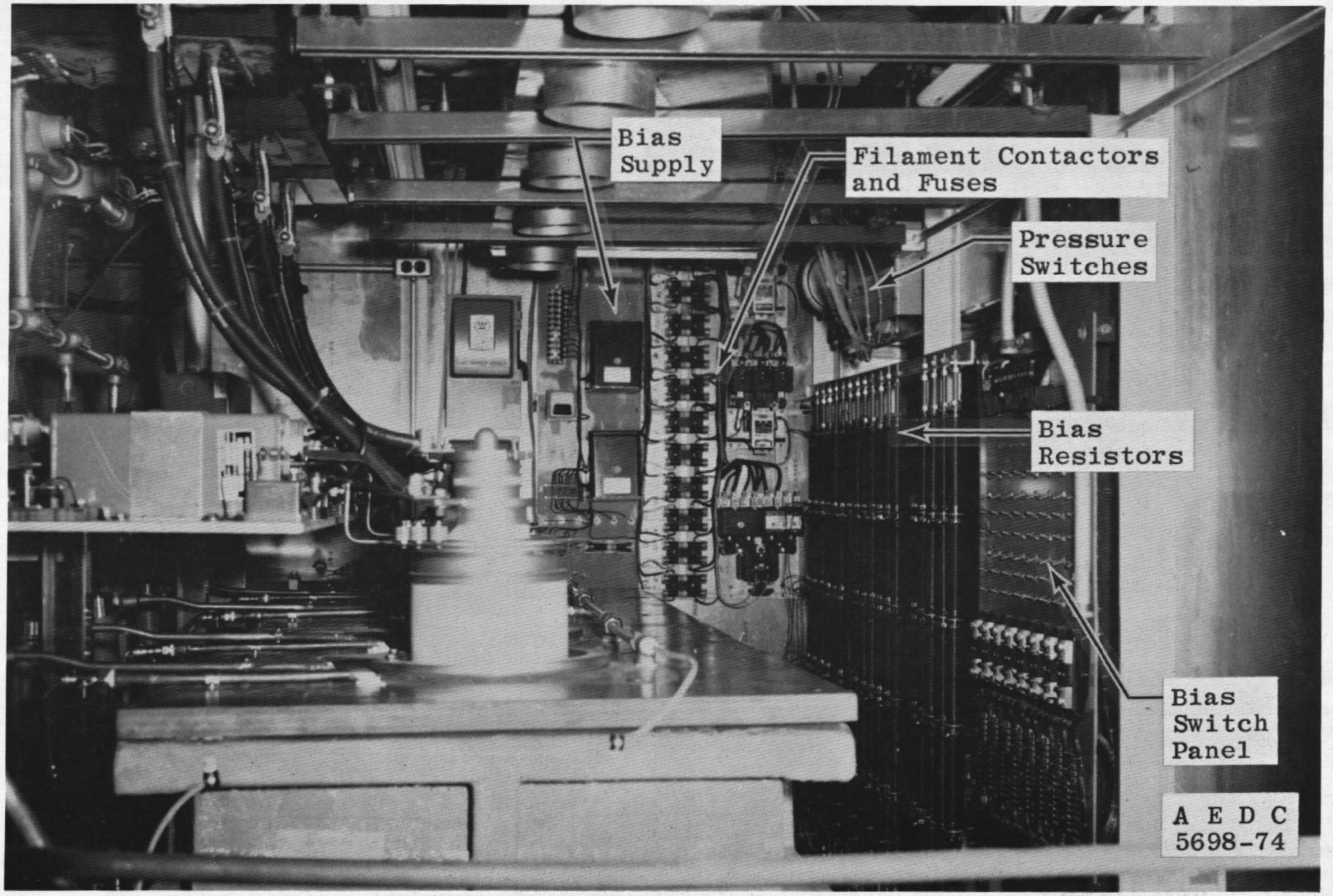

Figure 34. View of south and west walls of the enclosure.

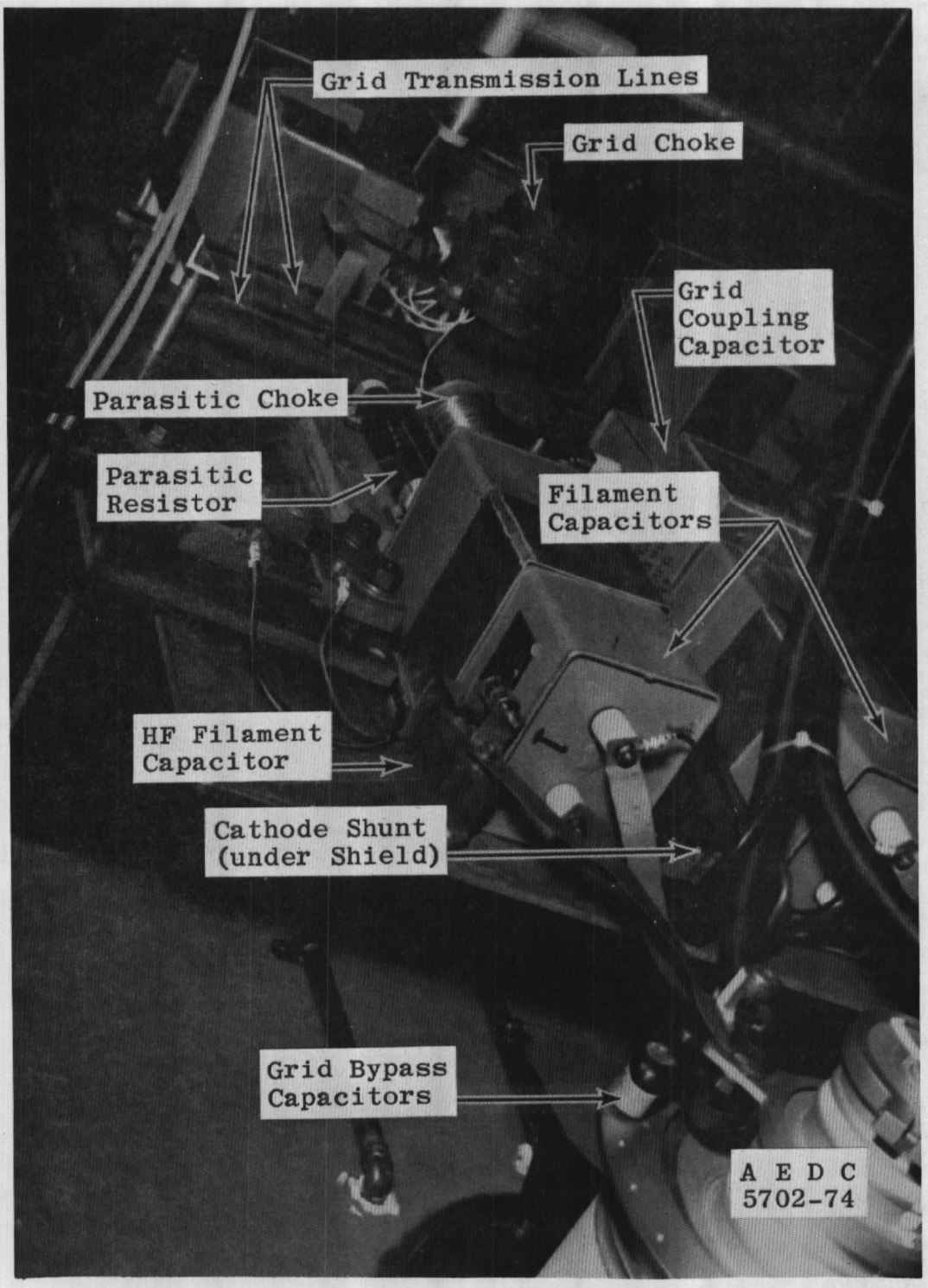

Figure 35. Arrangement of grid and filament circuit components.

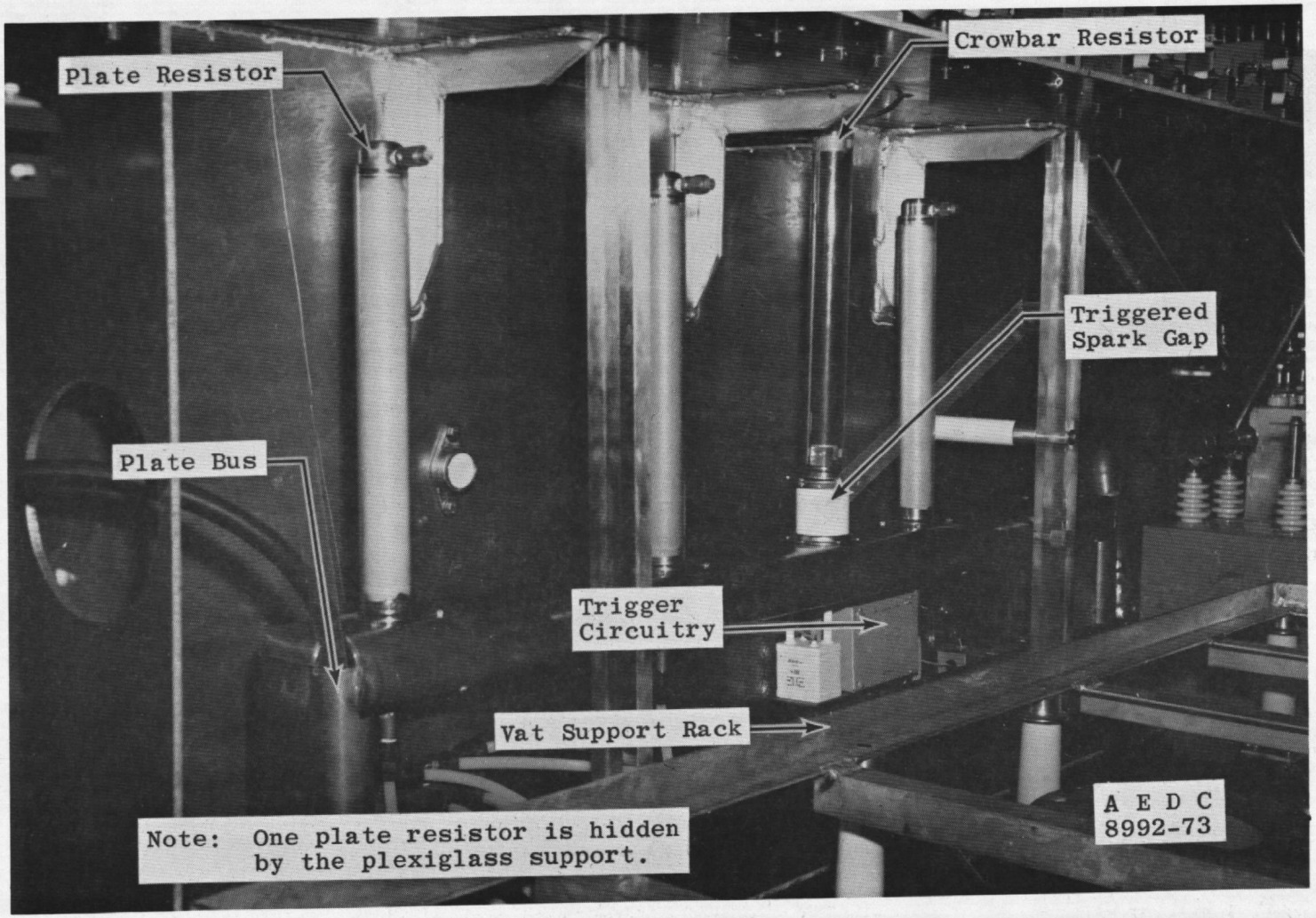

Figure 36. View of plate bus area, with vat removed.

6.0 PROTECTIVE DEVICES, SAFETY, AND INSTRUMENTATION

A photograph of the oscillator control panel is shown in Fig. 37. Meters are provided for measuring individual d-c grid and cathode currents, protective bias voltage, plate voltage, and total plate current. A meter and switch are provided for reading individual filament voltages. The grid and cathode meters include adjustable high limit contacts which will trip the power supply circuit breaker in the event of an ordinary overload. These are quite fast and provide adequate protection of the tubes from overheating.

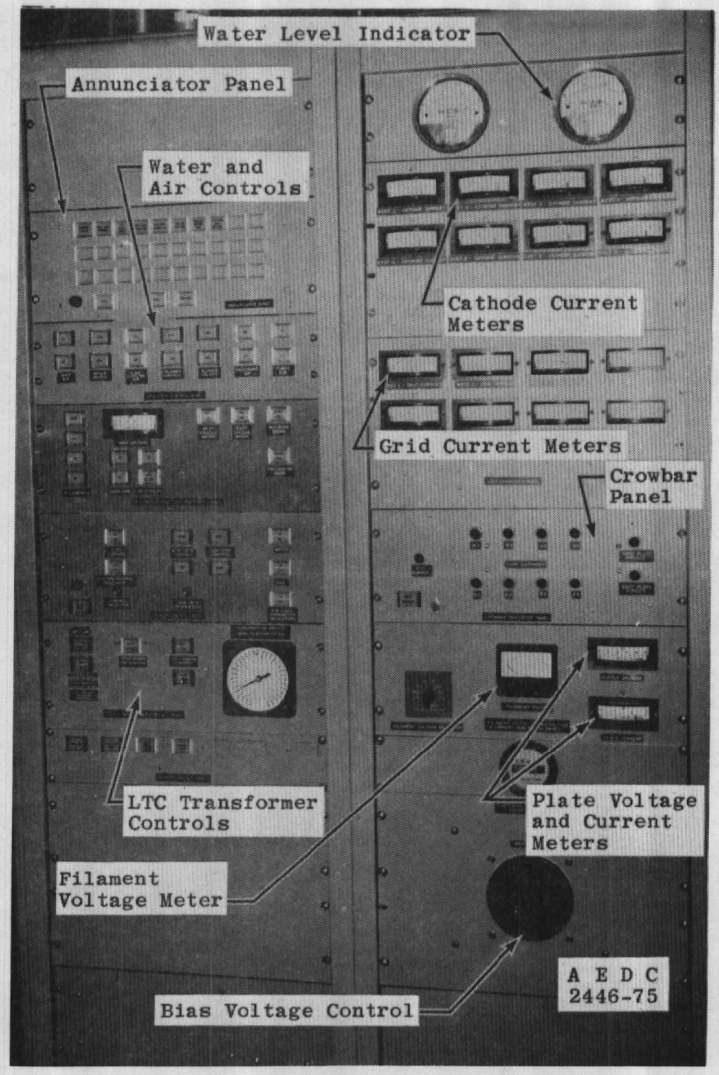

Figure 37. View of oscillator control panel.

6.1 PROTECTION OF VACUUM TUBES

In building large vacuum tubes, it seems to be practically impossible for manufacturers to remove the last traces of gas from the envelope. This gas will occasionally cause a flash-over to occur between the plate and the grid inside the tube, and in order to prevent the destruction of the tube, it is absolutely necessary to design the circuitry to limit the magnitude and duration of the resulting current flow. In the usual case of an rf amplifier or oscillator, it is the energy stored in the plate supply filter capacitor which damages the tube. Protection is obtained by short circuiting ("crowbarring") the filter capacitor by firing an ignitron when a flashover is detected.

In the present case, however, it is the energy stored in the tank capacitor which is dangerous, because of the low operating frequency, and because eight tubes are operating from a single tank circuit; the plate supply is unfiltered. Two means of protection have been incorporated in the circuit. The most reliable, and probably the most important, is the plate resistors. These are 4.5-ohm resistors placed in series with each plate. In the event of a flashover when the plate voltage is at its highest value, these resistors limit the peak current to 8500 amp or less. Perhaps even more important, during the flashover, most of the tank capacitor voltage appears across the resistor, and only a small portion of it appears across the low resistance arc within the tube. Thus, nearly all of the energy stored in the capacitor is dissipated in the resistor, not in the tube. The inductance of the plate resistors, which was calculated to be 15 μH, is also important, and limits the rate of rise of the arc current of 2,500 amp/μsec or less. The penalty for the use of the resistors is that they dissipate about 3 percent of the power output of the oscillator.

As a backup to the plate resistors, a crowbar, consisting of a triggered spark gap and a 0.5-ohm resistor in series, is connected between each plate bus and ground. After the spark gap is triggered, it diverts nine-tenths of the current from the tank capacitors around the tube. A ferrite ring is mounted inside the plate bus at the lower end of each plate resistor, so that the current through the resistor passes through it. A slot sawed in the ring prevents saturation because of the d-c plate current and causes the flux in the ring to be proportional to the instantaneous plate current. A coil wound on the ring then has a voltage induced in it proportional to dI/dt. The coils are connected to the trigger circuit shown in Fig. 38. When dI/dt in any tube becomes large enough to break down the spark gap (Fig. 38),

the trigger circuit fires the triggered spark gap, which discharges the tank capacitors.

While the triggered spark gap can easily handle the current and energy involved in discharging the tank capacitors, it cannot withstand a long duration follow-on current from the plate supply. It is therefore necessary to connect an ignitron in parallel with the plate supply and to fire it if either of the crowbar spark gaps fires. A small pickup loop is mounted near the grounded end of each crowbar resistor. The voltage induced in the loop by current in the resistor is used to fire the ignitron, through circuitry similar to that in Fig. 38. After the ignitron fires, the power supply circuit breaker must be opened to prevent destruction of the ignitron. A shunt in the cathode lead to the ignitron detects current in the ignitron and opens the circuit breaker through circuitry which will be discussed later in this section.

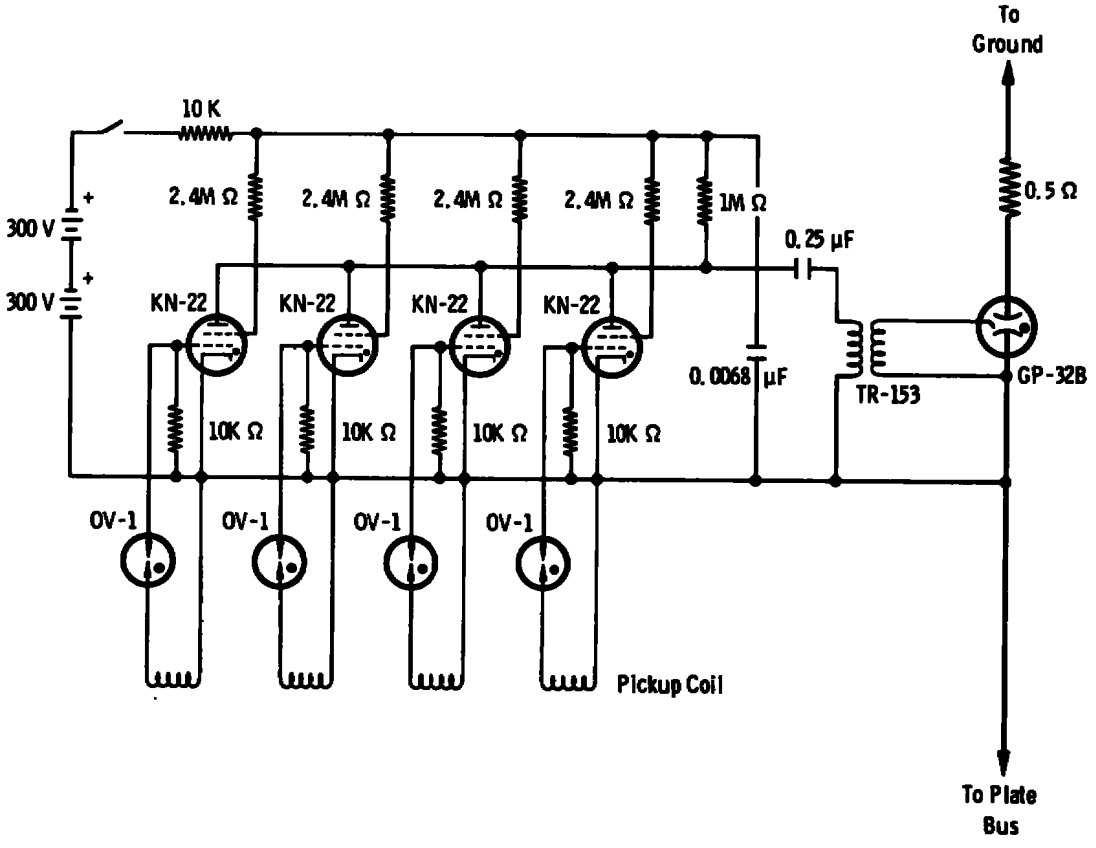

Figure 38. Crowbar trigger circuitry.

In order to protect the components connected to a tube from damage when a flashover occurs, spark gaps were connected across each grid coupling capacitor, across each feedback capacitor, and from one side of each filament to ground. These gaps are of a type which fire at a given voltage, regardless of the rate of rise of the voltage. A 1.5-ohm resistor was connected in series with the spark gaps across the feedback capacitors, since the gaps by themselves were not capable of handling the energy stored.

It seemed desirable to have an indication of which tube flashed over, so that a tube prone to flashover could be identified. The circuit shown in Fig. 39 was installed on each cathode current shunt in an attempt to accomplish this. It was not entirely successful, however, as will be discussed in Section 7.1. An identical circuit was installed across the shunt in the ignitron cathode lead and was used to trip the power supply circuit breaker. The SCR used, which is of an unconventional type with reversed polarity, was chosen because of its very fast turn-on time. The high speed was needed in order to detect the flashover before the crowbar fired and diverted the current from the tube.

The oscillator was also protected against loss of cooling water or filament air to the tubes. The "bubbler" arrangement shown in Fig. 40 was used to measure the water level in the jars. The pressure in the supply manifold is proportional to the water level in the jar with the lowest water level. This pressure is indicated (in inches of water) on the control panel and is also sensed by a pressure switch which will trip the power supply circuit breaker if the water level falls more than 3 in. below normal. Failure of the filament air is

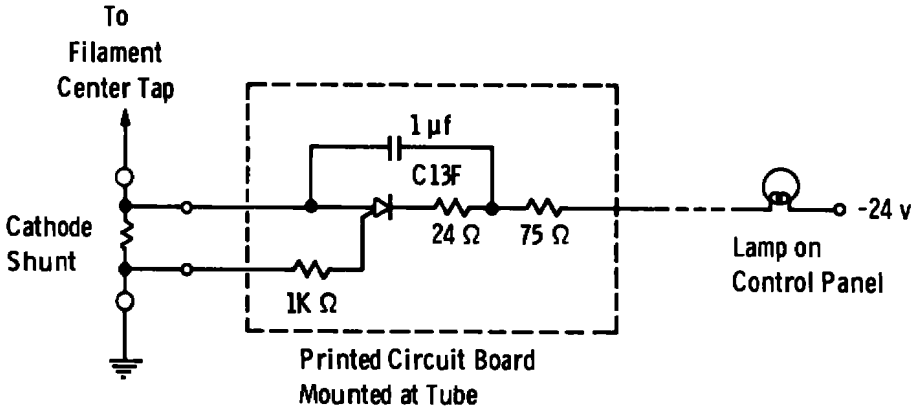

Figure 39. Flash-over detection circuit.

detected by the circuit shown in Fig. 41. If either filament air blower fails, the pressure seen by the pressure switch will fall to half its normal value, and the power supply circuit breaker will be tripped.

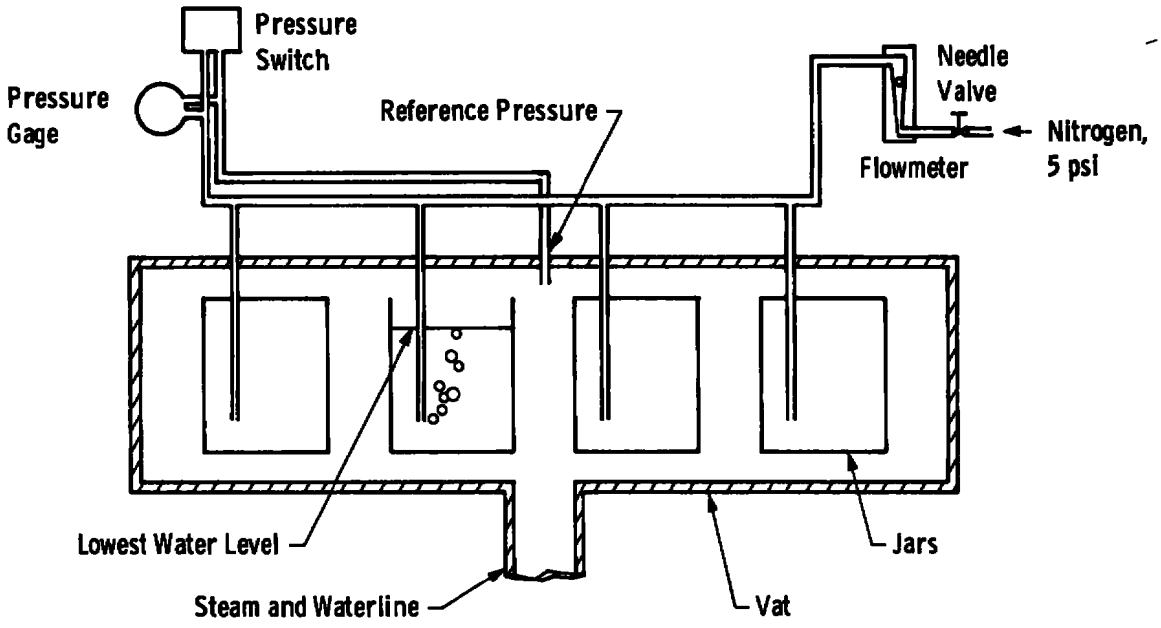

Figure 40. "Bubbler" circuit for measuring tube cooling water level.

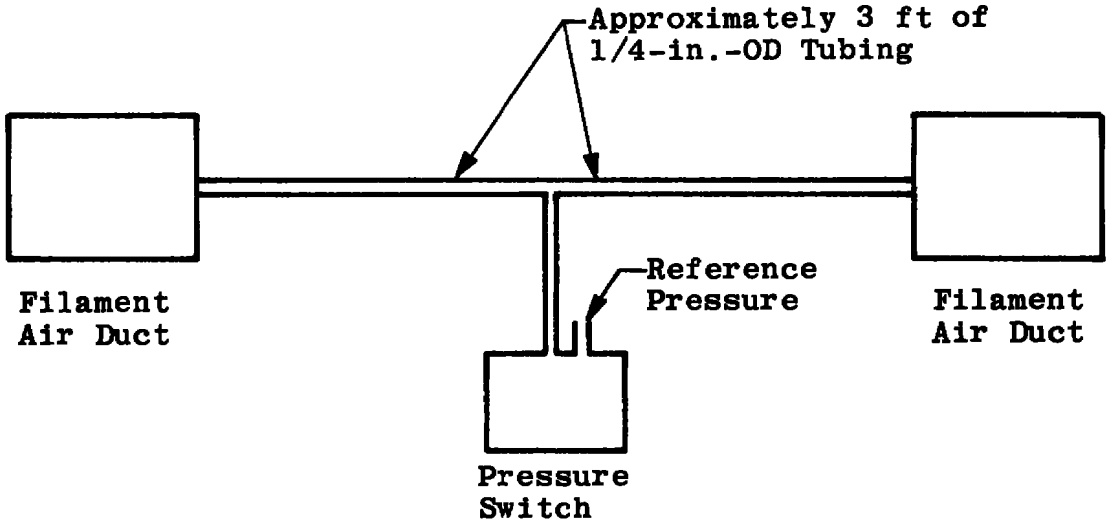

Figure 41. Filament air failure protection circuit.

There are several cases on record where violent explosions have occurred when a capacitor in an energy storage bank failed and the total energy stored in the bank was dissipated at the site of the fault. While the total energy stored in a tank capacitor bank is not especially large (about 250 J at most), it seemed quite possible that the circuit would continue to oscillate even after a capacitor in one of the banks failed. The entire tank current would then flow through the fault and would continue to dissipate energy, until perhaps the case of the capacitor ruptured. Some consideration was given to installing rupture disks on each capacitor, but this idea was rejected because of the possibility that a fault would cause flaming oil to be blown about the enclosure. Instead, a pressure switch was installed on each capacitor. (Automotive oil pressure switches were used.) A circuit was built which monitors these switches and trips the power supply circuit breaker if one of them operates. An SCR and a lamp indicate which switch operated. The feedback capacitors and the plate-coupling capacitors were not similarly protected, because oscillation will stop if they fail. The other capacitors in the oscillator were too small to require protection.

6.2 PROTECTION OF OPERATING PERSONNEL

In addition to protecting the components of the oscillator, it is necessary to provide protection for operating personnel. The principal danger is from energy stored in the various capacitors, which is quite sufficient to be lethal. Several levels of protection are provided, so that failure of a component or failure to carry out a procedure will not result in an unsafe condition. First, switches are provided which remove all power from the oscillator. The switch which connects the plate supply to the oscillator is arranged so that it can be locked in the open position. Another switch short circuits the plate supply voltage to ground. Two safety switches remove the power from the filament and bias supplies. These last three switches are located inside the enclosure, in view of anyone working on the oscillator. Second, bleeder resistors are installed wherever necessary so that all capacitors will discharge as soon as the plate supply voltage is removed. The time constants were chosen so that the enclosure will be safe 30 sec after the plate supply voltage is removed. Third, permanently connected ground straps are installed in the enclosure. On entering the enclosure, personnel are instructed to connect these ground straps to certain numbered points, in a prescribed order (see Fig. 2). It is possible to do so without being exposed

to contact with any high voltage point. With these ground straps in place, both terminals of every dangerous capacitor are directly grounded. Personnel are instructed that any sign of a spark when connecting the ground straps indicates an open bleeder resistor, and a potentially dangerous condition. In this event, they are to leave the enclosure and report the difficulty. It is important to realize that these procedures do not ensure safety unless the personnel who execute them are familiar in detail with the nature of the hazard.

The vacuum tubes used in the oscillator generate X-rays in rather large quantities. However, they are quite soft and are easily stopped, even by a 1/16-in. aluminum sheet. As has been mentioned, it was necessary to cover the windows of the enclosure with aluminum sheeting. Lead glass could probably have been used instead, if the windows had been absolutely necessary. The problem has been easy to handle, but should be kept in mind by anyone contemplating a penetration of the enclosure wall, or operation with the enclosure door open.

Before the oscillator was operated, there was some concern that it might generate a high level of ultrasonic noise, which could damage hearing without being audible. The opinion of a hearing conservation group was solicited. They cited literature (Ref. 7) which indicated that ultrasonic noise could not damage hearing, but could have other physiological effects if it were very intense. When the oscillator was operated, it was found that, at frequencies up to at least 100 kHz, it produced no ultrasonic noise which was measurable above the background noise of about 85 db in the test area.

6.3 ELECTROMAGNETIC INTERFERENCE

Some consideration has been given to the electromagnetic interference which might be produced by the oscillator, as there seemed to be a possibility that it could interfere with VLF radio services or with instrumentation on nearby aerospace test cells. Certain measures were included in the design, because if they were later found to be needed, they would have been nearly impossible to retrofit. The entire oscillator was enclosed in a carefully designed shielding enclosure. The number of penetrations of the shielding was minimized. Control and instrumentation wiring within the enclosure was done in conduit and was kept out of high field areas. Certain other measures were not taken, but could be added later at moderate expense if interference materializes. For instance, wiring leaving the enclosure could be

filtered, if necessary. To date, no interference of any kind has been detected. One concession is made, however: the oscillator is never operated when a solid rocket motor is installed in an adjacent test cell.

6.4 INSTRUMENTATION

During the design of the oscillator, an effort was made to provide for the measurement of accurate voltage and current waveforms. These would have been useful in diagnosing troubles with the oscillator, and would also have allowed a direct comparison of the actual performance of the oscillator with the performance predicted by the computer program. Although only moderate success was achieved, the approach which was taken will be described here. The difficulties which were encountered will be discussed in Section 7.3.

The goal of these measurements was to obtain accurate instantaneous waveforms of the two plate voltages, the eight grid voltages, and the eight cathode currents. Measurements of individual grid currents would also have been desirable, but no convenient means of obtaining them could be found. Direct-current coupling was used so that the actual load line could be obtained, and accurate transient response could be measured.

The plate voltage waveform was obtained from two voltage dividers which use the circuit diagram in Fig. 42. These can be seen in Fig. 33. These divers were connected to the two plate busses. To obtain the individual plate voltages, one must make a small correction for the voltage drop in the resistance (and perhaps the inductance) of the plate resistors. The voltage division is resistive below 1.59 kHz and capacitive above this frequency. The resistive ratio was adjusted to an accuracy of better than 0.1 percent by applying a d-c voltage to the divider. The capacitive ratio was adjusted by applying a step waveform to the divider, probably to an accuracy of about 1.0 percent. The coaxial output cable was connected to the divider during the adjustment. The grid voltages were to have been measured by dividers similar to (but much shorter than) the plate voltage dividers. However, difficulties with the measurements were discovered before they were constructed, and they have not been installed as yet.

The cathode current measurements were taken from the cathode shunts for each tube. In order to minimize the effect of the inductance of the shunt, the center lead of the cable connecting to the ungrounded side was laid along the blade of the shunt (Fig. 43).

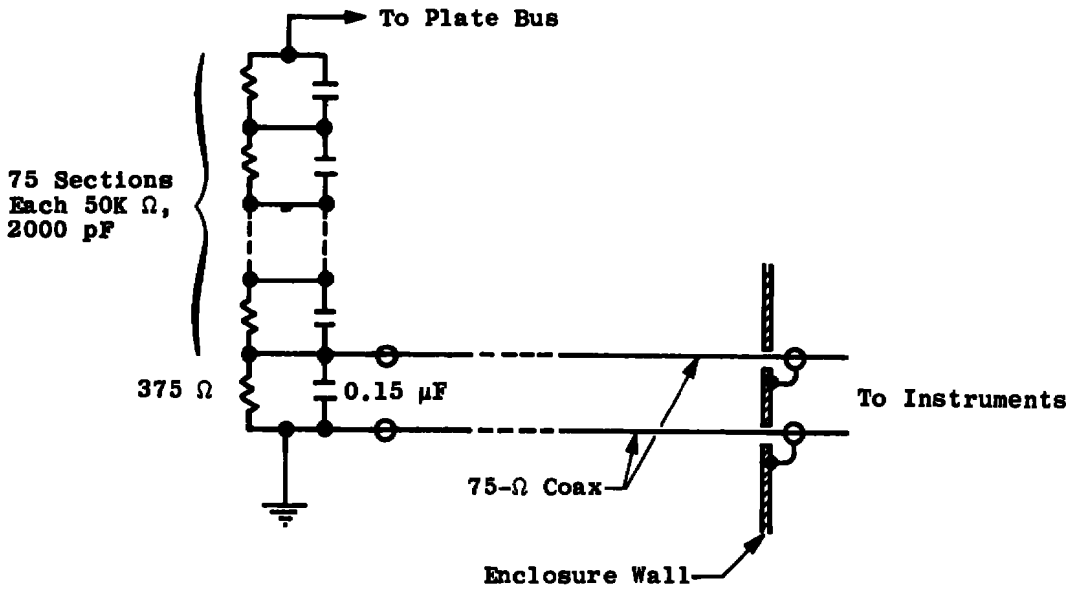

Figure 42. Voltage divider for measuring instantaneous plate voltage.

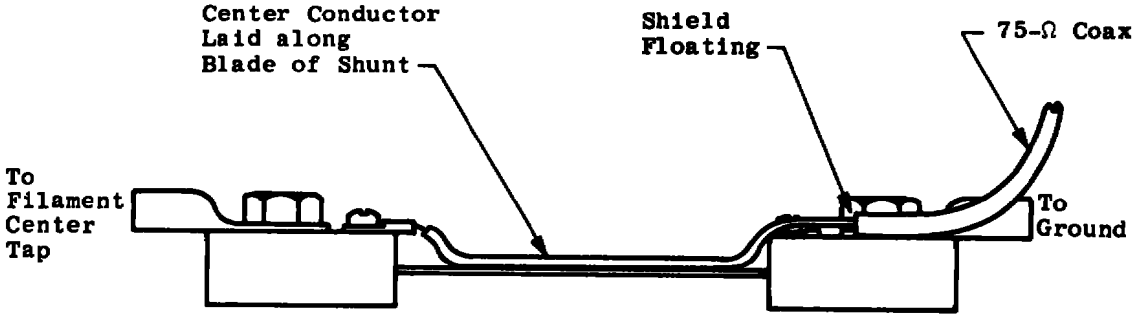

Figure 43. Method of connecting instrumentation leads to cathode current shunt to minimize the inductance of the shunt.

It was recognized that common mode voltages would be present, and in every case two coaxial cables were run for the measurement. One was connected to the ungrounded and one to the grounded side of the shunt (or divider). The cable shields were grounded where the cables left the enclosure and were floated at the shunt (or divider). Although the general approach taken seems to have been correct, the common mode voltages present on the cathode current measurements were too large to be handled by the instruments used.

7.0 OPERATING EXPERIENCE

Operation of the oscillator has been quite successful, and it is presently serving its intended function. In most cases the predictions of the design have been borne out. Some difficulties were encountered during shakedown, however, and it seems appropriate to discuss them here. First, the successes of the design were as follows:

1. A continuous power input of 3.5 MW has been achieved with operating conditions very close to those predicted by the design. In particular, the overall efficiency predicted in Section 2.0 was achieved. The limitations which prevent achievement of the full design power input of 4.6 MW can probably be removed without much trouble when more power is needed.
2. No flashovers of high voltage components have occurred.
3. No parasitic oscillations occur under any conditions.
4. No overheating or overloading of oscillator components has occurred.
5. Operation of the oscillator is quite stable, with no tendency toward blocking oscillations or unruly transient response.
6. Protection of the tubes against damage from flashover seems to be adequate.

7.1 TESTS OF TUBE PROTECTION CIRCUITRY

Shakedown of the oscillator was begun with a test of the flashover protection circuitry. This was carried out by disconnecting the plate choke, the tank coil, and the tank bleeder resistors, and charging first the tank capacitors and then the plate-coupling capacitor to the desired voltage. The tubes had not yet been installed. The top of a plate resistor was then shorted to ground by a loop of 0.010-in.-diam molybdenum wire connected to a ground strap. (The actual grid wires in the tubes are 0.012-in.-diam platinum-clad molybdenum.) No damage to the molybdenum wire could be detected after shorting to

ground, even at a plate voltage of 45 kv. It was found that the crowbar fired whenever the plate voltage was above about 8 kv. Shorts were made to the top of each plate resistor to verify that all eight crowbar trigger circuits were operable. It was very difficult to measure the time required for the crowbar to fire, but it appeared to be about 2.0 μsec after initiation of the fault. A high voltage tester was used to verify that the spark gaps in the grid and filament circuits fired at the proper voltages. It was verified that firing of either crowbar triggered the ignitron across the plate voltage supply.

It has been mentioned that the flashover detection circuits (Fig. 39) were not entirely successful. When these circuits were tested individually with a d-c input, they were found to fire at voltages ranging from 0.40 to 0.56 v, which correspond to cathode currents of 200 to 280 amp. However, in operation, the circuits were found to be too sensitive, and often fired under normal conditions, even at low plate voltages. It was eventually necessary to disconnect them in order to continue the shakedown. When a flashover did finally occur, the crowbar and ignitron fired properly, but the plate supply circuit breaker was not tripped, and the shunt on the ignitron cathode was eventually destroyed. By this time, the plate supply had been short circuited long enough so that the flashover had cleared, and when the shunt opened and plate voltage returned, the oscillator went back into normal operation.

The reason for the excess sensitivity is difficult to identity. It may be that the SCR fires at a lower voltage if the rise time is fast. It could also be that the inductance of the shunt is not neglible, and that too much voltage is applied to the SCR. When time permits, the circuits will be replaced with some circuit with better voltage discrimination and known high frequency response. Inductive, rather than resistive coupling to the cathode will probably also be used.

The shakedown of the oscillator was carried out with the oscillator output connected to a dummy load consisting of a bank of water-cooled stainless steel tubes. The power output was calculated from the flow rate and temperature rise of the cooling water. The tank capacitor was operated in configuration 9 at a frequency of 22.7 kHz, because this configuration had the highest var capability and was therefore the most conservative. A number of trivial problems were located and corrected, among them the difficulties with the flashover detector circuits and tube cooling water flow rate, which have already been discussed. Eventually it became possible to achieve a power input

of 3.5 MW routinely, with a measured efficiency of 66 to 71 percent. This compares favorably with the efficiency of 70.5 percent calculated in Section 2.0.

7.2 LOAD DIVISION BETWEEN TUBES

The ultimate limit to the power output of the oscillator is at present imposed by unbalanced loading of the tubes. The oscillator was operated over a wide range of plate voltages and tank Q values. It was found that while a moderate unbalance in cathode current between tubes existed under all conditions, any condition which required a high peak plate current greatly increased the unbalance. The variation of individual cathode currents as plate supply voltage changed in a typical case is shown in Fig. 44. The same effect was obtained by holding plate supply voltage constant and lowering the tank Q, which also increased the peak plate current. Evidently the tubes differ most markedly in the low plate voltage, high plate current region of the characteristic. Perhaps the difference is caused by variations in the secondary emission characteristics of the grids, which could be appreciable even if the geometry of the tubes were identical.

In early runs it was found that the tubes on the east side of the component support consistently drew more current than those on the west side, and that swapping tubes did not alter this condition. Voltage measurements made on the grid lines and on the south end of the component support (Fig. 45) suggested that the tank coil was inducing voltages which unbalanced the grid drive voltages, increasing the drive on the east side and decreasing the drive on the west. The shield shown in Fig. 46 was installed. Although it could not be as effective as might have been desired because it had to avoid existing components, it was successful in reducing the unbalance in grid voltages by a factor of 7 (see Fig. 45) and in reducing the voltage induced in the component support by a factor of 9. With the shield in place, the systematic unbalance between east and west tubes disappeared, but intolerable unbalances remained. The data plotted in Fig. 44 were taken with the shield in place.

Unbalanced loading of the tubes had of course been anticipated, and provisions had been made for adjusting the individual bias resistors on the tubes in 5.0-Ω steps from 0 to 395 Ω, the nominal design value being 295 Ω. Changing bias resistance was rather ineffective, however, and perfect balance could be achieved under

only one operating condition. At other conditions, the grid resistors had to be readjusted. Note the behavior of the tube W2 in Fig. 44.

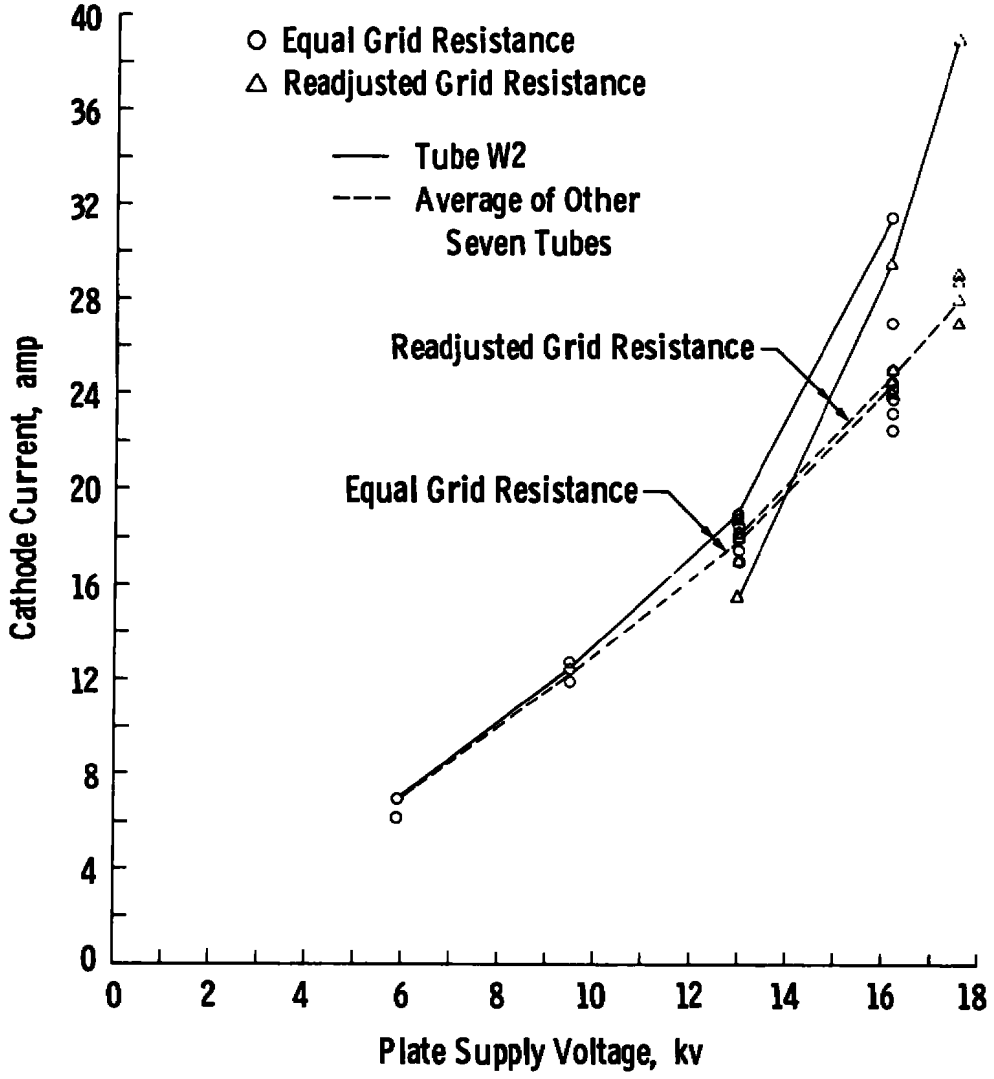

Figure 44. Variation of individual cathode currents with plate supply voltage.

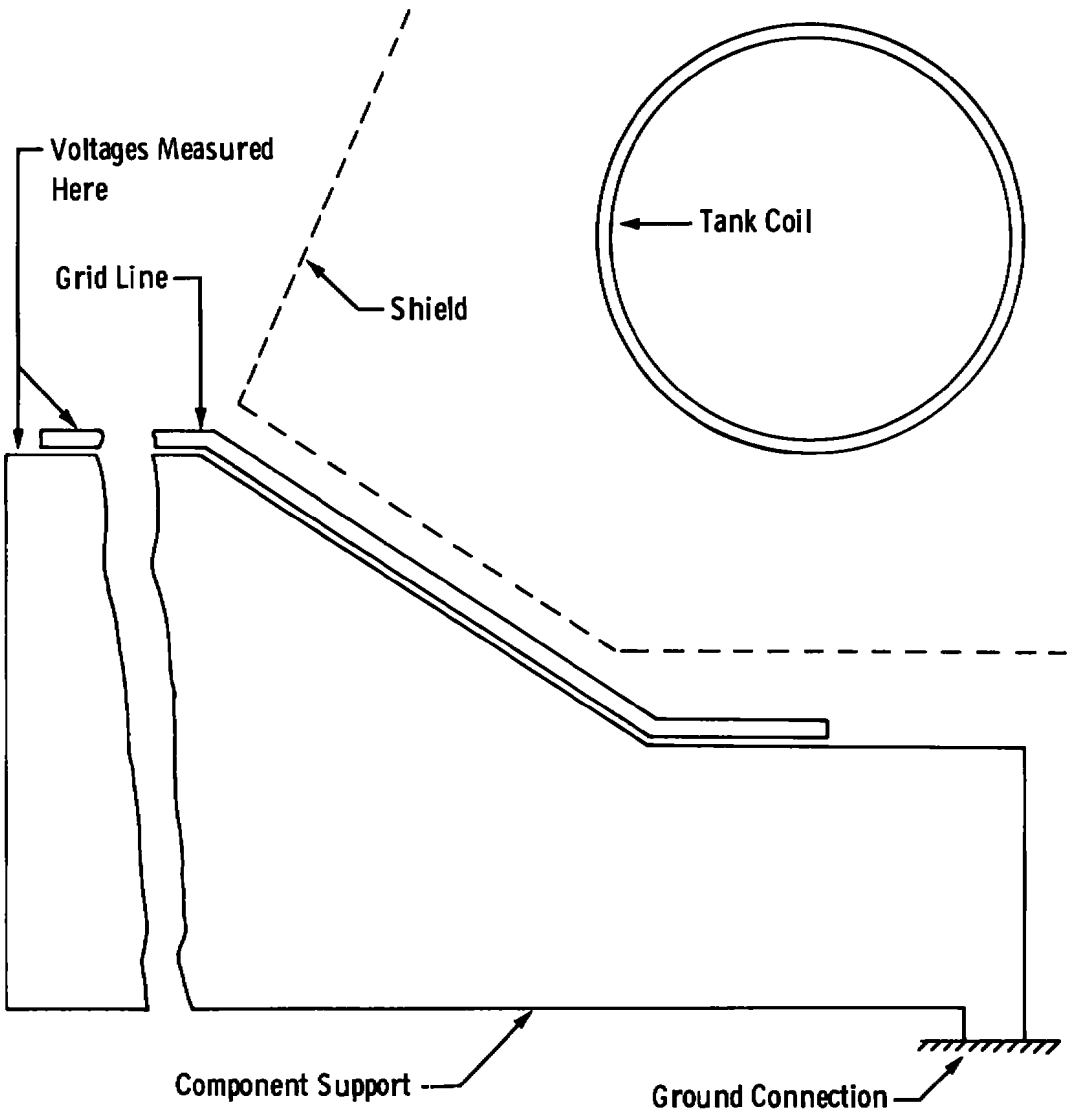

Peak-to-Peak Voltages on Tap 11

	Without Shield	With Shield
West Grid Line	1432	1564
East Grid Line	1335	1550
Component Support	95	10

Figure 45. Voltages induced by tank coil.

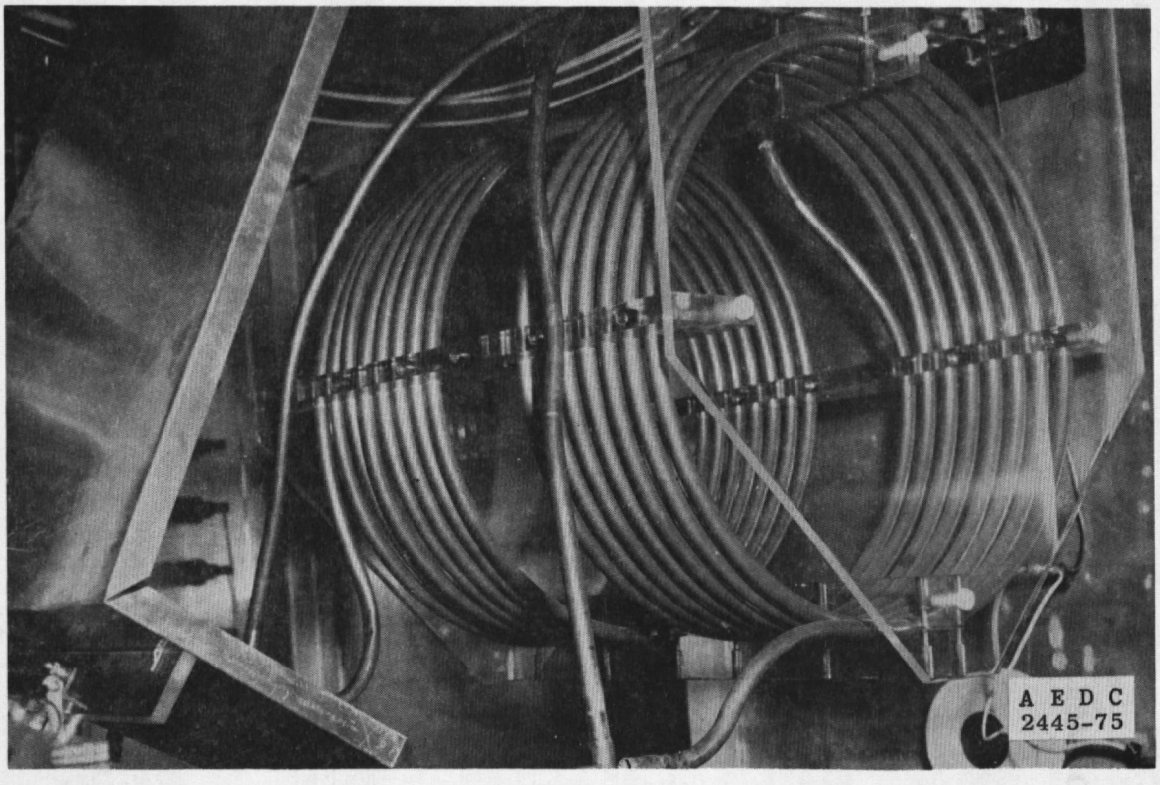

Figure 46. View showing the shield which was installed around the tank coil.

It is difficult to document exactly why the change in grid resistance is ineffective, because attempts at accurate measurement of instantaneous electrode voltages were only partially successful. Something like the following sequence of events probably occurs. Figure 47 shows the tube characteristic near the low voltage end of the load line. Increasing the grid resistor on one tube will increase the bias on that tube and thus will decrease the peak positive grid voltage, but will have little effect on the peak rf plate voltage or peak rf grid voltage, because there are seven other tubes in operation. Thus, the load line on this one tube will be moved downward (dashed line in Fig. 47). Increasing the bias voltage from 1,000 to 1,100 v (the case depicted in Fig. 47), an increase of 10 percent, decreases the peak grid current from 28 to 21 amp, a decrease of 25 percent. As a very rough approximation one can assume that all grid current flows at this condition. Then the percentage change in grid resistance needed to establish the new conditions is

$$\frac{\Delta R}{R} = \frac{\Delta E}{E} - \frac{\Delta I}{I}$$

$$= 0.1 - (-0.25) = 35 \text{ percent}$$

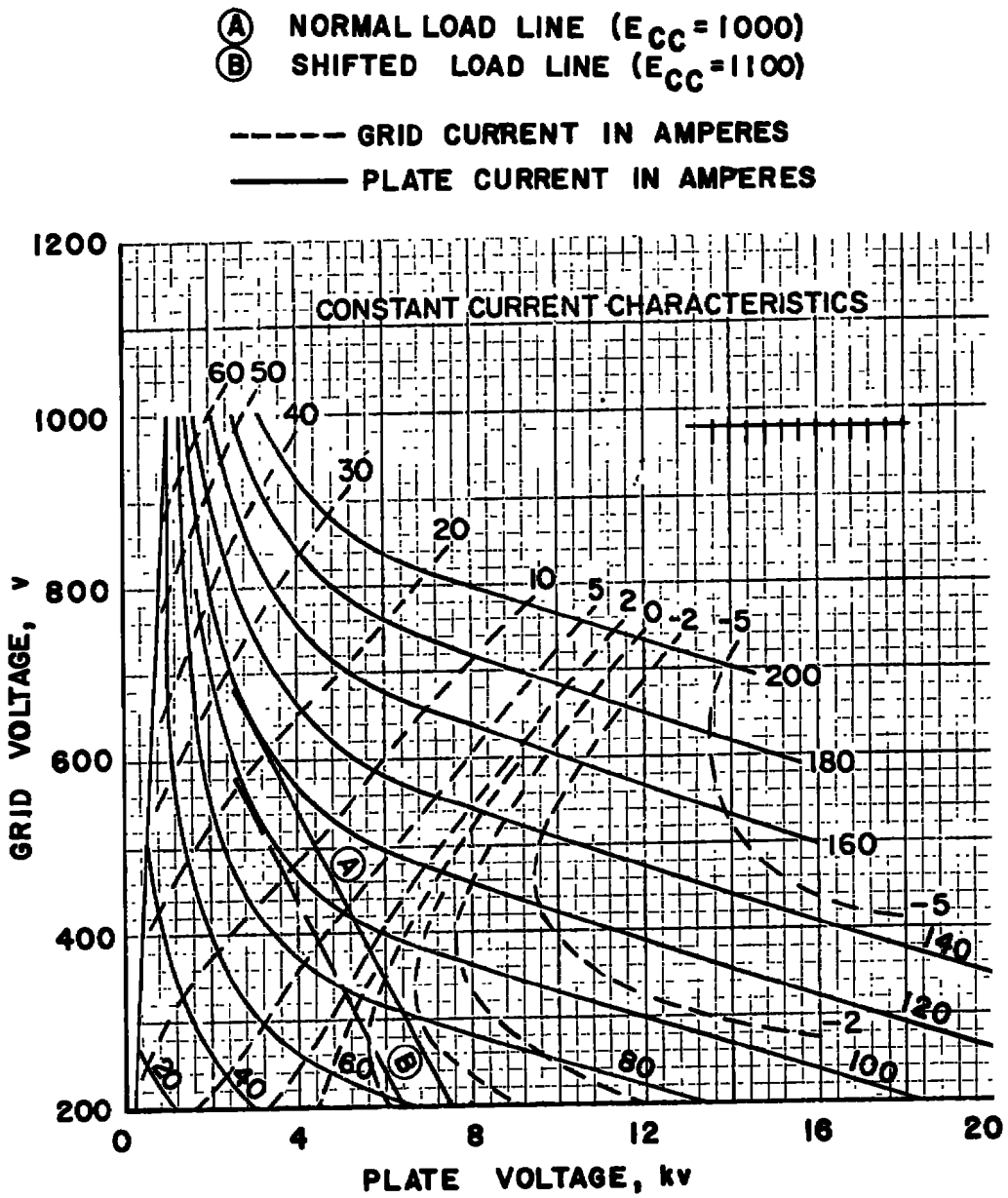

Figure 47. High current region of tube characteristic, showing the effect of increased bias voltage.

Furthermore, the peak plate current changes only from 119 to 99 amp, a decrease of 17 percent. So a 35-percent increase in bias resistance produces a 25-percent decrease in grid current, and only a 17-percent decrease in plate current. Data taken during the shakedown confirm that the bias resistors are more effective in changing grid current than plate current.

An attempt has been made here to balance the tubes, by applying the same rf driving voltage to each tube, and by varying the individual bias voltages. In retrospect, it appears that it would have been better to apply the same bias voltage to each tube, and to vary the individual rf driving voltages. The circuit of Fig. 48 would accomplish this, and would have the additional advantage that balance is automatically achieved, and does not require cut-and-try adjustment. Any unbalance between cathode currents induces a voltage in the balancing transformer, which tends to increase the drive on one tube and decrease the drive on the other. A similar circuit is often used to balance currents between silicon diodes in parallel. Calculations indicate that the transformers would not be difficult to build.

Incorporation of these transformers was considered very early in the design. They were not included because of the uncertain impedance they add to the cathodes of the tubes. Had parasitic oscillations occurred, the transformers would have been immediately suspect, and would have to have been removed. Since the oscillator seems to be rather immune to parasitic oscillations, the balancing transformers will probably be added at a later date.

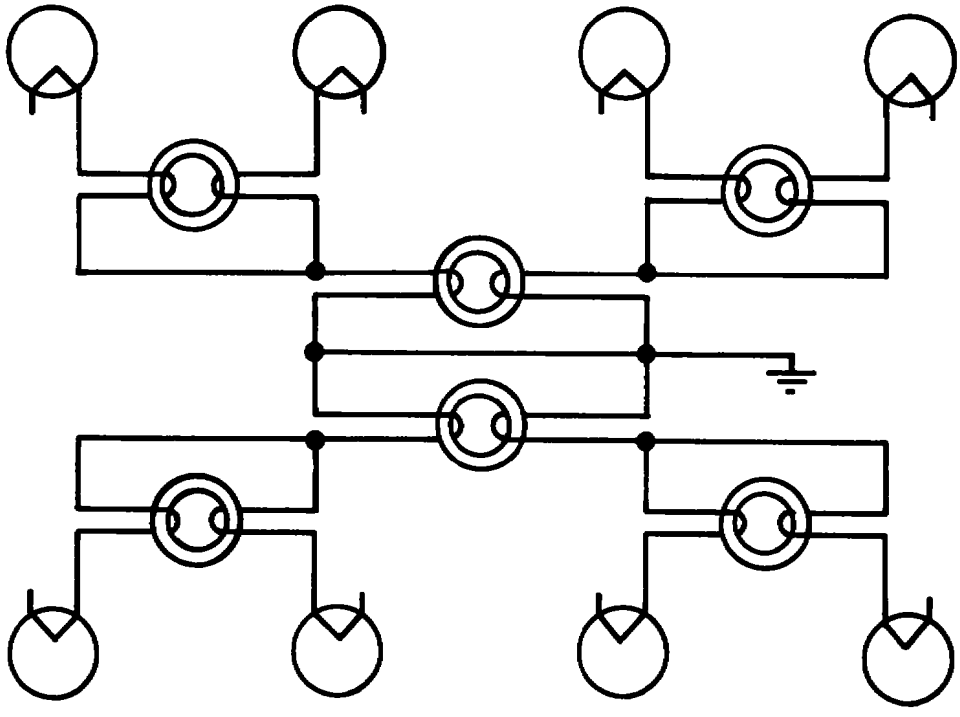

Figure 48. Possible arrangement of balancing transformers for equalizing cathode currents of the tubes.

7.3 PROBLEMS WITH INSTRUMENTATION

Of the instantaneous waveform measurements which were attempted, only the plate voltage measurements were particularly successful. Since the compensated voltage dividers used in the plate voltage measurement appeared to operate properly, successful grid voltage measurements could probably be made. At present there seems to be no way to make accurate cathode current waveform measurements, for two reasons.

First, the desired signal taken from the cathode shunt, which is of the order of 0.1 v in magnitude, must be measured in the presence of the common mode voltage of about 10 v, which is present on the component support. The common mode voltage capability of oscilloscopes is not good enough to make accurate measurements under these conditions, especially since frequency components up to 100 kHz or more are involved.

Second, the inductance of the shunt is apparently not negligible. In an attempt to overcome the common mode problems, an isolation transformer wound on a ferrite core was constructed and was connected to a cathode shunt. The waveform obtained from the transformer was roughly believable, except that it showed a negative cathode current at the end of the conduction period. This was attributed to inductance in the shunt, and a compensating network was introduced which was capable of eliminating the effect of this inductance. By adjusting the network, one could eliminate the negative portion of the waveform. However, almost any shape could be obtained for the positive portion of the waveform, and since the actual waveform was unknown, the proper setting for the compensating network could not be found. Perhaps it will eventually be possible to make accurate measurements by coupling inductively to the cathode.

7.4 OSCILLATOR DESIGN IN RETROSPECT

Now that construction of the oscillator has been completed and the experience of several dozen runs has been accumulated, it is becoming possible to be objective about the decisions which were made during the design. The general form of the circuit (push-pull Colpitts with shunt-fed grids and plates) has been very satisfactory. The means chosen for varying the feedback capacitor has proven to be convenient and reliable. The tank capacitor bank is probably about the most

economical which would allow any versatility, but changing configurations is certainly awkward. Apparently the possible causes of parasitic oscillations were correctly identified and eliminated, because no such oscillations materialized.

The tube protection circuitry seems to be entirely adequate, except for the circuits which indicate which tube flashed over. The plate resistors are the heart of the protection. They offer the important advantages that they are entirely passive and very reliable, and they are certainly worth the small amount of output power they consume. The crowbars are also worthwhile, and have been reliable up to this point, but they suffer a distinct disadvantage in that they are not passive. If the operator allows the bateries to run down, or fails to turn them on, protection is lost.

The method which was chosen for equalizing loading among the tubes was inadequate, and has the further disadvantage that it must be adjusted by trial and error, and must be readjusted for every change in operating conditions. The use of some method which automatically balances tubes without adjustment would be much more desirable.

The use of vapor cooling has been a mixed blessing. Although it was quite economical of water usage, provided somewhat better cooling, and probably did result in some saving in construction cost, it complicated the mechanical design of the oscillator much more than was originally anticipated. The fact that plate dissipation cannot be measured directly is also an inconvenience, if not to the designer, at least to the user, who has no direct means of calculating the power input to his experiment.

The time devoted to the computer simulation program was considered well spent. The program takes into account many effects which must be ignored when using classical methods, and it is applicable to a much broader range of problems.

The features which were included in the oscillator design for protection of operating personnel are considered adequate and permit safe operation and maintenance. However, it must be kept in mind that these features are not automatic, and that the oscillator is very dangerous to an operator who does not understand and use the established procedures.

REFERENCES

1. Terman, F. E. Electronic and Radio Engineering. (Chapter 13, "Tuned Power Amplifiers" and Chapter 14, "Vacuum-Tube Oscillators.") McGraw-Hill Book Company, Inc., New York, 1955.

2. Ryder, J. D. Engineering Electronics. (Chapter 11, "Oscillators and Class C Amplifiers.") McGraw-Hill Book Company, Inc., New York, 1957.

3. Stern, T. E. Theory of Nonlinear Networks and Systems. (Chapter Two, "Network Elements and Network Equations.") Addison-Wesley Publishing Company, Inc., Reading, Mass., 1965.

4. Conte, S. D. and DeBoor, C. Elementary Numerical Analysis. (Chapter Six, "The Solution of Differential Equations.") McGraw-Hill Book Company, Inc., New York, 1972 (Second Edition).

5. Milne, W. E. Numerical Solution of Differential Equations. (Chapter Five, "Methods of Runge-Kutta.") John Wiley and Sons, Inc., New York, 1953.

6. Spangenburg, K. R. Vacuum Tubes. (Sections 9.6 and 9.7.) McGraw-Hill Book Company, Inc., New York, 1948.

7. Parrack, H. O. "Effect of Air-Borne Ultrasound on Humans." International Audiology, Vol. 5, 1966, p. 294.

NOMENCLATURE

A	Dimensionless parameter relating vacuum tube and capacitor voltage ratings, see Eq. (39)
B	Dimensionless parameter relating vacuum tube and capacitor voltage ratings, see Eq. (40)
C	Capacitance of an individual capacitor
C_b	Capacitance of a tank capacitor bank
C_f	Capacitance of a feedback capacitor bank
C_t	Effective plate-to-plate tank capacitance

E_b	Voltage across a tank capacitor bank, rms
E_{bb}	Plate supply voltage
E_{br}	Voltage rating of a tank capacitor bank, rms
E_{cc}	Bias voltage, DC
E_{pr}	Plate-to-plate voltage rating of vacuum tubes, rms
E_r	Voltage rating of an individual tank capacitor, rms
E_t	Plate-to-plate voltage across tank capacitor, rms
f	Frequency, Hz.
I	Current (general)
I_b	Current through a tank capacitor bank, rms
I_{bb}	Total d-c plate current of vacuum tubes
I_{bbr}	Rated total d-c plate current of vacuum tubes
I_{br}	Current rating of a tank capacitor bank, rms
I_r	Current rating of an individual tank capacitor, rms
I_t	Current Circulating in tank circuit, rms
k	Ratio of a-c grid voltage to a-c plate voltage
L	Inductance of tank inductor
ℓ	Ratio of the highest voltage across an individual capacitor in a bank to the voltage across the bank
m	Ratio of the highest current through an individual capacitor in a bank to the total current through the bank
n	Number of capacitors in a bank
P	Total power output of vacuum tubes
P_m	Maximum power which can be obtained from oscillator when capacitor voltage rating is more restrictive than plate supply voltage rating
P_r	Total rated power output of vacuum tubes
Q	Quality factor of tank circuit
Q_o	Dimensionless parameter relating vacuum tube and tank capacitor rating see Eq. (38)
R	Load resistance coupled into tank inductor

t	Time
V_{br}	Rating of a tank capacitor bank, vars
V_r	Rating of an individual tank capacitor, vars
V_t	Reactive power being handled by tank circuit, vars
Z_t	Plate-to-plate tank circuit impedance at resonance
ω	Frequency, radians per sec
ω_h	Frequency at which rated current and rated var capability of a capacitor will be reached simultaneously
ω_ℓ	Frequency at which rated voltage and rated var capability of a capacitor will be reached simultaneously
ω_o	Resonant frequency of tank circuit